



Summer School
Recent Developments in Wave Physics
of Complex Media
Institut d'Etudes Scientifiques de
Cargèse

2 – 6 May, 2011



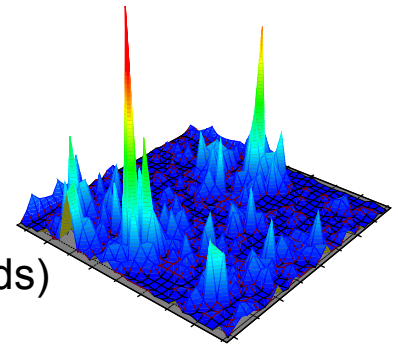
Anderson localization of ultrasonic waves in three-dimensional “mesoglasses”

John Page
University of Manitoba

At Manitoba, we use ultrasound to study mesoscopic wave phenomena in complex media, and to probe the physical properties of mesoscopic materials.



- ballistic and diffusive **wave transport in random media**
- field fluctuation spectroscopy (DSS, DAWS...)
- wave transport & focusing in phononic crystals
- ultrasound in complex materials (e.g., soft matter, foods)



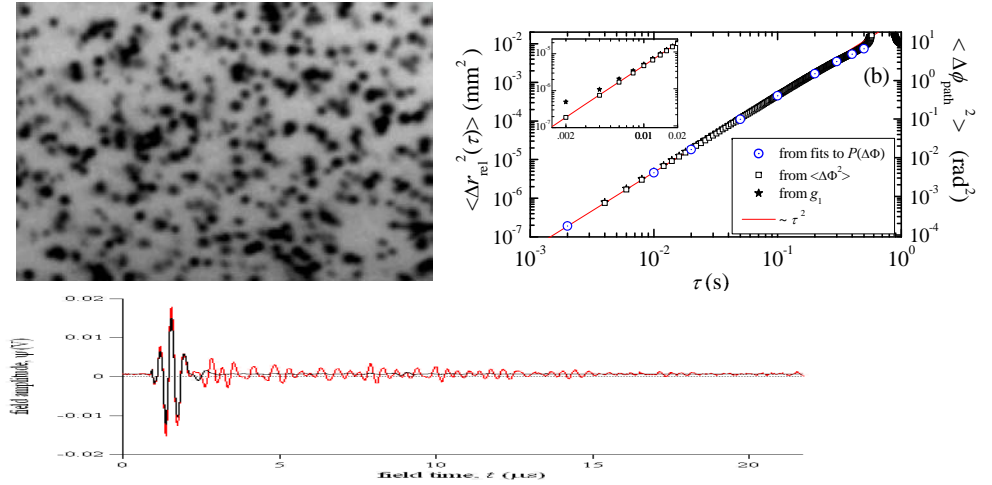
www.physics.umanitoba.ca/~jhpage

Mesososcopic wave physics with ultrasound

Wave transport in random media



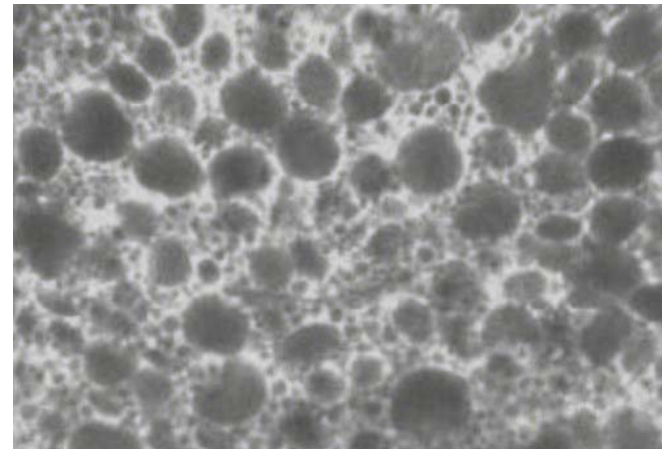
Field fluctuation spectroscopy (e.g., DAWS)



Phononic crystals



Spectroscopy of complex materials, e.g. foods



Collaborators/Acknowledgements:

- Hefei Hu, Anatoliy Strybulevych, Kurt Hildebrand*, Laura Cobus*, Eric Lee (University of Manitoba, Winnipeg, Canada)
 - Sergey Skipetrov*, Bart van Tiggelen (Université J. Fourier & LPMMC, Grenoble)
 - Alexandre Aubry*, Arnold Derode (Institut Langevin, ESPCI, Paris)
- Sanli Faez, Ad Langedijk (FOM Institute for Atomic & Molecular Physics, Amsterdam)



* Special thanks for contributions to the slides in this presentation

Outline: Anderson Localization of Ultrasonic Waves

- Introduction to Anderson localization

See Physics Today, August 2009



- Localization of elastic waves in 3D

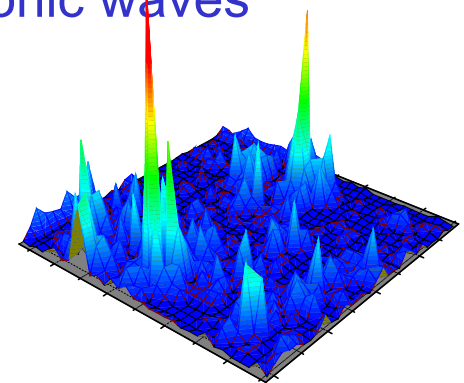
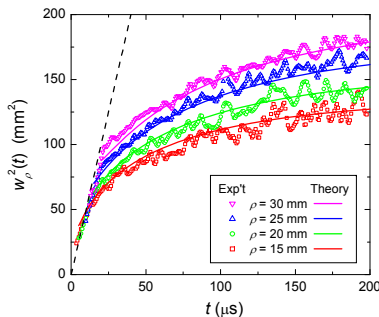
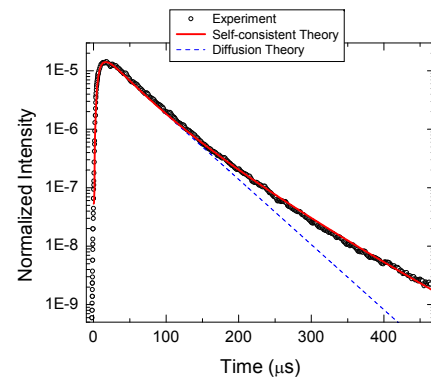
I. Why elastic waves?

Our samples & their basic (wave) properties

II. Time-dependent transmission, $I(t)$

III. Transverse confinement of ultrasonic waves due to localization

IV. Coherent Backscattering



IV. Statistics and Correlations – non-Rayleigh statistics, variance, multifractality, long-range correlations.

- Conclusions

Hu *et al.*, *Nature Physics*, **4**, 945 (Dec, 2008) arXiv:0805.1502

Introduction: Anderson localization of electrons (quantum particles)

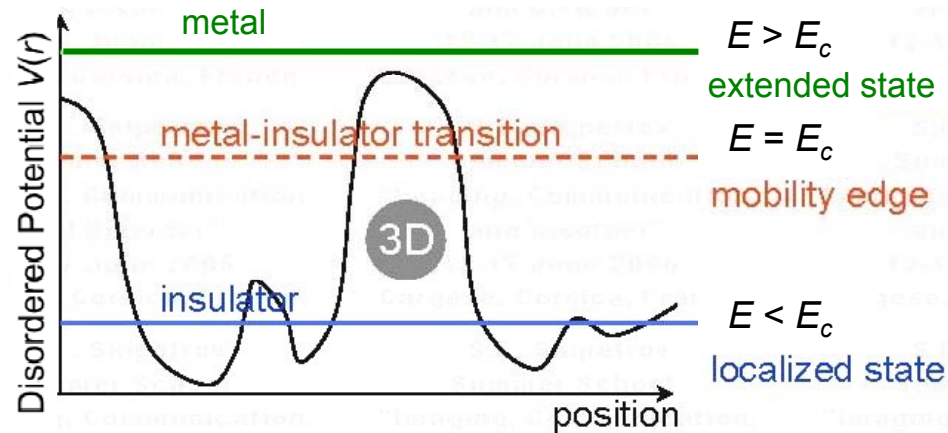


P.W. Anderson
1958

(~50 years ago)

Schrodinger equation:
 $V(\mathbf{r})$ varies randomly
in space

$$\left[-\frac{\hbar^2}{2m} \nabla^2 + V(\mathbf{r}) \right] \psi(\mathbf{r}) = E\psi(\mathbf{r})$$



PHYSICAL REVIEW

VOLUME 109, NUMBER 5

MARCH 1, 1958

Absence of Diffusion in Certain Random Lattices

P. W. ANDERSON

Bell Telephone Laboratories, Murray Hill, New Jersey

(Received October 10, 1957)

This paper presents a simple model for such processes as spin diffusion or conduction in the "impurity band." These processes involve transport in a lattice which is in some sense random, and in them diffusion is expected to take place via quantum jumps between localized sites. In this simple model the essential randomness is introduced by requiring the energy to vary randomly from site to site. It is shown that at low enough densities no diffusion at all can take place, and the criteria for transport to occur are given.

[# citations > 4200 !]

Introduction: Anderson localization of electrons (quantum particles)

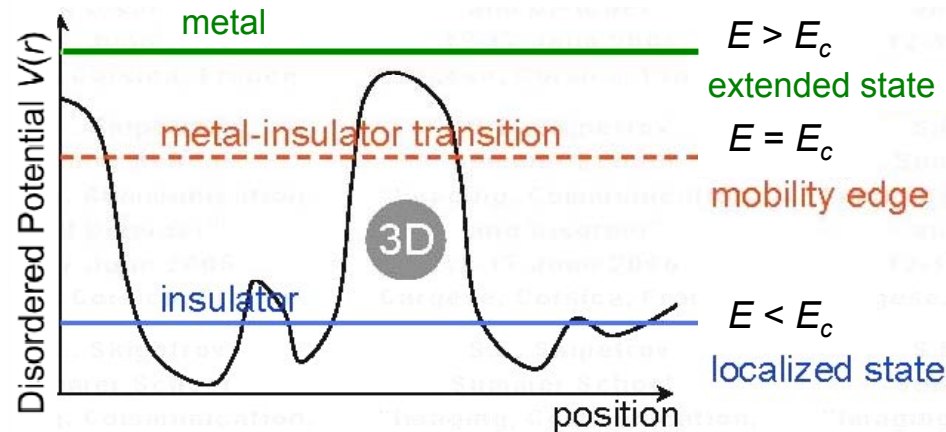


P.W. Anderson
1958

(~50 years ago)

Schrodinger equation:
 $V(\mathbf{r})$ varies randomly
in space

$$\left[-\frac{\hbar^2}{2m} \nabla^2 + V(\mathbf{r}) \right] \psi(\mathbf{r}) = E\psi(\mathbf{r})$$



"Localization [...], very few believed it at the time, and even fewer saw its importance, among those who failed to fully understand it at first was certainly its author. It has yet to receive adequate mathematical treatment, and one has to resort to the indignity of numerical simulations to settle even the simplest questions about it."

P.W. Anderson, Nobel Lecture, 1977

Many theoretical breakthroughs:

e.g. Scaling theory (1979) (~30 years ago)
Self consistent theory (1980)

Experiments:

Hampered by interactions and
finite temperatures

Introduction: Anderson localization of electrons (quantum particles)

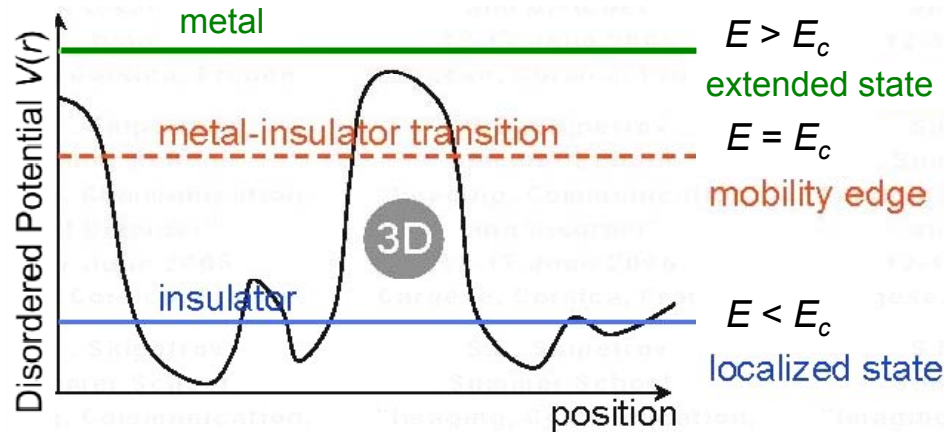


P.W. Anderson
1958

(~50 years ago)

Schrodinger equation:
 $V(\mathbf{r})$ varies randomly
in space

$$\left[-\frac{\hbar^2}{2m} \nabla^2 + V(\mathbf{r}) \right] \psi(\mathbf{r}) = E\psi(\mathbf{r})$$



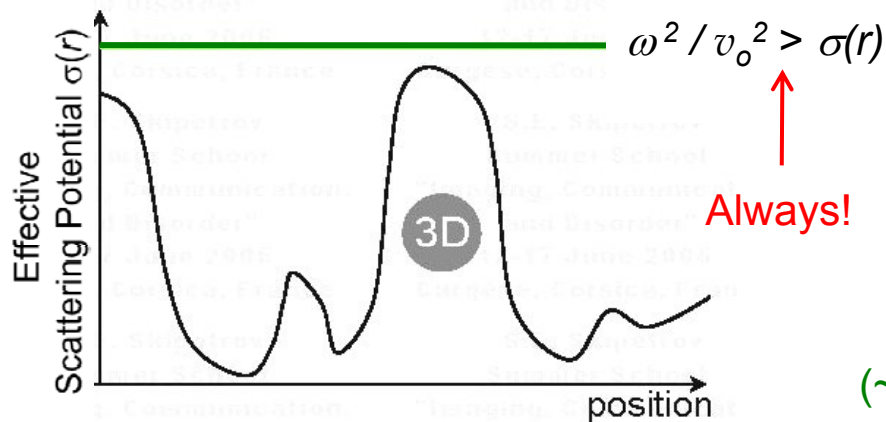
Localization of classical waves (sound or light)

e.g., scalar wave equation with disorder:

$$\left[-\nabla^2 + \sigma(r) \right] \psi(r) = \frac{\omega^2}{v_0^2} \psi(r)$$

where $\sigma(r) = \frac{\omega^2}{v_0^2} - \frac{\omega^2}{v^2(r)}$

deviations from a uniform medium with velocity v_0



Sajeev John
1983

(~25 years ago)

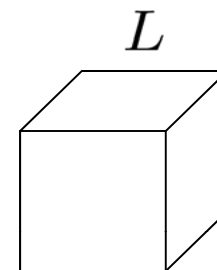
Introduction - basic concepts:

With sufficient disorder, wave interference can suppress the diffusion coefficient and hence the conductivity.

Localized state: confined within a length scale ξ

Extended (diffusive) state: extends over the entire sample, L^d

Thouless criterion - distinguishing localized and extended states by their sensitivity to boundary conditions



2 important frequencies (and time scales)

- $\delta\omega$ \equiv the frequency shift of a mode when boundary conditions are changed from symmetric to antisymmetric.
 - frequency width is due to **time scale** τ_T (“**Thouless time**”) required for change in boundary conditions to be **communicated** to the wave function ($\delta\omega \sim 1/\tau_T$).
- $\Delta\omega$ \equiv the average frequency separation between neighbouring states
 - Inversely proportional to the **density of states** [$\rho = 1/(\Delta\omega L^d)$]
 - $\tau_H \sim 1/\Delta\omega$ is called the “**Heisenberg time**”

Dimensionless Thouless conductance:

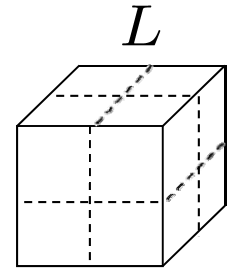
$$g \equiv \frac{\delta\omega}{\Delta\omega}$$

$g > 1 \Rightarrow$ diffusive/extended states

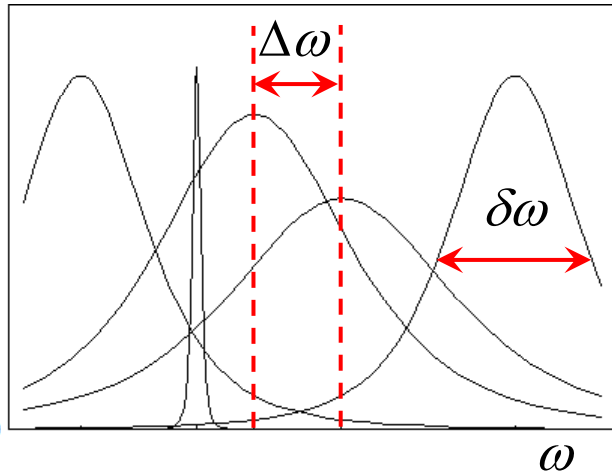
$g < 1 \Rightarrow$ localized states

Scaling of the Thouless conductance with system size L :

What happens if small samples are coupled together to make larger ones?



Extended/diffuse states ($\delta\omega > \Delta\omega$; states overlap in frequency):



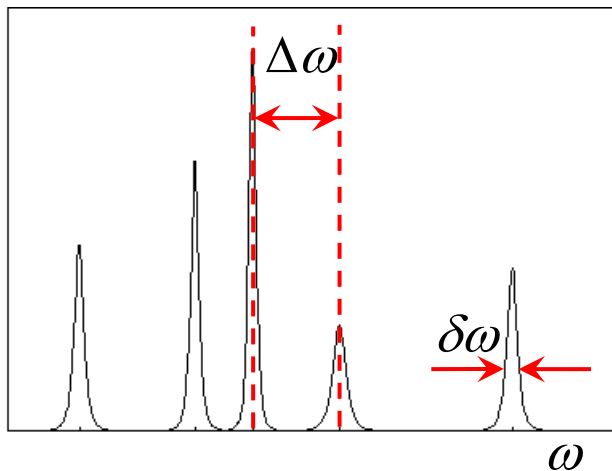
$$\delta\omega \sim \frac{1}{\tau_T} = \frac{1}{\tau_D} = \frac{D}{L^2} \quad \Delta\omega = \frac{1}{\rho L^d} \propto L^{-d}$$

Characteristic diffusion time

$$\therefore g \equiv \frac{\delta\omega}{\Delta\omega} \propto L^{d-2}$$

g increases with L in 3D,
 g decreases with L in 1D

Localized states ($\delta\omega < \Delta\omega$; states well separated in frequency):



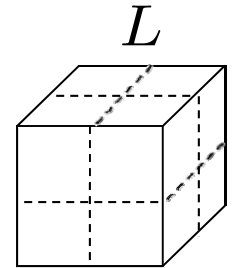
$$\delta\omega \sim \frac{1}{\tau_T} \sim \exp(-L/\xi) \quad \Delta\omega = \frac{1}{\rho L^d} \propto L^{-d}$$

$$\therefore g \equiv \frac{\delta\omega}{\Delta\omega} \propto \exp(-L/\xi) \quad (\text{for } L > \xi)$$

g always decreases with L

Scaling of the Thouless conductance with system size L :

What happens if small samples are coupled together to make larger ones?



Extended/diffuse states:

$$g \equiv \frac{\delta\omega}{\Delta\omega} \propto L^{d-2}$$

g increases with L in 3D,
 g decreases with L in 1D

Localized states:

$$g \equiv \frac{\delta\omega}{\Delta\omega} \propto \exp(-L/\xi) \quad (\text{for } L > \xi)$$

g always decreases with L

Consequences:

• **In 3D:** g increases with L for diffuse states (large g), but decreases with L for localized states (small g).

⇒ transition from diffuse transport to localization at $g = g_c \approx 1$.

• **In 1D:** g always decreases as L increases.

⇒ No transition, all states are localized.

• **2D** is the “marginal” dimension for localization. Higher order terms indicate that all states are localized in 2D as well (no transition).

Scaling Theory of Localization [Abrahams et al., P.R.L., 42, 637 (1979)]

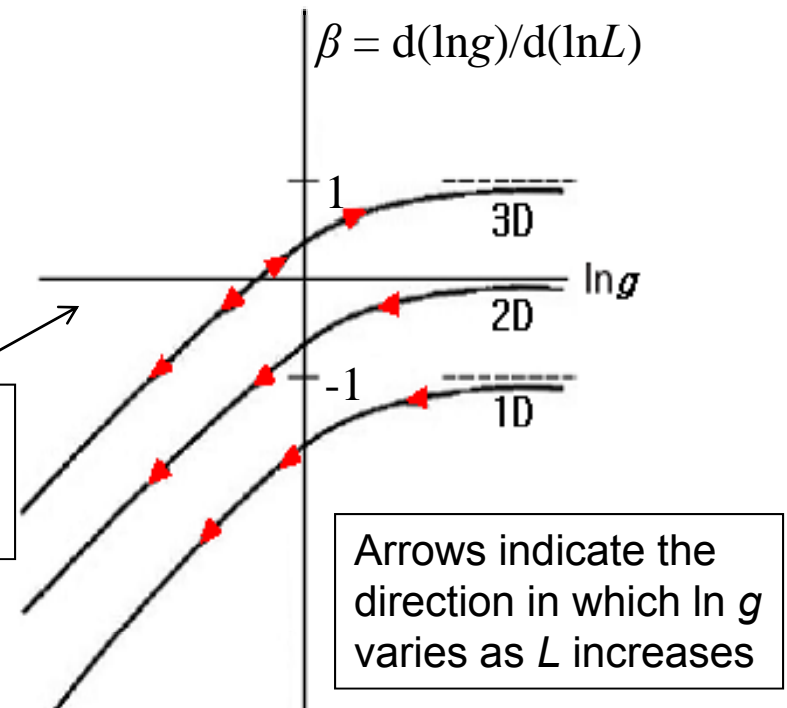
The scaling of g with L is given by

$$\ln g(L) \propto \begin{cases} (d-2)\ln L & \text{extended states} \\ -\exp(\ln L) & \text{localized states} \end{cases}$$

and captured by the scaling function

$$\beta(g) = \frac{d \ln g}{d \ln L}$$

$\beta > 0$ extended states
 $\beta < 0$ localized states
 $\beta = 0$ at g_c



Scaling hypothesis: β is a function of g only

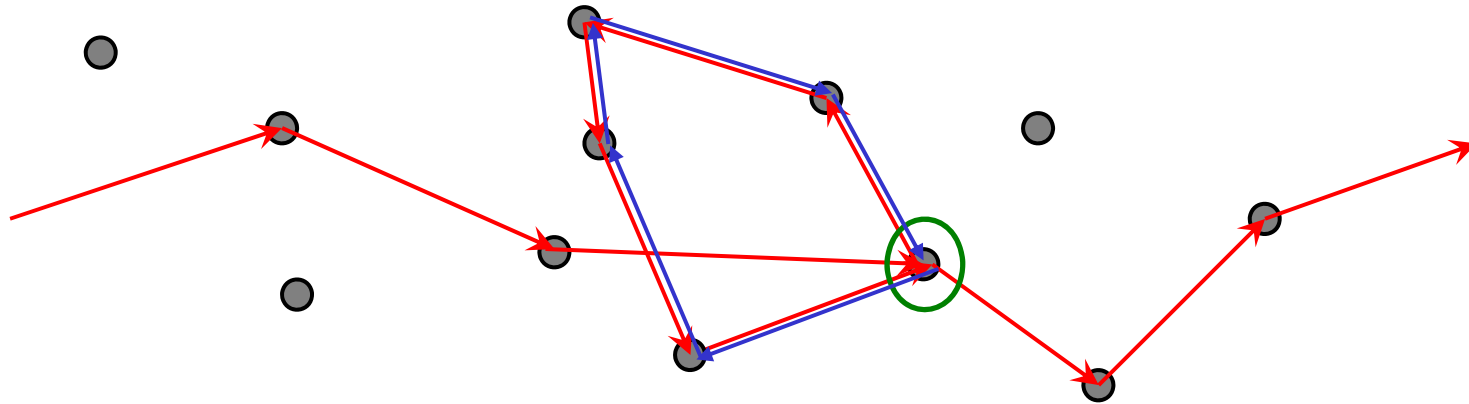
\Rightarrow Effect of changing the disorder can be compensated by changing L (g depends on both disorder and L).

Predictions:

- Only in 3D is there a real transition (i.e., a critical point at $g = g_c$) from extended to localized modes
- At g_c , $g \sim DL^{d-2} \approx 1$ is scale independent ($\beta = 0$) $\Rightarrow D \sim 1/L$ is renormalized
- All states in 1D and 2D are localized (if the sample is big enough).

Self-Consistent (SC) Theory

[Vollhardt & Wölfle, P.R.L., **45**, 842 (1980)]



Wave paths with multiple scattering loops lead to constructive interference, which enhances the probability for the wave to return to the same spot.

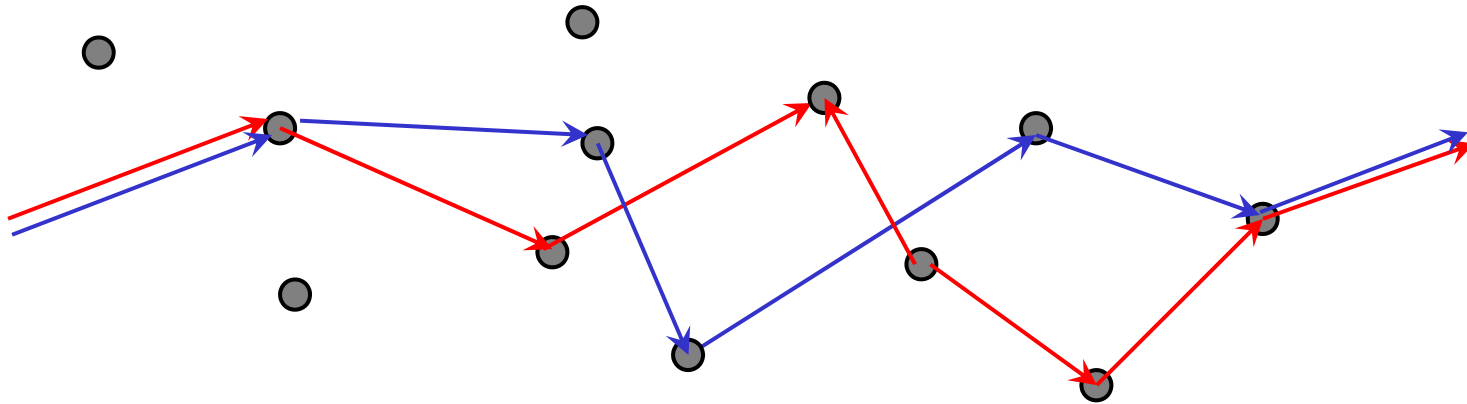
Consider two wave paths a and b . The wave energy is

$$|\psi_a + \psi_b|^2 = |\psi_a|^2 + |\psi_b|^2 + 2\text{Re}\psi_a\psi_b^*$$

Interference term

Self-Consistent (SC) Theory

[Vollhardt & Wölfle, P.R.L., **45**, 842 (1980)]



Wave paths with multiple scattering loops lead to constructive interference, which enhances the probability for the wave to return to the same spot.

Consider two wave paths a and b . The wave energy is

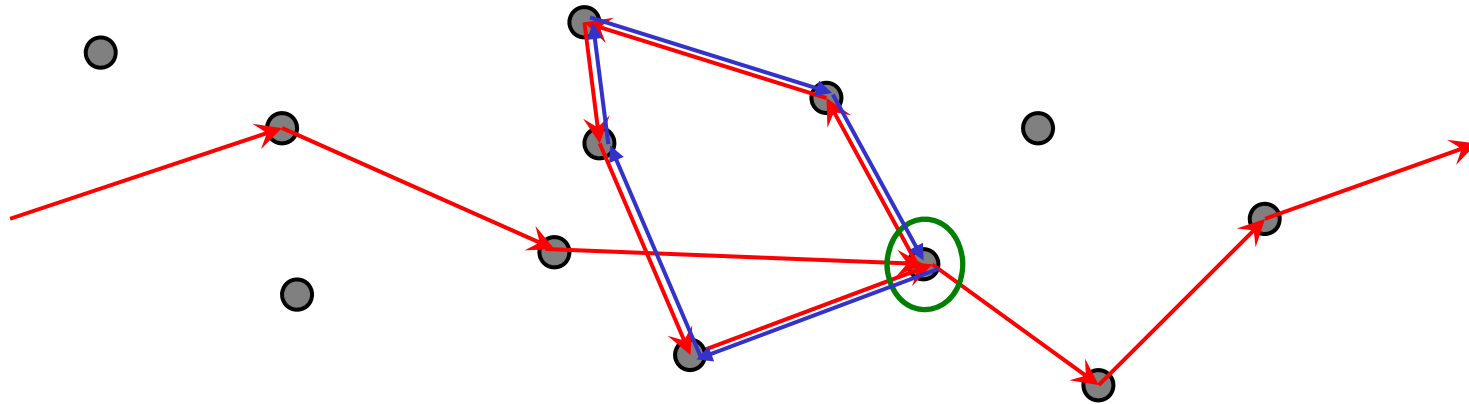
$$|\psi_a + \psi_b|^2 = |\psi_a|^2 + |\psi_b|^2 + 2\text{Re}\psi_a\psi_b^*$$

Interference term

for different paths, cancels on average (diffusion approximation)

Self-Consistent (SC) Theory

[Vollhardt & Wölfle, P.R.L., **45**, 842 (1980)]



Wave paths with **multiple scattering loops** lead to **constructive interference**, which enhances the probability for the wave to return to the same **spot**.

Consider two wave paths a and b . The wave energy is

$$|\psi_a + \psi_b|^2 = |\psi_a|^2 + |\psi_b|^2 + 2\text{Re}\psi_a\psi_b^*$$

Interference term

for different paths, cancels on average (diffusion approximation)

for loops, doubles the energy locally (time reversed paths)

⇒ **Diffusion slows down** and conductivity (transmission) is reduced, becoming scale dependent.

SC theory provides physical insight into how localization occurs.

Question: when does the amount of energy returning to the source position become significant?

A simple (approximate) argument can be constructed that **this occurs when $kl \sim 1$** , where k is the wave vector and ℓ is the mean free path.

Ioffe Regel criterion for localization: $kl \leq 1$

Why has it been difficult to observe Anderson localization of electrons experimentally?

For “quantum” particles (electrons), observations are hindered by:

- Need for low temperatures:

$$L_{\text{coh}} \sim 1/T^\alpha$$

(Anderson’s “absence of diffusion” only holds for $T = 0$)

- Need for small samples:

$$\text{size} < L_{\text{coh}} \sim 1 \mu\text{m}.$$

- Mutual interactions between electrons
- Electron-phonon interactions

Experiments with classical waves have some advantages.

For “quantum” particles (electrons), observations are hindered by:

- Need for low temperatures:
 $L_{\text{coh}} \sim 1/T^\alpha$
(Anderson’s “absence of diffusion” only holds for $T = 0$)
- Need for small samples:
size $< L_{\text{coh}} \sim 1 \mu\text{m}$.
- Mutual interactions between electrons
- Electron-phonon interactions

For light (photons) or sound (phonons),

- Experiments can be done at room temperature.
 $L_{\text{coh}} \sim$ is independent of T
- Samples can be of “human” size:
 L_{coh} is very large.
- No photon-photon or phonon-phonon interactions in a linear medium.
- Photon-phonon interactions are negligible

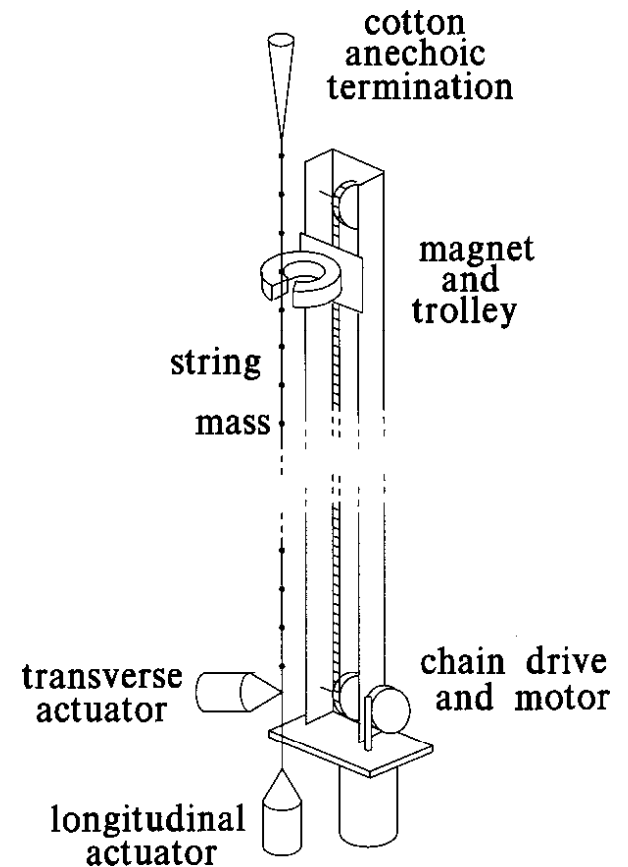
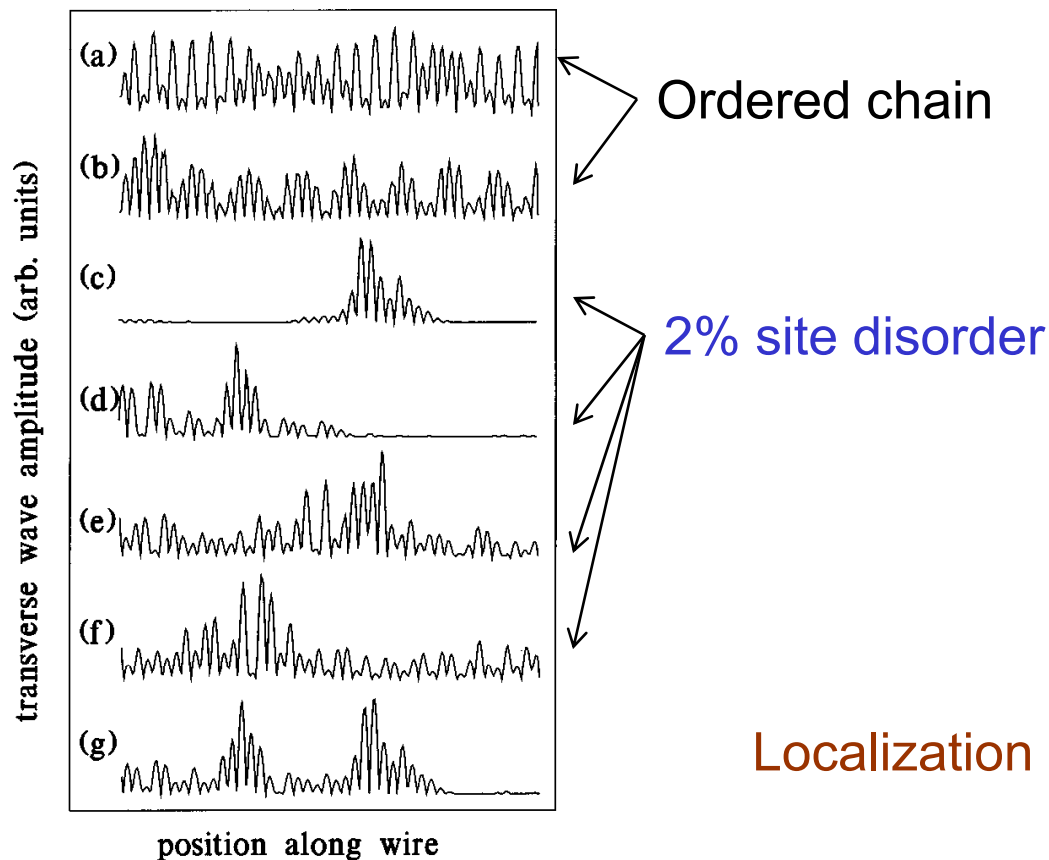
(but it is important to avoid complications due to absorption)

Previous acoustic experiments in 1D:

A disordered chain of masses and springs - measure the transverse displacements for different amounts of disorder
[He and Maynard, PRL, **57**, 3171]:

Diagonal disorder: vary the positions of the masses.

Off-diagonal disorder: vary the sizes of the masses.



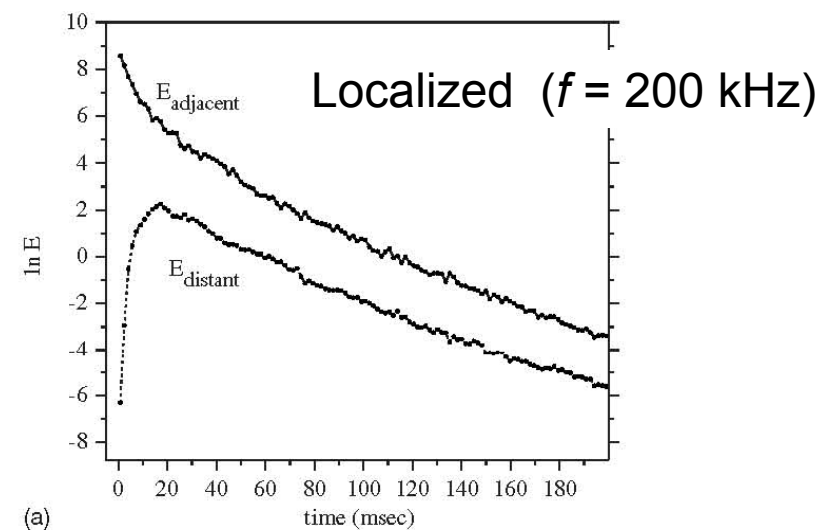
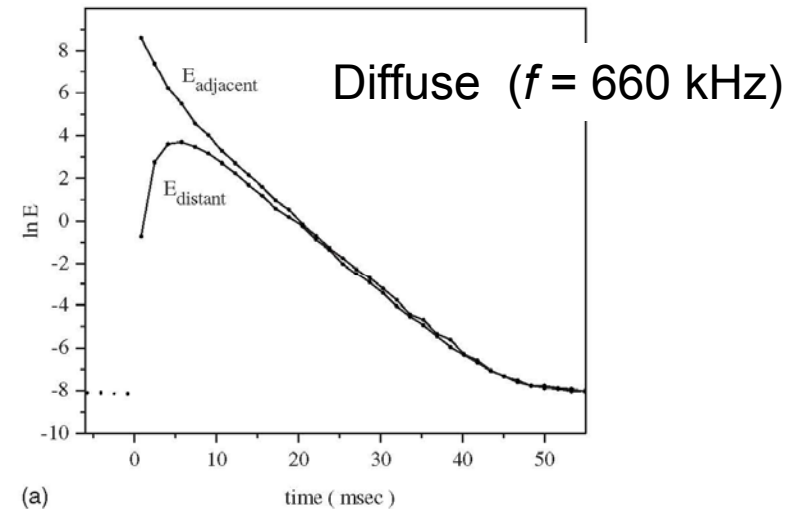
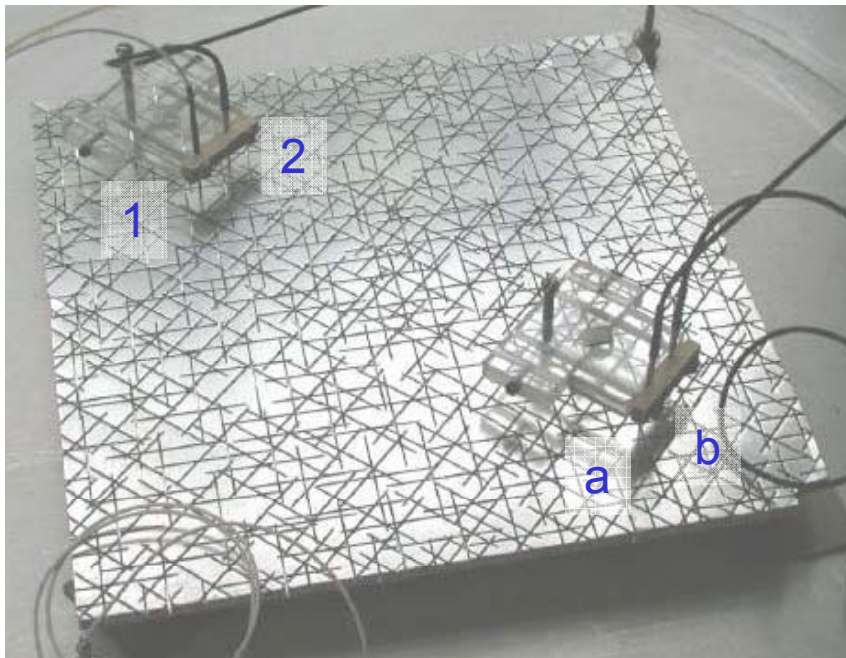
Localization is easy to observe in 1D!

Previous ultrasonic experiments in 2D:

Ultrasound in a disordered plate with random slots [Weaver, *Wave Motion*, **12**, 129-142(1990) ; Lobkis and Weaver, *J. Acoust. Soc. Am.* **124**, 3528 (2008)]:

Measure (with 4 small transducers):

$$R(r,t,f) = \frac{[E_{1b}E_{2a}E_{2b}E_{1a}]^{1/4}}{[E_{12}E_{ab}]^{1/2}} = \frac{E_{\text{distant}}}{E_{\text{adjacent}}}$$

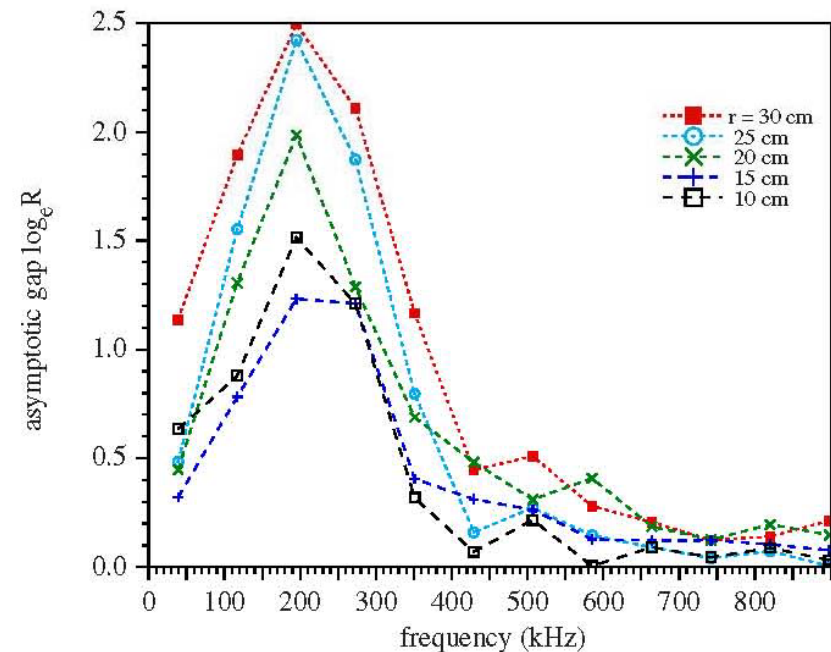
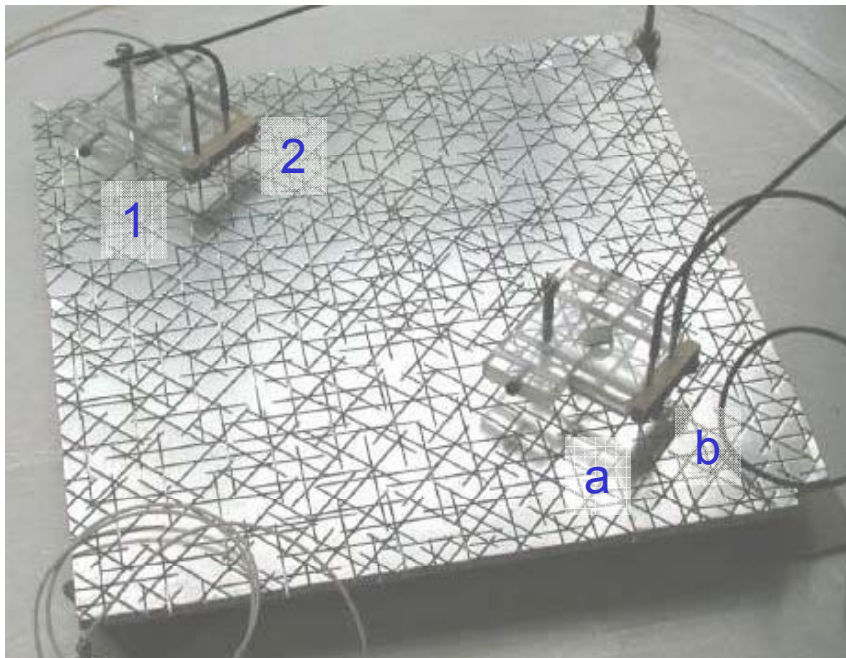


Previous ultrasonic experiments in 2D:

Ultrasound in a disordered plate with random slots [Weaver, *Wave Motion*, **12**, 129-142(1990) ; Lobkis and Weaver, *J. Acoust. Soc. Am.* **124**, 3528 (2008)]:

Measure (with 4 small transducers):

$$R(r,t,f) = \frac{[E_{1b}E_{2a}E_{2b}E_{1a}]^{1/4}}{[E_{12}E_{ab}]^{1/2}} = \frac{E_{\text{distant}}}{E_{\text{adjacent}}}$$

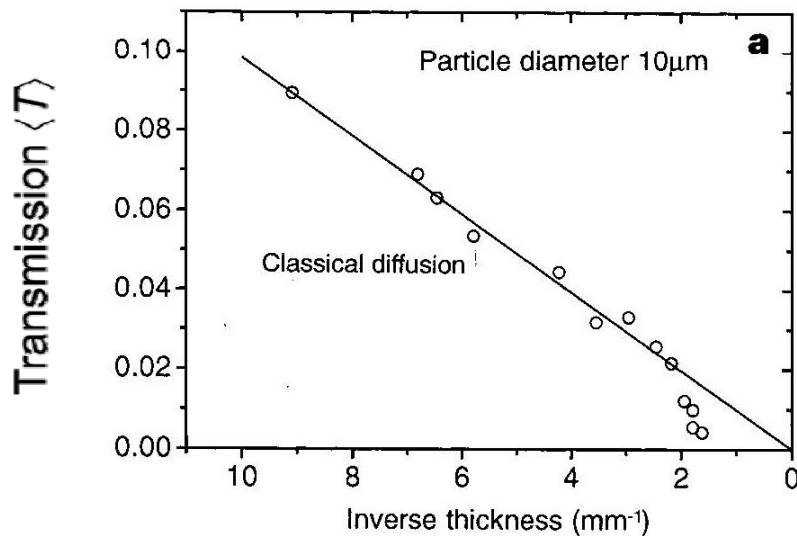


Anderson localization near 200 kHz

Localization length ~ 12 cm

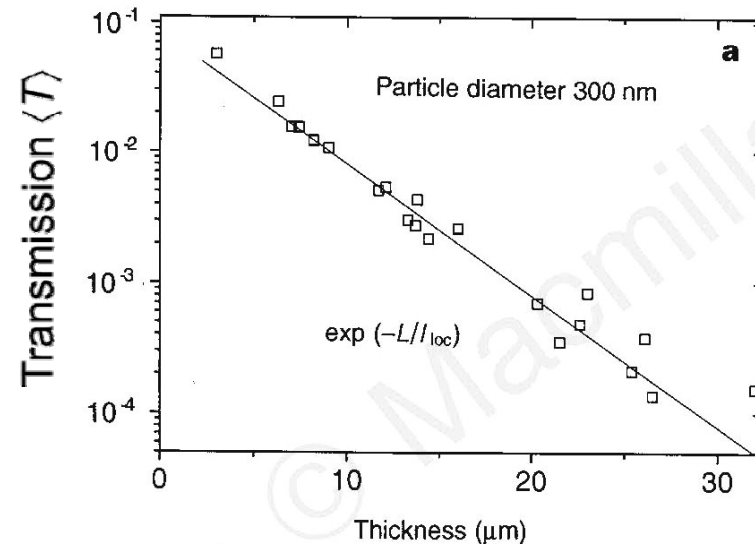
Previous experiments with light in 3D:

Exponential scaling of the average transmission (for monochromatic waves) with thickness L . [Wiersma *et al.*, *Nature* **390**, 671 (1997)]



Diffuse regime:

$$\langle T \rangle \propto \frac{l^*}{L}$$



Localized regime

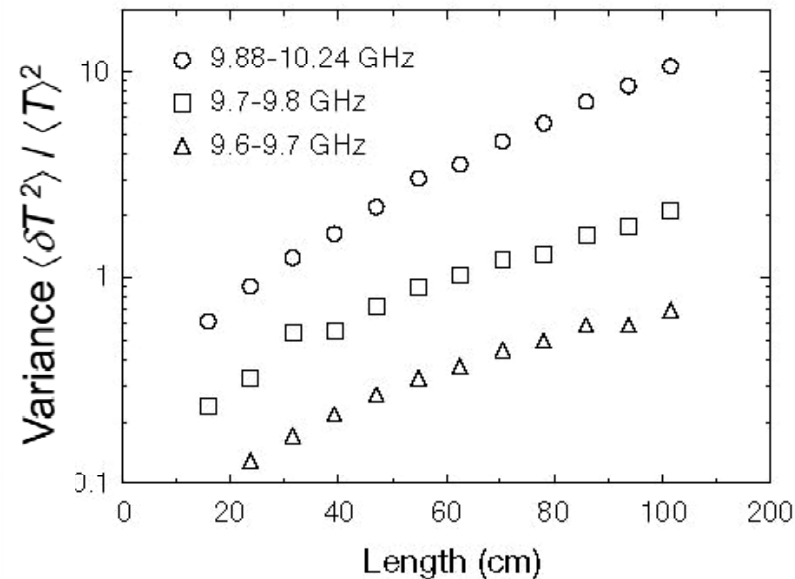
$$\langle T \rangle \propto \exp\left[-\frac{L}{\xi}\right]$$

- Difficult to distinguish from effects of absorption ($\propto \exp[-L/\ell_a]$)

Previous experiments with microwaves in quasi-1D:

Enhanced fluctuations of total transmission.

[Chabanov *et al.*, *Nature* **404**, 850 (2000)]



Diffuse regime:

$$\frac{\langle \delta T^2 \rangle}{\langle T \rangle^2} \ll 1$$

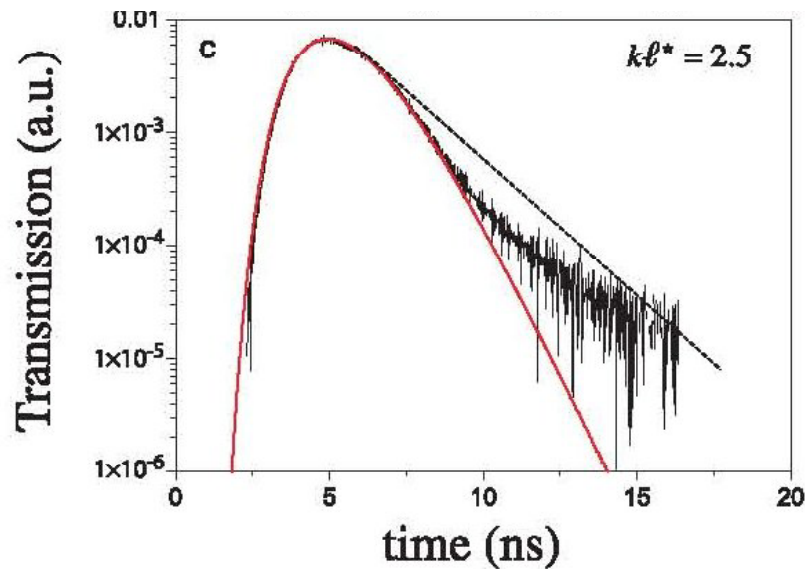
Localized regime

$$\frac{\langle \delta T^2 \rangle}{\langle T \rangle^2} > \text{const} \sim 1$$

- Chabanov *et al.* proposed that this criterion for localization is independent of absorption, but their experiments were limited to quasi-1-dimensional samples.

More recent experiments with light in 3D:

Time-dependent transmission through thick samples of TiO_2 particles
[Störzer et al., *PRL* **96**, 063904 (2006)]



Non-exponential tail at long times:
interpreted as a slowing down of diffusion with propagation time due to localization.

Current status (~50 years after Anderson's discovery):

- The subject is more alive than ever!
- Activity in optics, microwaves, acoustics, seismic waves, and atomic matter waves.

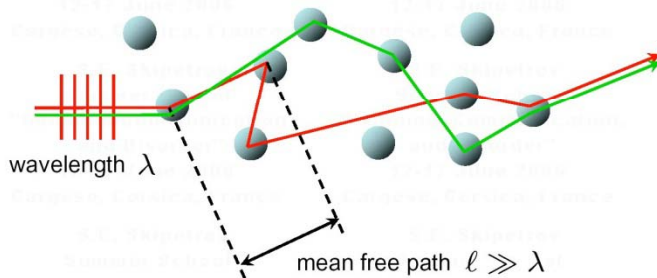
Question: Can we convincingly observe the localization of ultrasound due to disorder in 3D, and, if so, can we learn something new?

N.B.: Scaling theory \Rightarrow Only in 3D is there a real transition from **extended** to **localized** modes (*i.e.*, a mobility edge) ; unambiguous evidence has been elusive.

Weak disorder ($k\ell \gg 1$):

Diffuse propagation

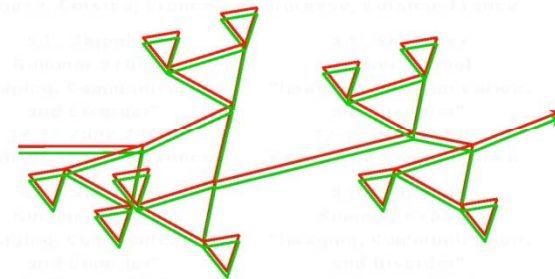
$D_B = \frac{1}{3} v_E \ell_B^*$ (neglect interference)



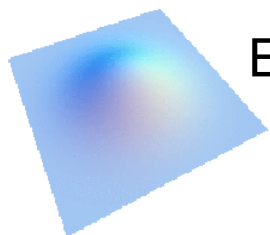
Strong disorder ($k\ell \sim 1$):

Anderson localization

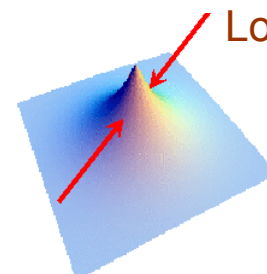
(interference is important!)



e.g., After a short pulse of ultrasound is incident on the medium...



Energy density spreads diffusively from the source



Localization length ξ

Energy remains localized the vicinity of the source

Our samples: “Mesoglasses” fabricated by brazing aluminum beads together to form a solid porous **3D elastic network**.

- good control of elastic coupling between beads
- low intrinsic absorption.

Aluminum volume fraction: $\phi = 0.55$

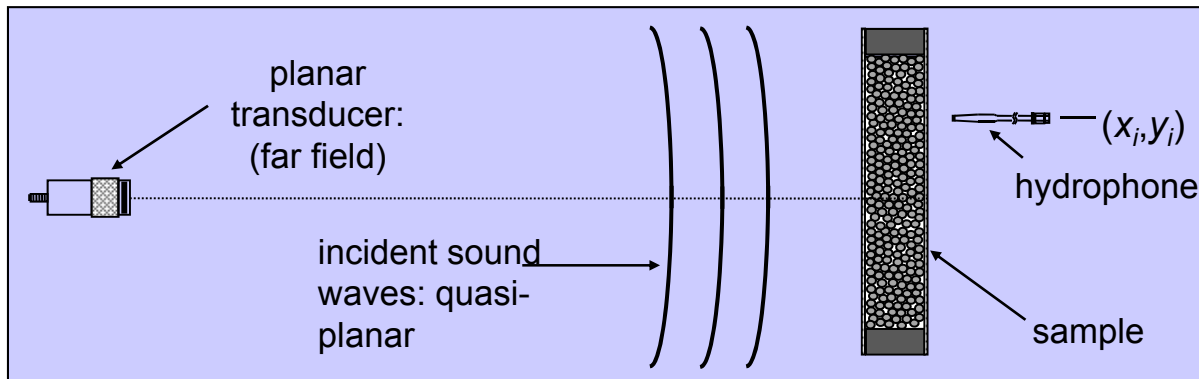
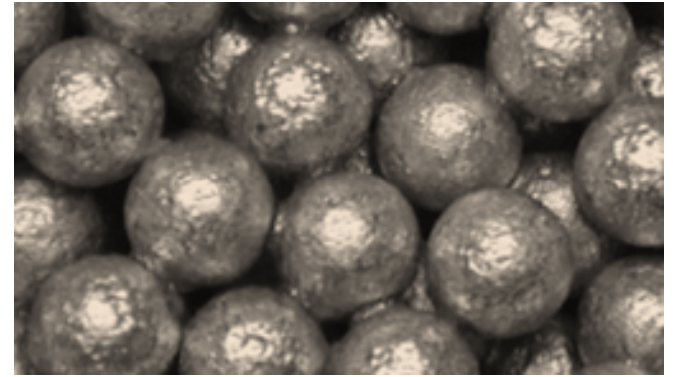
Monodisperse beads:

radius, $a_{\text{bead}} = 2.05 \text{ mm}$

Sample width \gg thickness (L : 8 to 23 mm)

Pulsed ultrasonic transmission measurements
(waterproofed samples, in a water tank)

Frequency range: 0.1 to 3 MHz ($6 \geq \lambda/a \geq 1$)



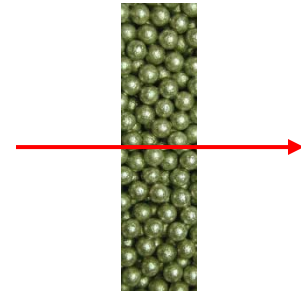
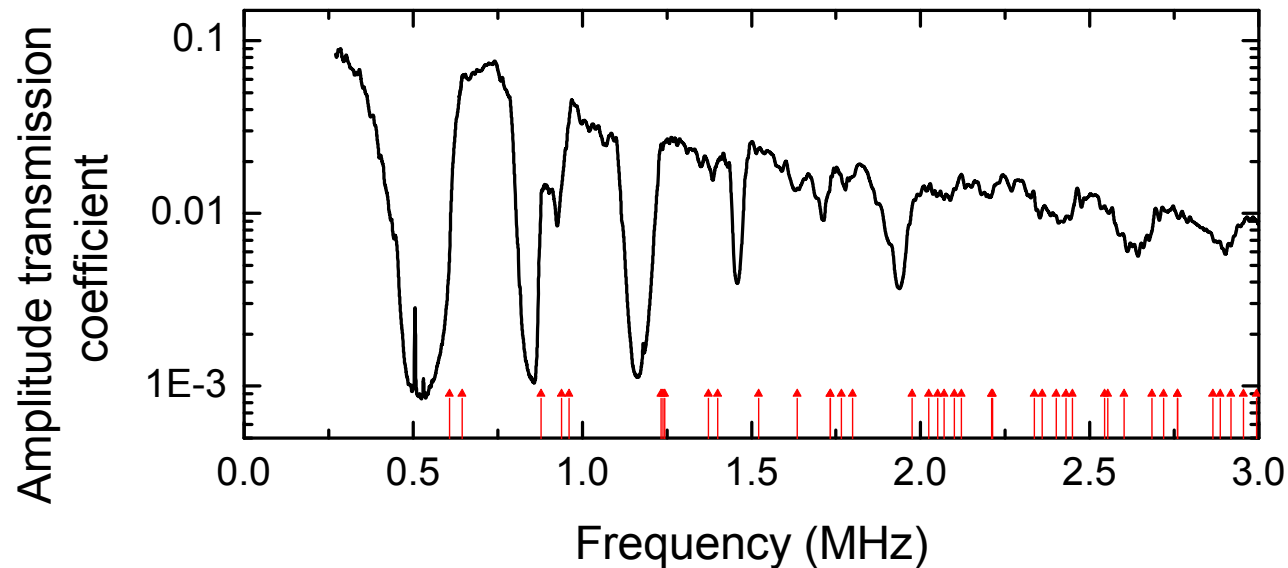
Coherent transport in disordered Al mesostructures:

Ballistic transport: Average the transmitted field to recover the weak coherent pulse and measure :

- phase velocity: $v_p = \omega/k$
- group velocity: $v_g = d\omega/dk$
- scattering mean free path, ℓ : $I = I_0 \exp[-L / \ell]$

Amplitude transmission coefficient:

Bandgaps arise from weakly coupled resonances of the aluminum beads (Turner & Weaver, 1998)



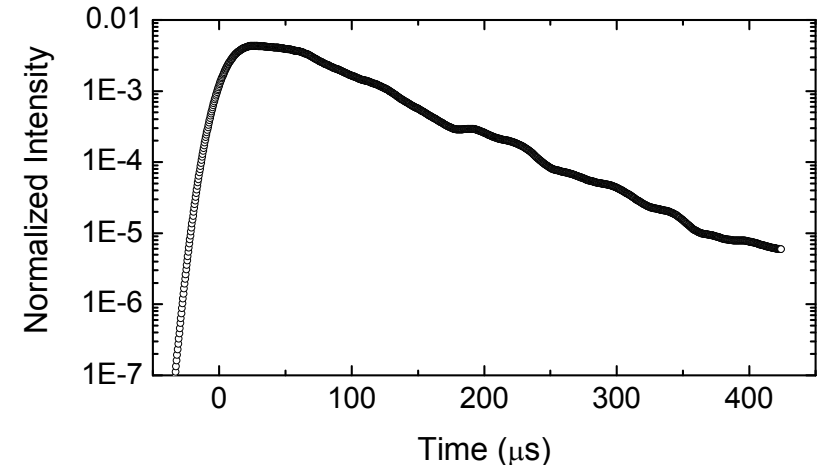
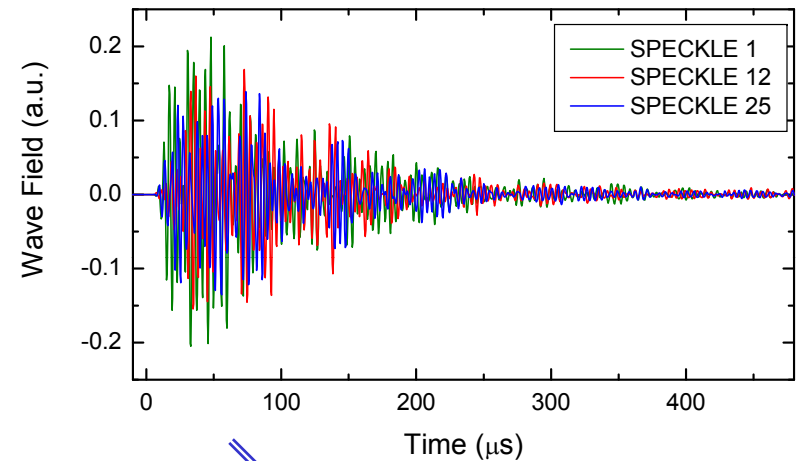
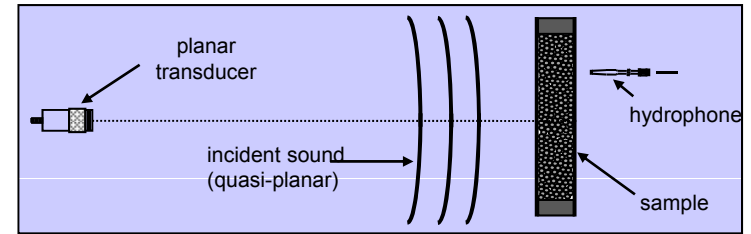
Very strong scattering in the intermediate frequency regime (0.2 – 3 MHz) :

$$1 \leq k\ell \leq 2.5$$

(outside the bandgaps)

II. Time-dependent transmission, $I(t)$.

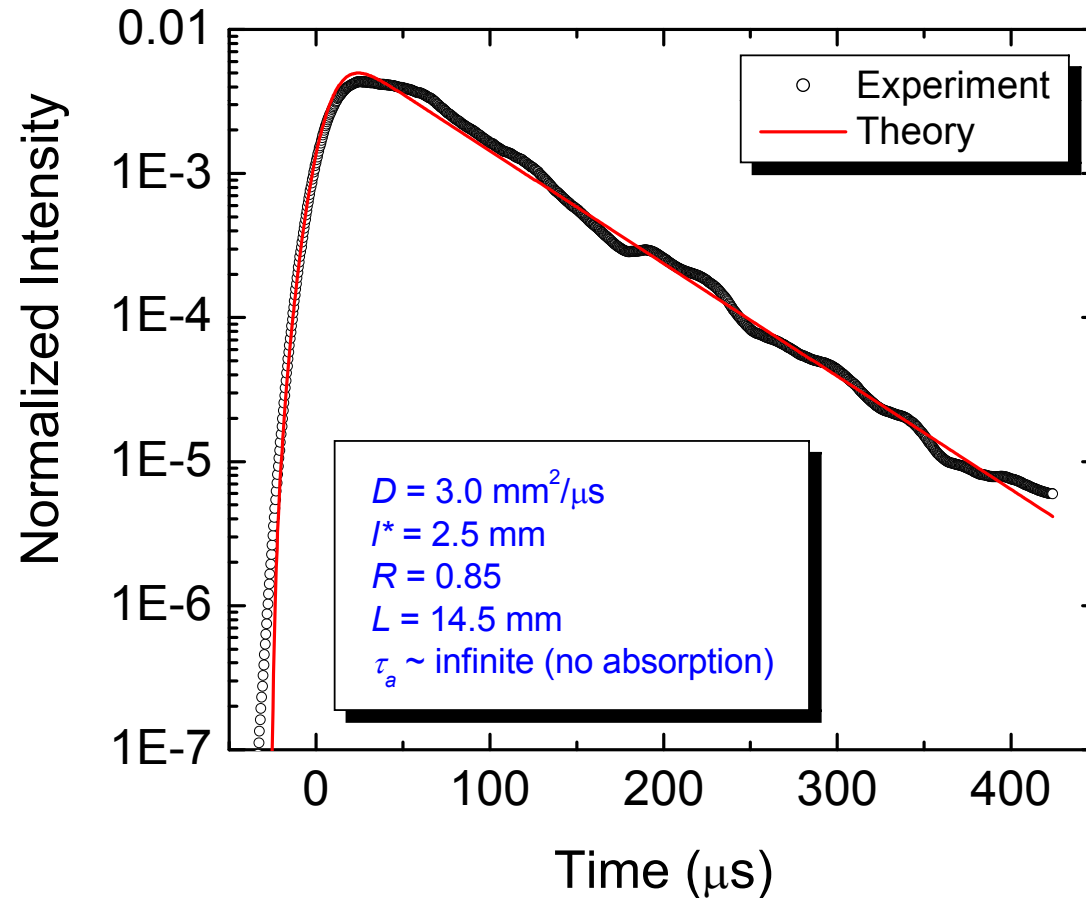
- Measure multiply scattered field in many independent speckles by scanning the hydrophone.
- Digitally filter the field to limit bandwidth (~5% usually)
- Determine $I(t)$ by averaging the squared transmitted pulse envelopes. (Normalize by the peak of the input pulse)
- First compare with the diffusion model, using realistic boundary conditions (e.g. see Page *et al.*, Phys. Rev. E **52**, 3106 (1995) for ultrasonic waves)
[z_0 - extrapolation length; z' - penetration depth; τ_a - absorption time]
- For elastic media, the diffusion coefficient $D_B = \frac{1}{3} v_E \ell^*$ is the energy-density weighted average of longitudinal and transverse waves.



Time-dependent transmission at low frequencies:
(below the lowest band gap)

Good fit to the predictions of the diffusion approximation for a plane wave source \Rightarrow measure D . (Absorption is too small to measure.)

$f = 0.2$ MHz:



$I(t)$ decays exponentially at long times

$$I(t) \sim \exp[-t/\tau_D]$$

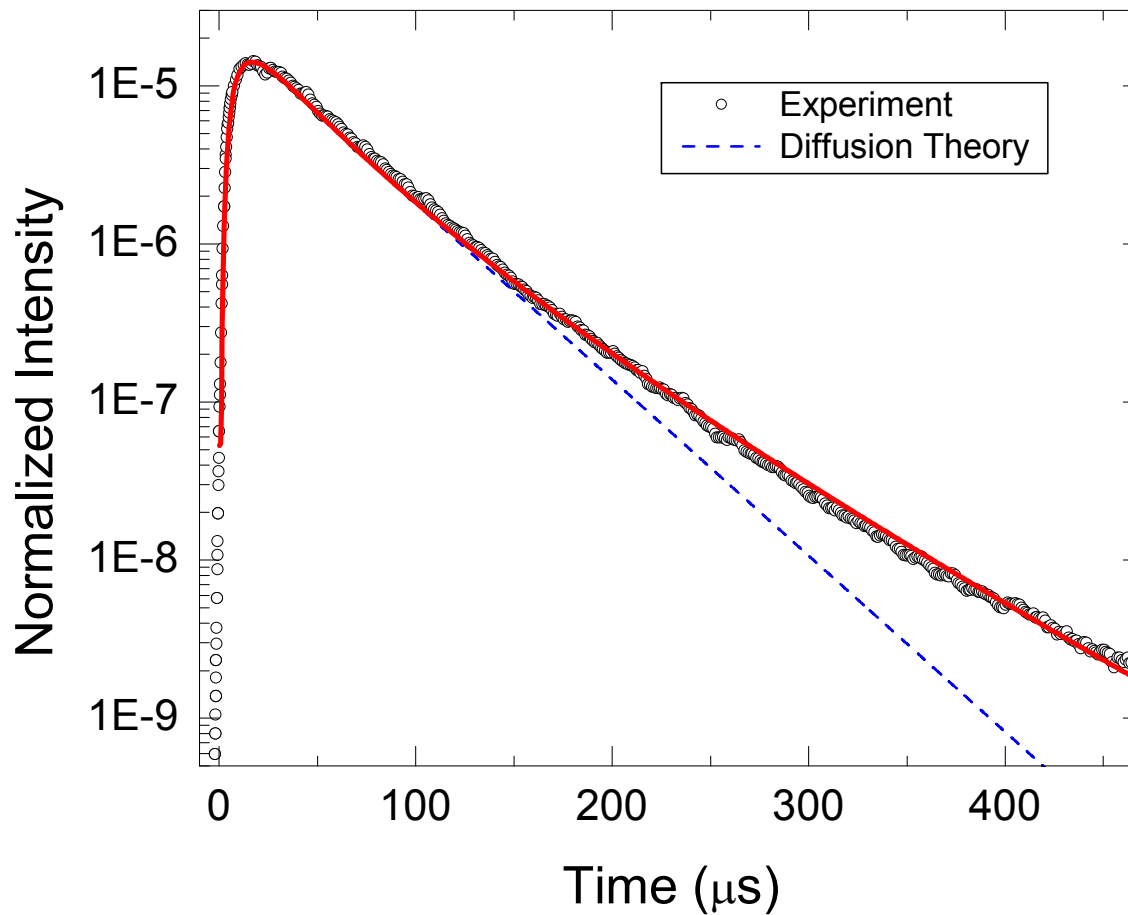
with

$$\tau_D = (L + 2z_0)^2 / \pi^2 D_B$$

Normal diffusive behaviour

$I(t)$ at higher frequencies (e.g. 2.4 MHz)

Find non-exponential decay of $I(t)$ at long times ($t \gg \tau_D$) \Rightarrow Looks like a diffusion process with $D(t)$ decreasing with propagation time.



Suggests that sound may be **localized**

Quantitative analysis of $I(t)$ at high frequencies (2.4 MHz)

– fit the (plane wave) data directly with the recently improved self-consistent theory of localization [Skipetrov & van Tiggelen (2006)]

Basic idea:

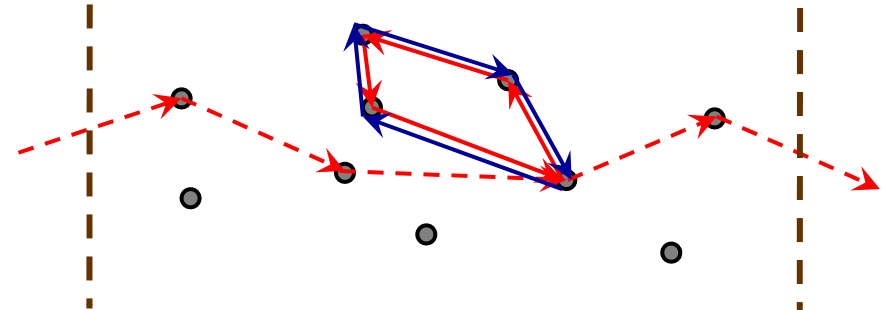
The presence of loops increases the return probability as compared to 'normal' diffusion



Diffusion slows down



Diffusion constant should be renormalized



$$D_B \rightarrow D < D_B$$

Generalization to Open Media:

Loops are less probable near the boundaries



Slowing down of diffusion is spatially heterogeneous



Diffusion constant becomes position-dependent

$$D_B \rightarrow D(\mathbf{r}) < D_B$$

Quantitative analysis of $I(t)$ at high frequencies (2.4 MHz)

– fit the (plane wave) data directly with the recently improved self-consistent theory of localization [Skipetrov & van Tiggelen (2006)]

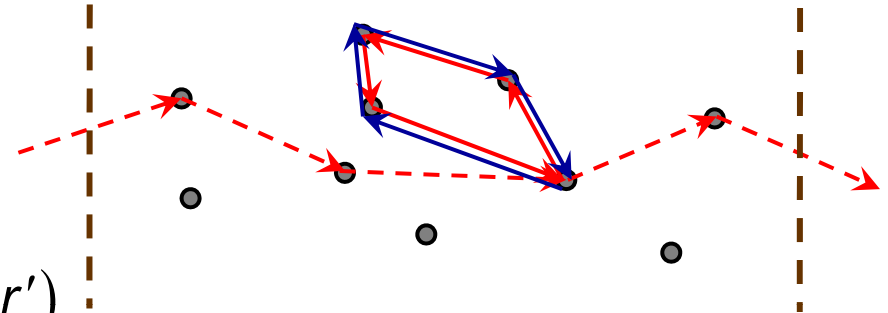
Mathematical formulation:

Diffusion equation

$$\left[-i\Omega - \nabla \cdot D(r, \Omega) \nabla \right] G(r, r', \Omega) = \delta(r - r')$$

+

($G(r, r', \Omega)$ – Intensity Green's function)



Self-consistent equation for the diffusion coefficient

$$\frac{1}{D(r, \Omega)} = \frac{1}{D_B} + \frac{3}{\pi \rho(\omega) D_B} G(r, r' = r, \Omega)$$

+

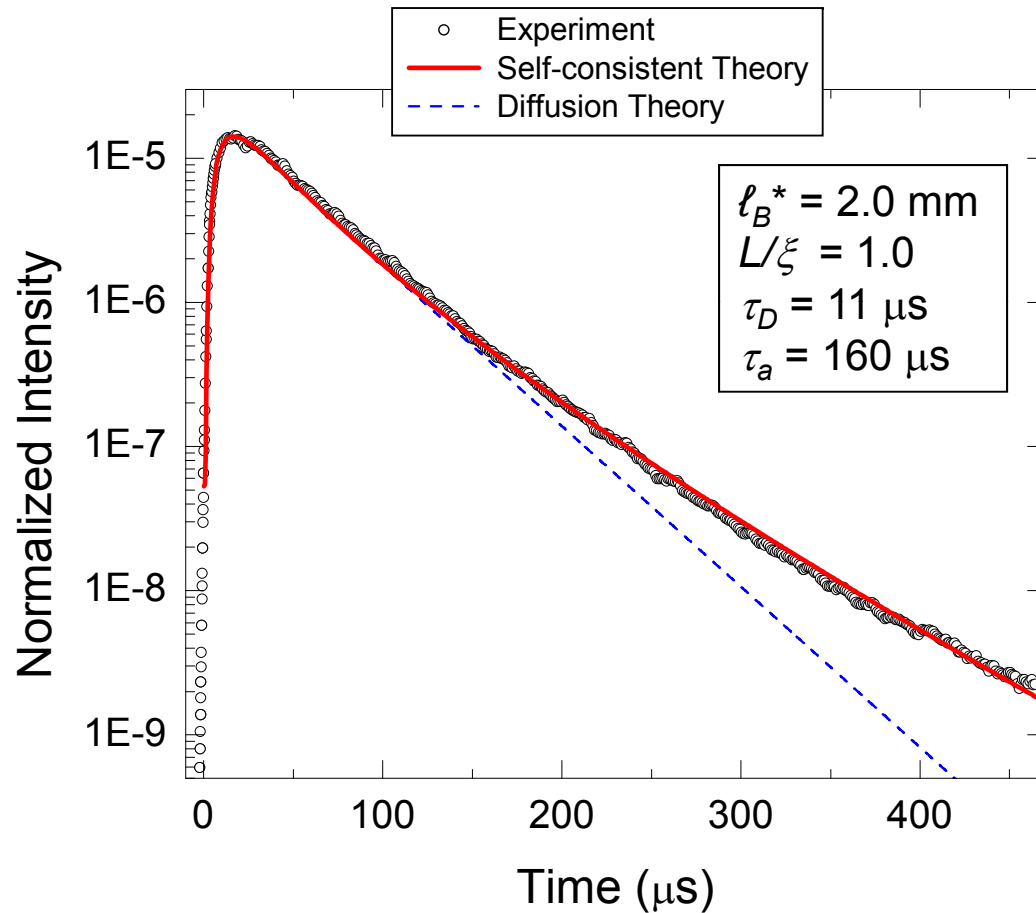
($\rho(\omega)$ – density of states)

Boundary conditions

$$G(r, r', \Omega) - z_0 \frac{D(r, \Omega)}{D_B} (\mathbf{n} \cdot \nabla G(r, r', \Omega)) = 0$$

Diffusion coefficient depends on position \mathbf{r} and frequency Ω

Quantitative analysis of $I(t)$ at high frequencies (2.4 MHz)
– fit the (plane wave) data directly with predictions of the self
consistent theory of localization for $D(r,\Omega)$ [Skipetrov & van Tiggelen (2006)]



Input parameters:

$L = 14.5 \text{ mm}$ (sample thickness)

$\ell = 0.6 \text{ mm}$ (scattering mean free path)

$R = 0.82$ (internal reflection coeff.)

$z_0 = \ell_B^* \sqrt[2]{3} (1+R)/(1-R) = 6.7 \ell_B^*$

$v_p = 5.0 \text{ km/s}$ (phase velocity)

$k\ell = 1.82$

Fitted parameters:

ℓ_B^* (“bare” transport mean free path)

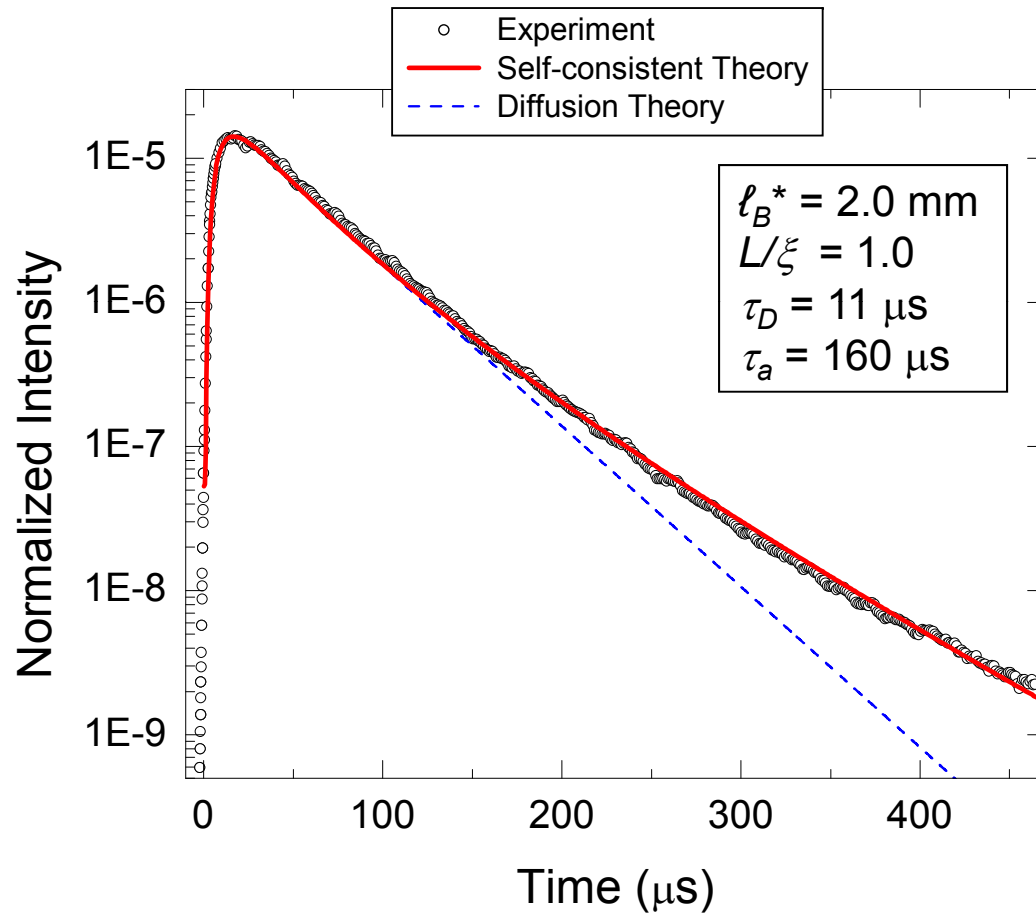
L/ξ (ξ is the localization length)

τ_D or D_B (bare diffusion coefficient)

τ_a (absorption time)

Excellent fit at all propagation times.

Quantitative analysis of $I(t)$ at high frequencies (2.4 MHz)
 – fit the (plane wave) data directly with predictions of the self
 consistent theory of localization for $D(r, \Omega)$ [Skipetrov & van Tiggelen (2006)]



Localization length ξ :

$$\frac{\xi}{l_B^*} = \left[\frac{6}{(k l_B^*)_c^2} \right] \frac{\chi^2}{1 - \chi^4}$$

where $\chi = kl / (kl)_c$

Localization regime:

$$\xi > 0, \quad kl < (kl)_c$$

Diffuse regime:

$$\xi < 0, \quad kl > (kl)_c$$

Excellent fit at all propagation times with $\xi > 0$ ($L > \xi > L/4$)

⇒ Strong (but indirect) evidence for the localization of sound

Self consistent theory of localization predicts **a strong and rapid renormalization of D in our samples:**

$$\frac{1}{D(\Omega, r)} = \frac{1}{D_B} + \beta G(r, r' = r, \Omega)$$

where $\beta = 3/\pi\rho(\omega)D_B$,
 $\rho(\omega) = \text{D.O.S.}$

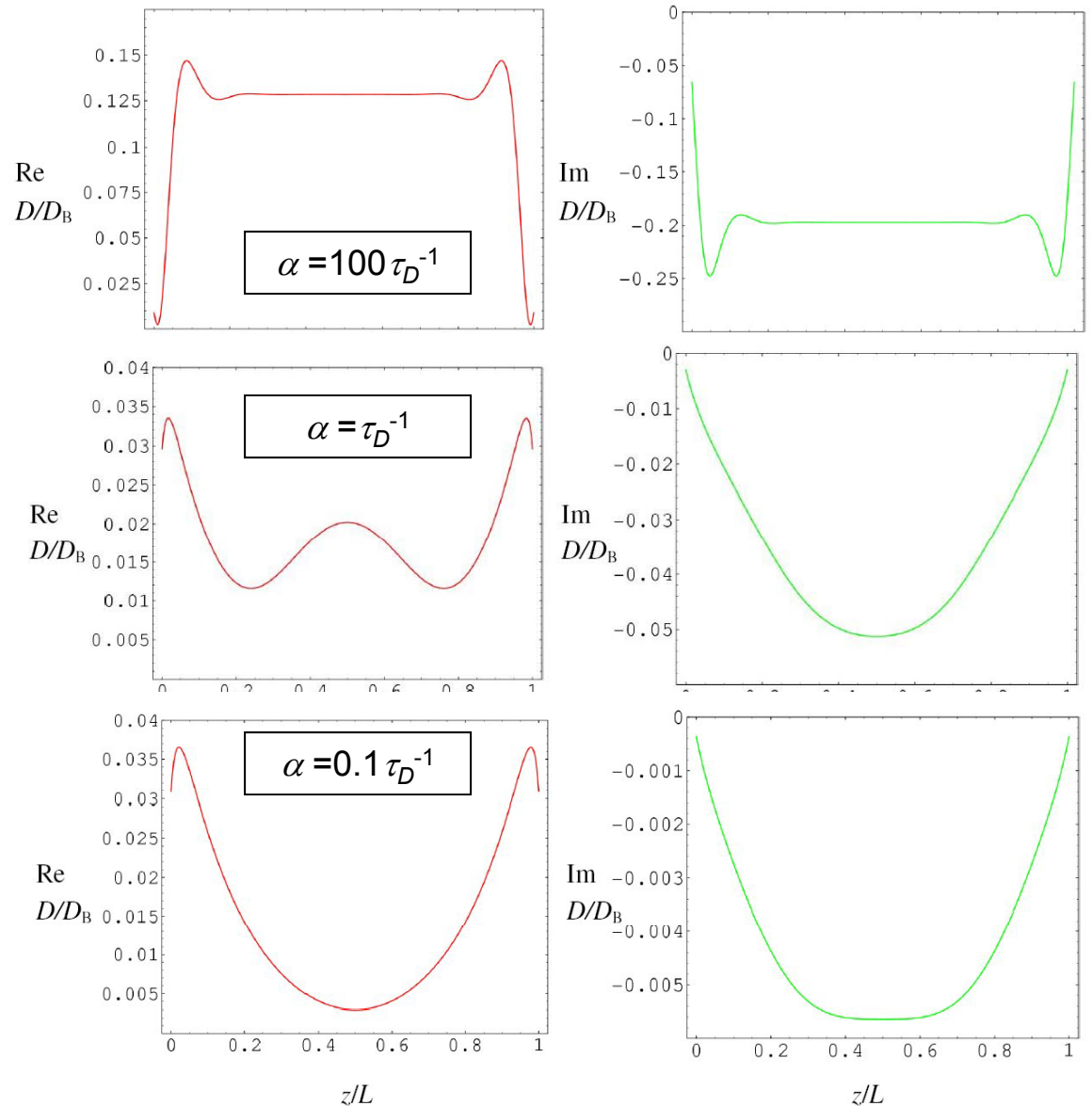
$\Rightarrow D_B$ cannot be measured directly, even for $t < \tau_D$.

($D(\Omega, z)/D_B \ll 1$ for all accessible t).

\Rightarrow Best fits have: surprising large D_B (and hence large v_E)

Question: Can this be explained by a reduced density of states (D.O.S.)?

Typical curves $D(\Omega = -i\alpha + \varepsilon, z)$



Density of states – direct measurements!

- Unusual behaviour below the first bandgap (~ constant).
- For $f > 0.6$ MHz, average DOS is consistent with standard predictions:

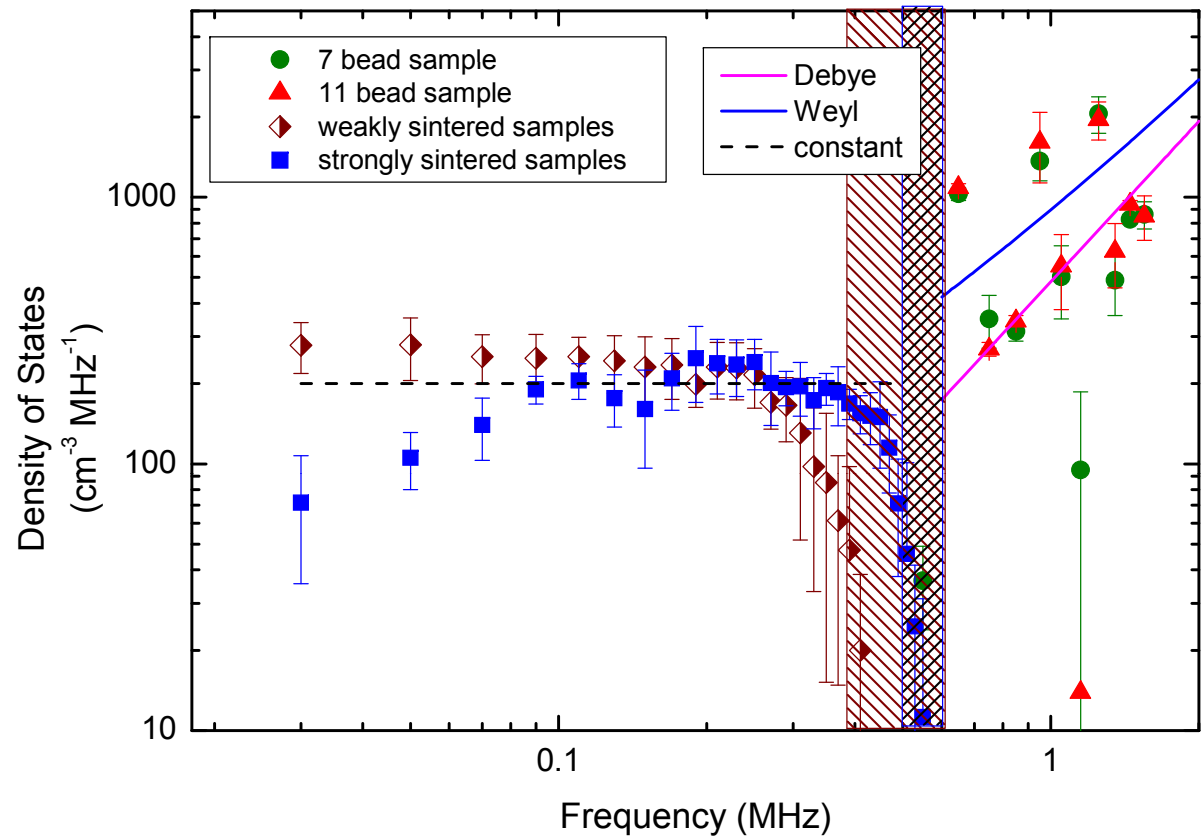
Debye:

$$\frac{D(f)}{V} = \phi \frac{12\pi f^2}{\bar{V}^3}$$

Weyl (includes surface modes)

$$D(f) = n \left\{ \frac{12\pi V_{\text{sphere}}}{\bar{V}^3} f^2 + \frac{\pi S_{\text{sphere}}}{2} \frac{2 - 3(v_L / v_T)^2 + 3(v_L / v_T)^4}{v_L^2 [(v_L / v_T)^2 - 1]} f \right\}$$

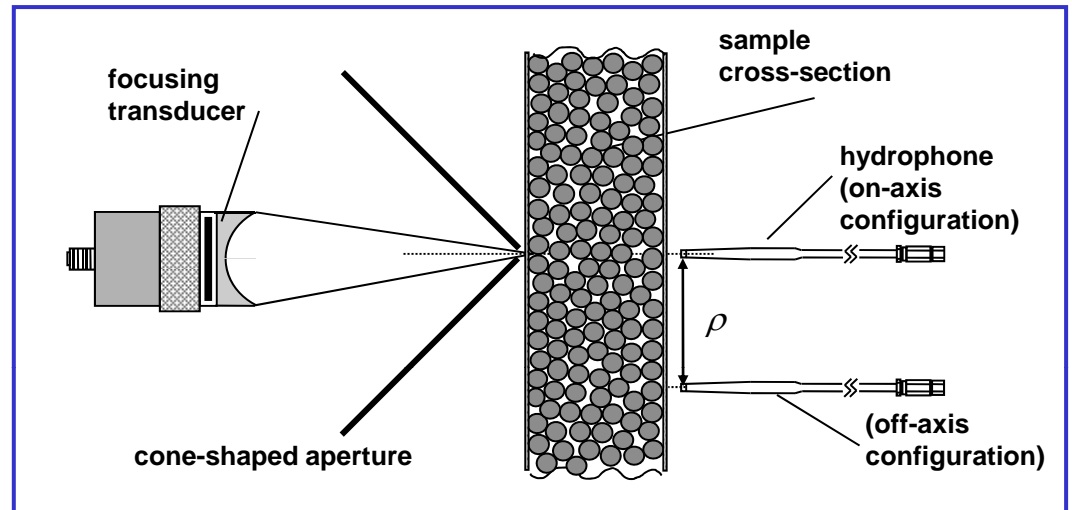
Conclude: Large values found for v_E cannot be explained by anomalously low DOS (due to short range correlations or bandgap effects)



III. Transverse confinement (“transverse localization in 3D”)

Experiment (displaced point source technique):

- Point source (focusing transducer + small aperture)
- Point detector, placed a transverse distance ρ away
- Scan x - y position of the sample to determine $I(\rho, t)$.



The ratio $I(\rho, t)/I(0, t)$ probes the transverse growth (dynamic spreading) of the intensity profile.

- Diffuse regime – measure the effective width of the “diffuse halo”, which provides a method of measuring D independent of boundary conditions and absorption. [Page *et al.*, Phys. Rev. E **52**, 3106 (1995)]

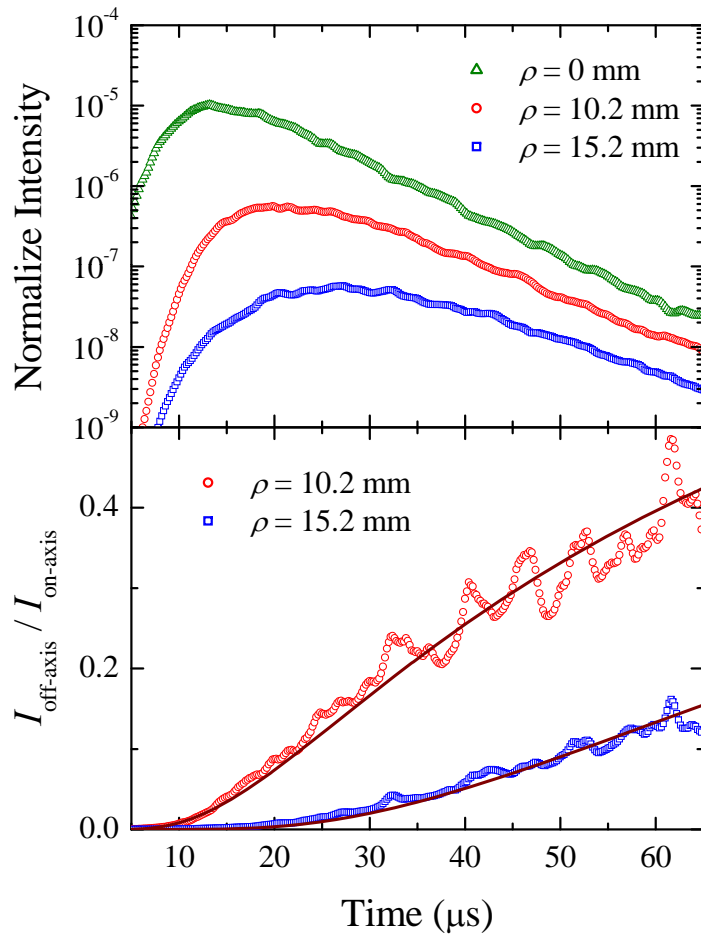
$$\frac{I(\rho, t)}{I(0, t)} = \exp\left[-\rho^2/4Dt\right] \equiv \exp\left[-\rho^2/w^2(t)\right]$$

so the effective width $w(t)$ is

$$w^2(t) = -\frac{\rho^2}{\ln[I(\rho, t)/I(0, t)]} = 4Dt$$

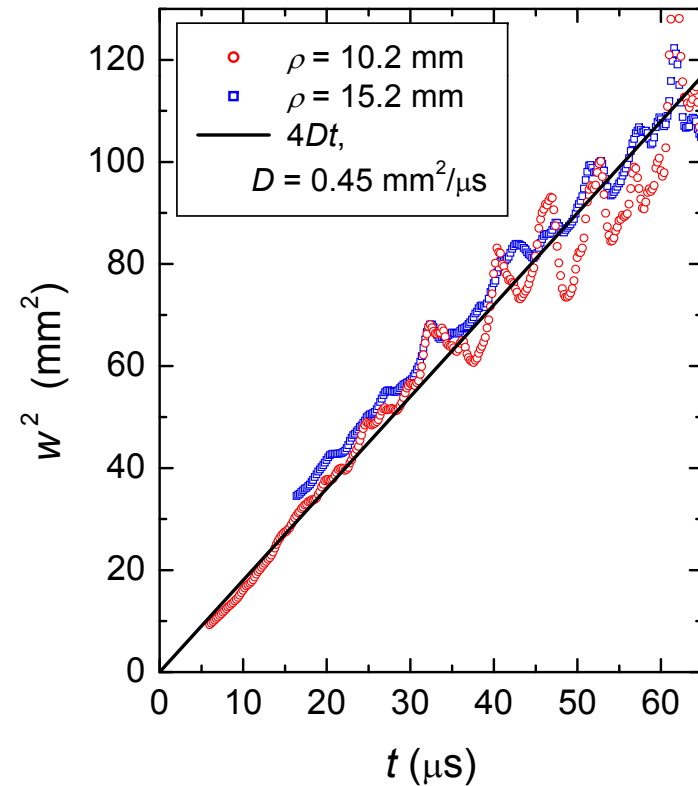
Diffuse regime –the effective width of the “diffuse halo” grows linearly in time

Data (from 1995) on a suspension of glass beads in water ($k\ell \sim 7$)
 [Page *et al.*, Phys. Rev. E **52**, 3106 (1995)]



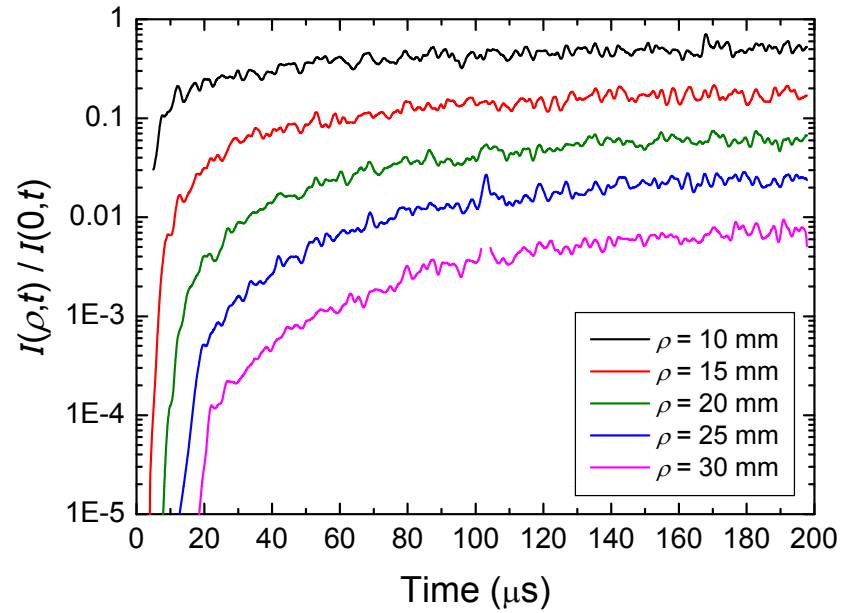
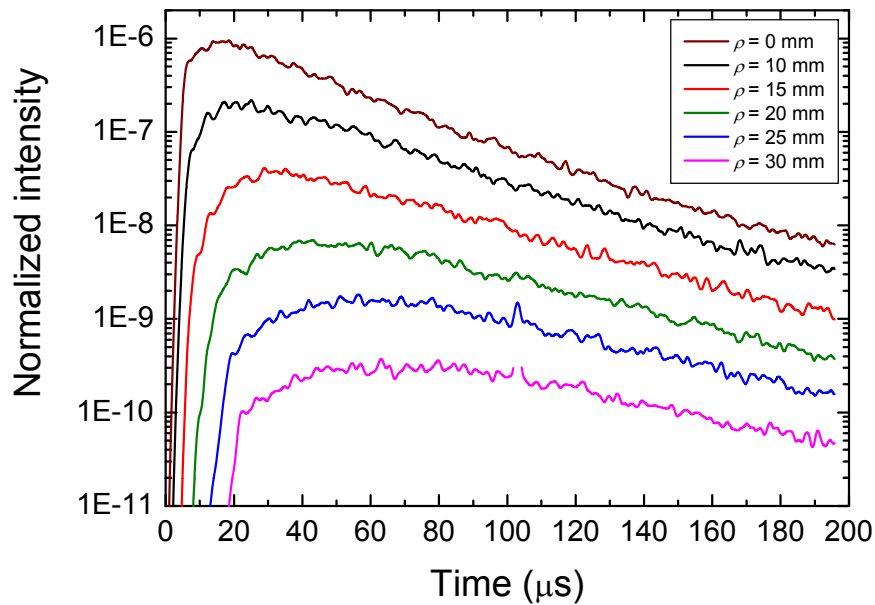
$$\frac{I(\rho, t)}{I(0, t)} = \exp\left[-\rho^2 / 4Dt\right] \equiv \exp\left[-\rho^2 / w^2(t)\right]$$

$$w^2(t) = -\frac{\rho^2}{\ln[I(\rho, t)/I(0, t)]} = 4Dt$$



Measure D_B independent of boundary conditions and absorption.

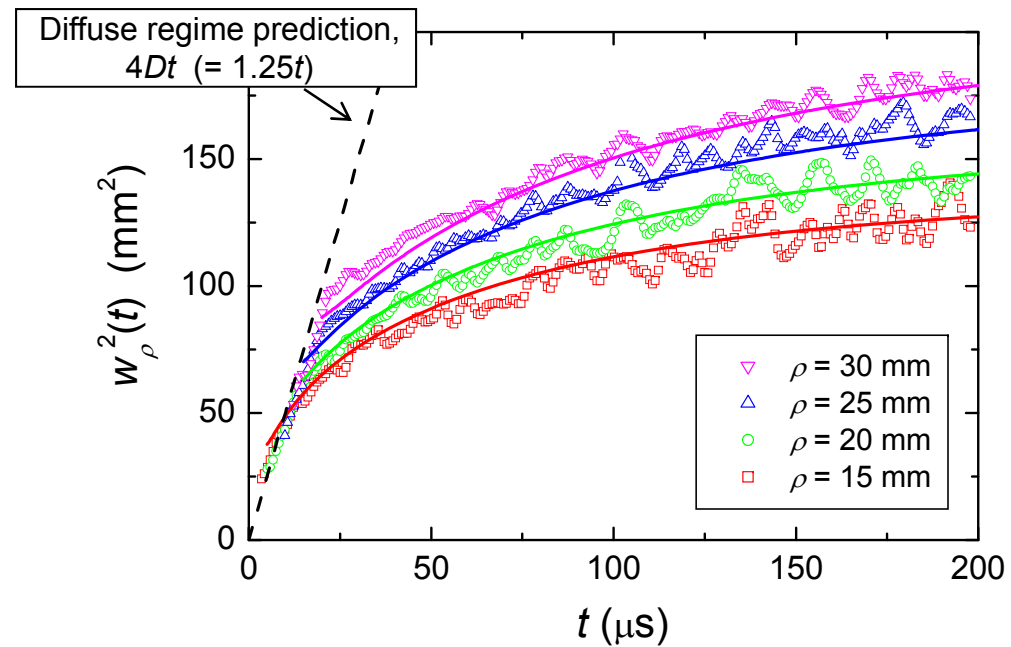
Question: What happens to $I(\rho, t)$ & $w(t)$ in the localization regime?



Dynamic transverse width at 2.4 MHz:

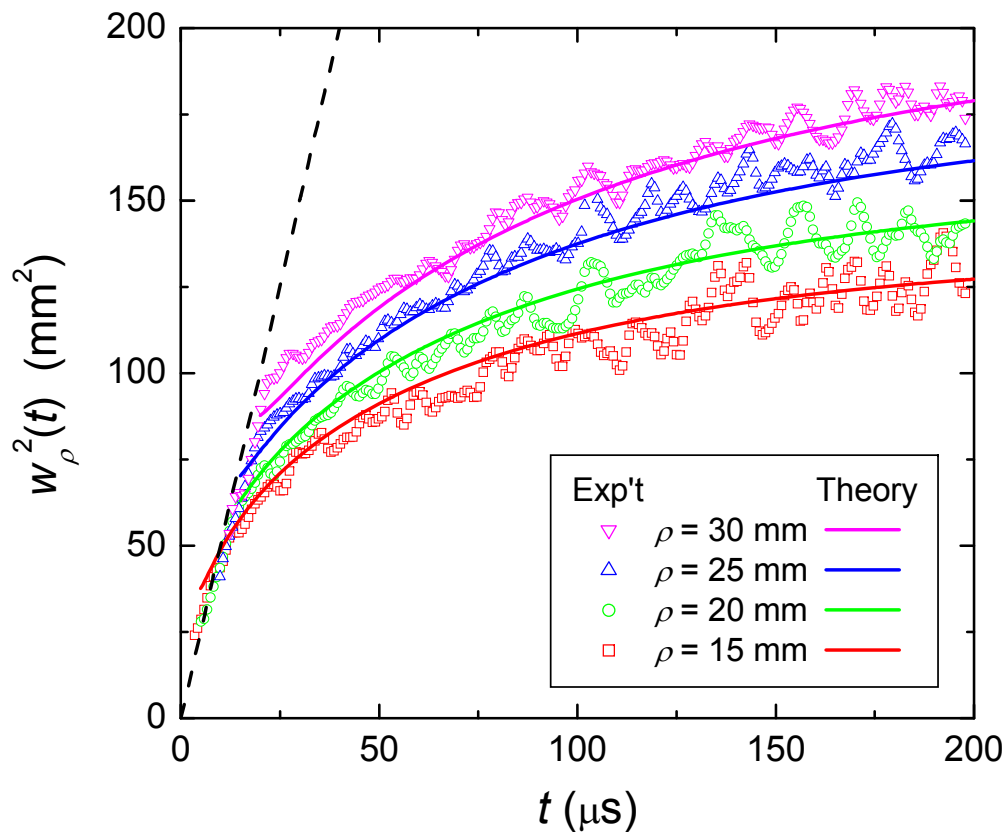
Localization dramatically inhibits the expansion of the intensity profile in the transverse direction.

$$\frac{I(\rho, t)}{I(0, t)} = \exp\left[-\rho^2 / w^2(t)\right]$$



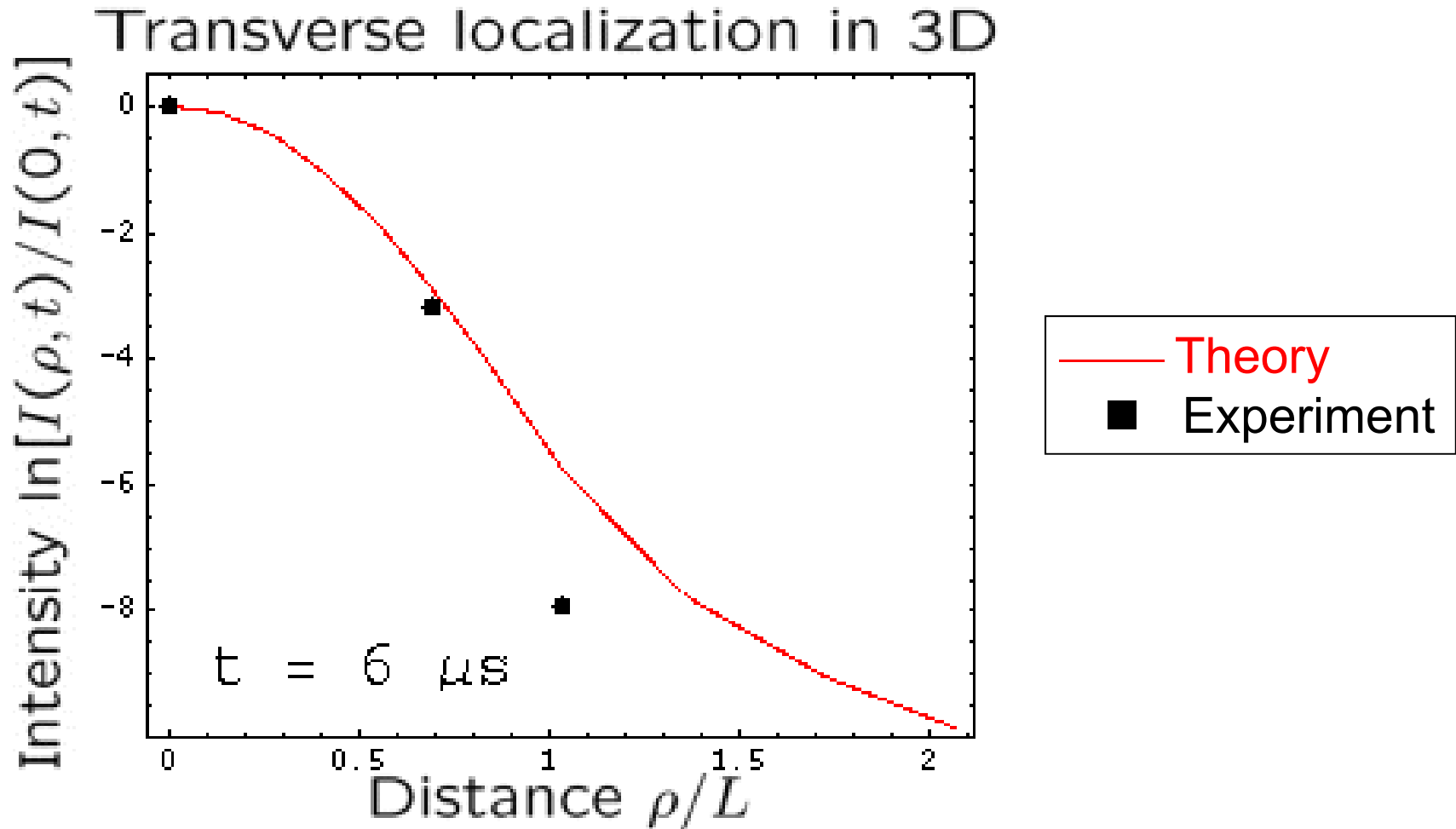
Quantitative analysis of the dynamic transverse width, $w(t)$:

- Fit the data using the new self consistent theory that allows for the position dependence of the renormalized diffusion coefficient in 3D.



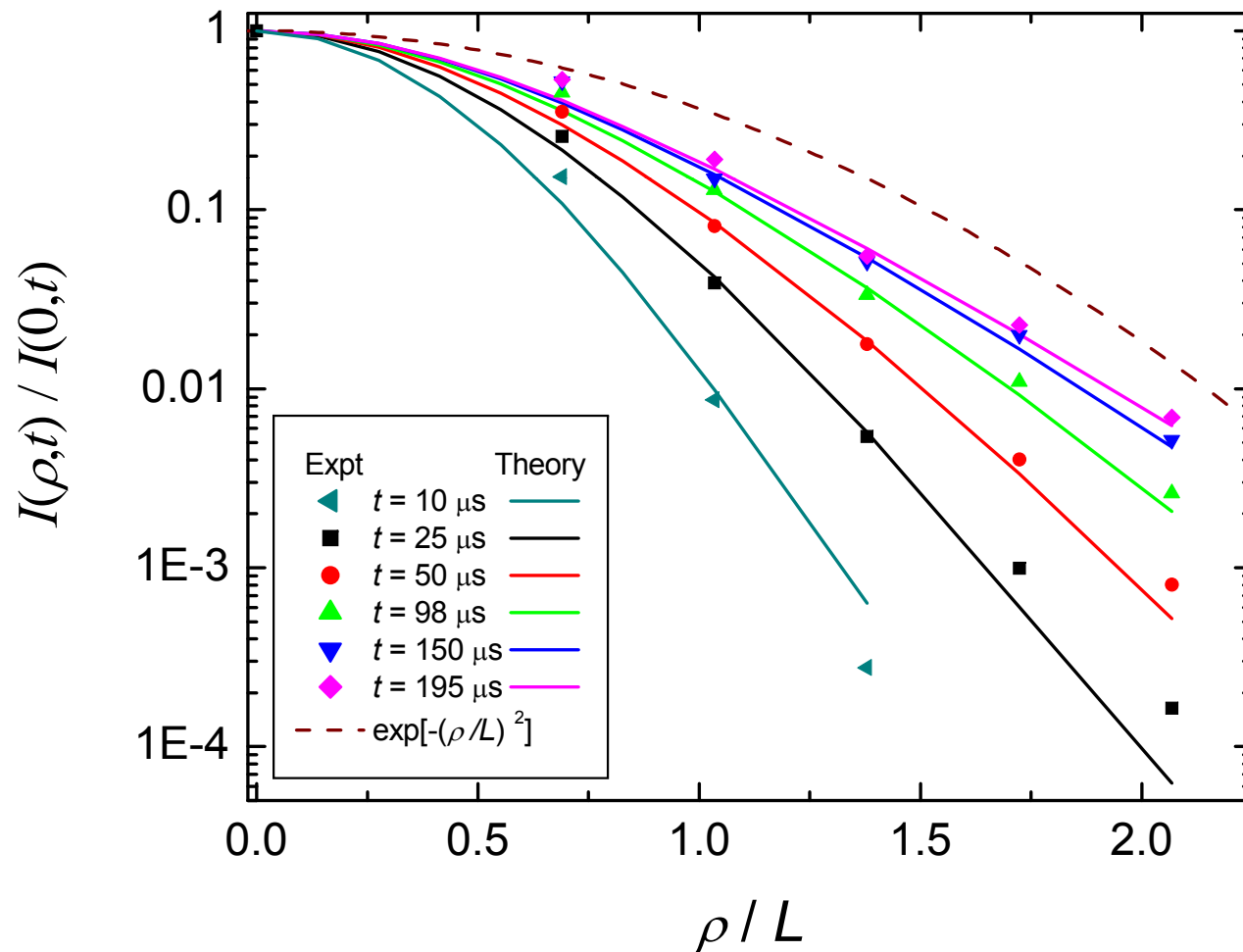
- Excellent fit for all four ρ with:
 - $l_B^* = 2.0$ mm
 - $L/\xi = 1.0$
 - $\tau_D = 17$ μ s
 - (τ_a cancels in ratio)
- Fit is more sensitive to ξ than plane wave $l(t)$
- Again, find $\xi > 0 \Rightarrow$ classical wave localization is convincingly demonstrated in this 3D “phononic” mesoglass.
- First direct measurement and theory for the transverse structure of localized waves in 3D. Find $w \sim 12-14$ mm $\sim \xi$ for this sample

3D Transverse Localization: this animation (prepared by Sergey Skipetrov) shows the “freezing” of the transverse profile at long times (saturation of $I(\rho,t)/I(\rho,0)$ occurs for $t > t_{\text{loc}} \sim 100 \mu\text{s}$ in this case.)



Decrease of $I(\rho, t)$ with transverse distance ρ is not Gaussian
 \Rightarrow Near the mobility edge ($k\ell / (k\ell)_c = 0.99$ for this sample at this frequency), w varies somewhat with transverse displacement ρ .

The self-consistent theory (solid curves) captures the experimentally observed dependence of $w(t)$ on ρ very well.

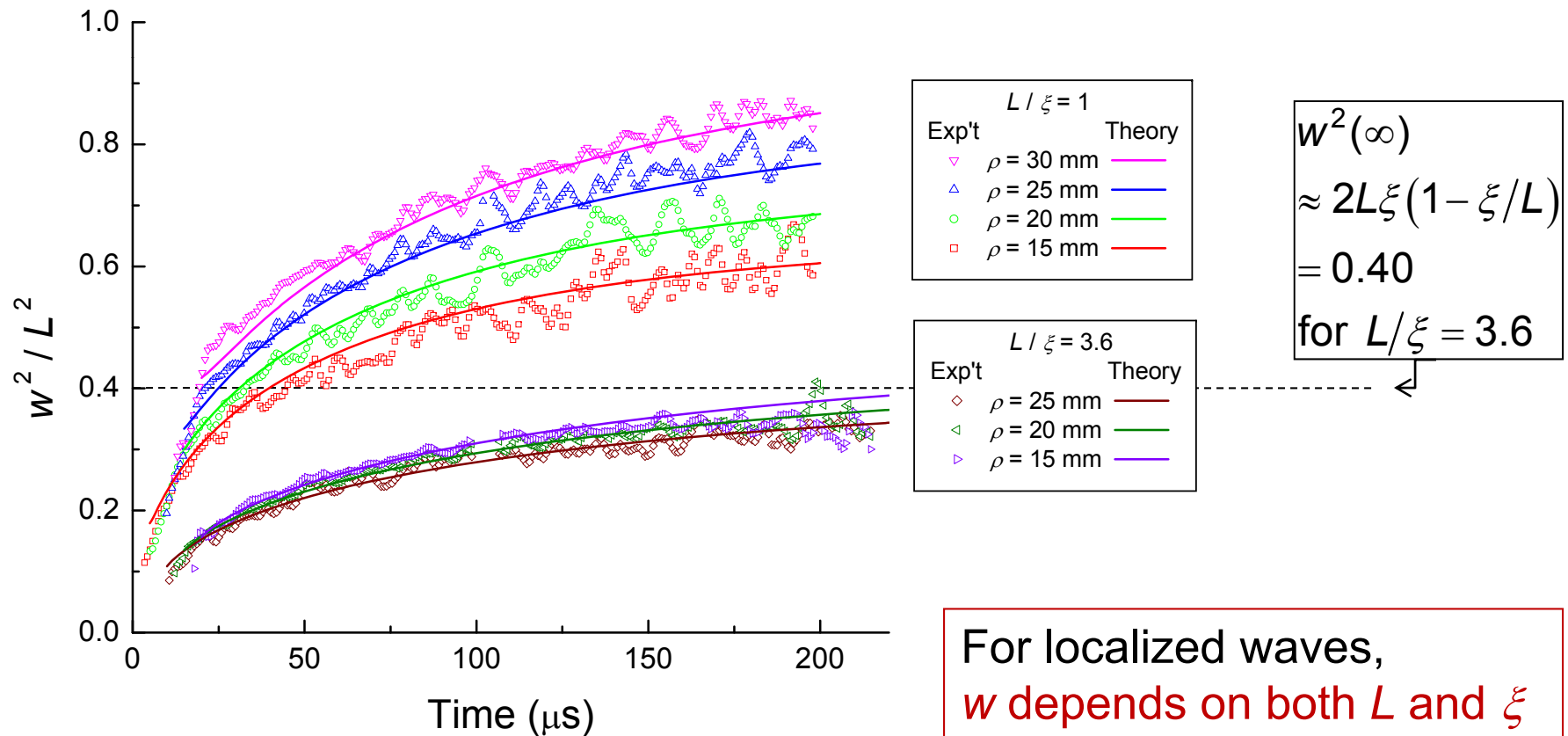


Question: What determines the magnitude of the dynamic transverse width $w_\rho(t)$ in transmission?

- For thick samples, w becomes independent of ρ .
- Behaviour at long times: SC theory predictions for the saturated width when $L \gg \xi$:

$$w^2(t \rightarrow \infty) \approx 2L\xi(1 - \xi/L)$$

[Cherroret, Skipetrov and van Tiggelen, aiXiv:0810.0767v1]

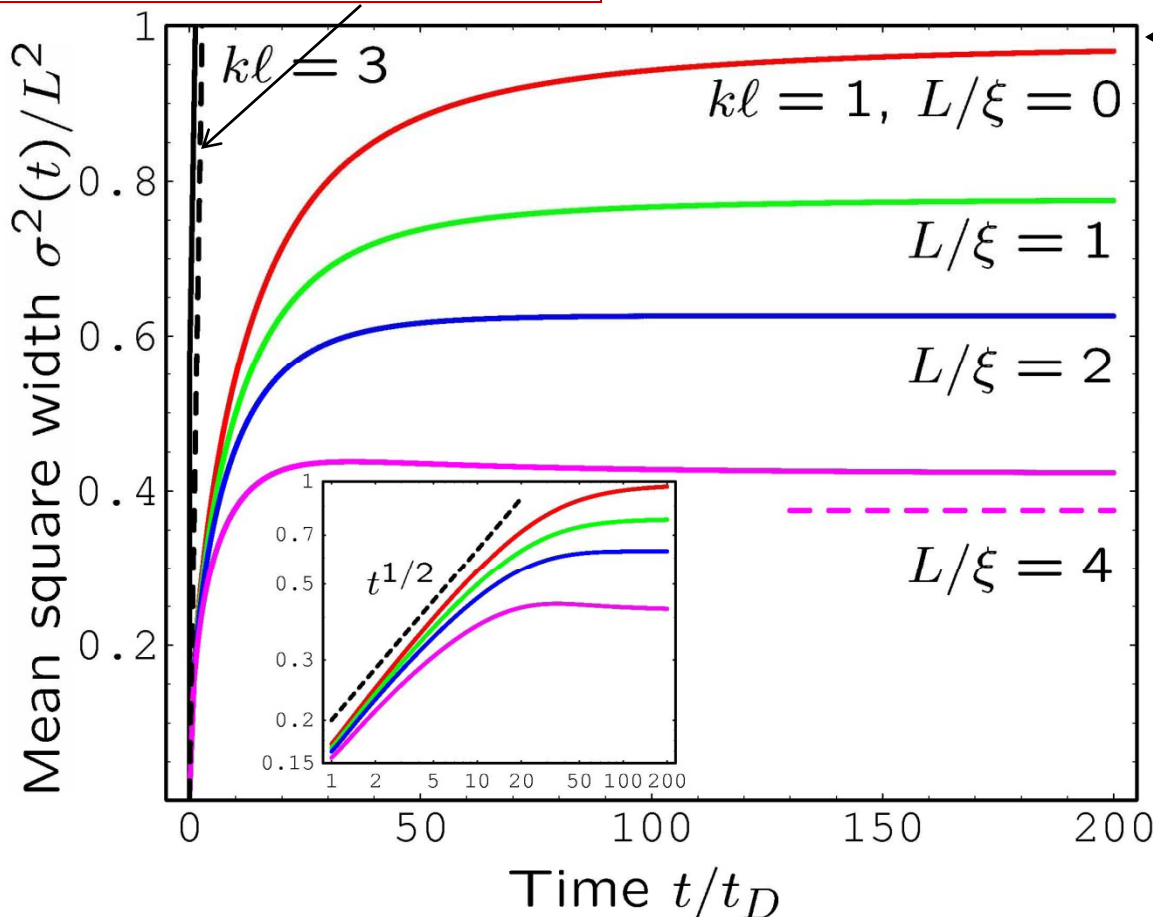


The saturation of $w(t)$ at long times is predicted *even* at the mobility edge [Cherret, Skipetrov and van Tiggelen, arXiv:0810.0767v1].

Numerical calculations using the dynamic self-consistent theory:

In the diffuse regime:
 $w^2(t \rightarrow \infty) = 4D [1 - (k\ell)^{-2}] t$

At the mobility edge:
 $w(t \rightarrow \infty) \approx L$



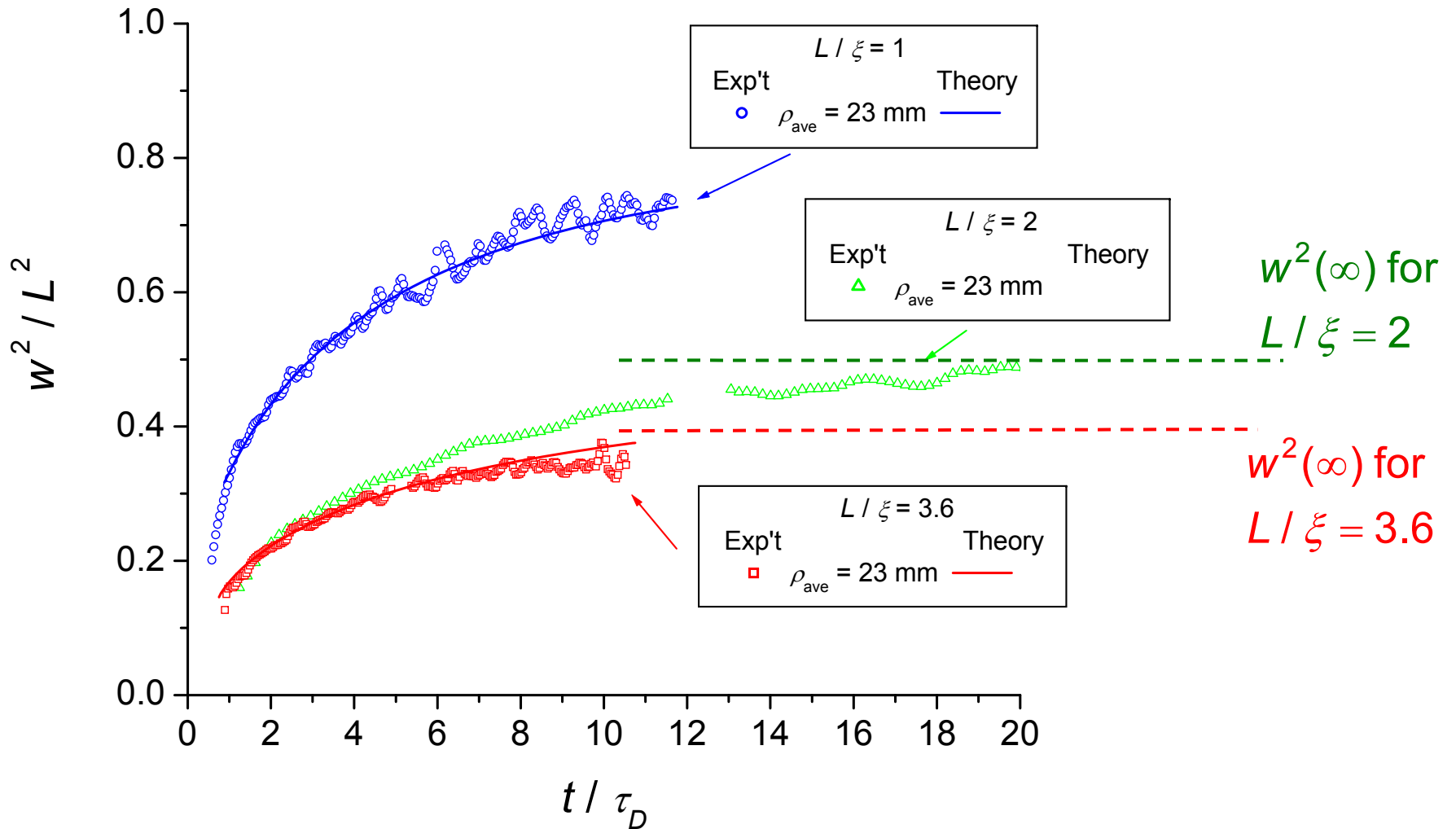
Deep in the localization regime:

$$w^2(t \rightarrow \infty) \approx 2L\xi(1 - \xi/L)$$

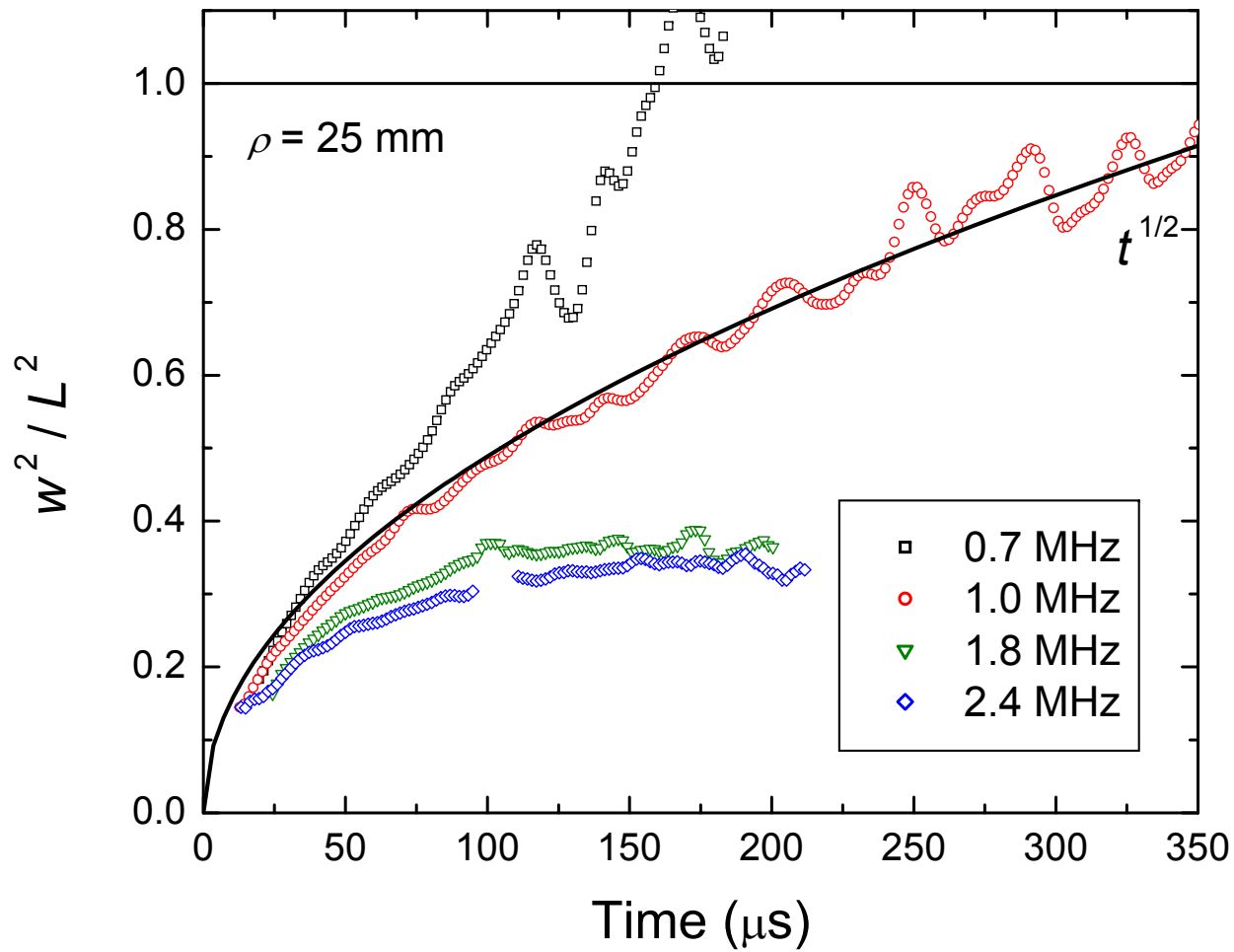
Similar trends are seen in the experiments (for $t/\tau_D < 20$)

- Compare three representative samples with different amounts of disorder (same measuring frequency $f = 2.4$ MHz).

$L = 14.5$ mm, $\xi = 15$ mm; $L = 23.05$ mm, $\xi = 12$ mm; $L = 23.5$ mm, $\xi = 6.5$ mm;



What happens when we vary the frequency?

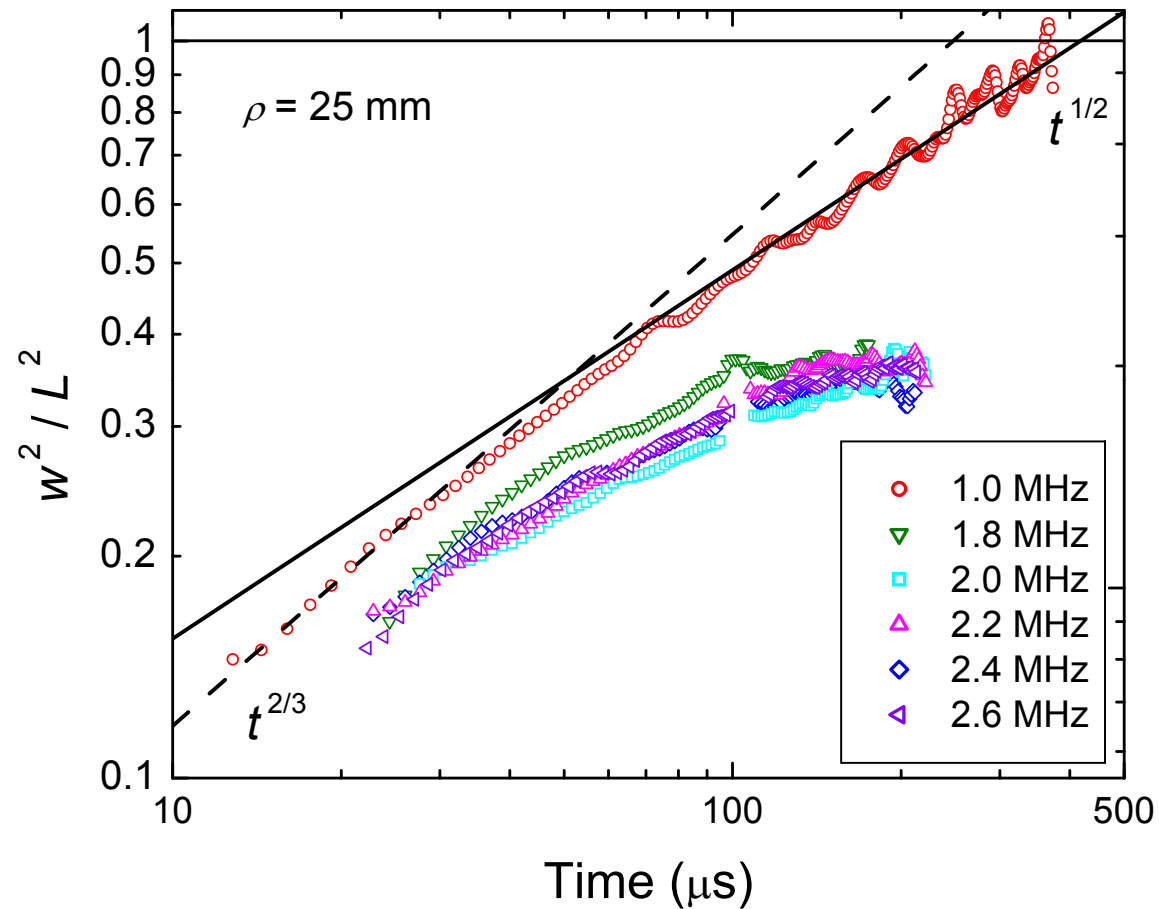


At 0.7 and 1.0 MHz, $w^2(t)$ does not saturate \Rightarrow above the mobility edge.
(at 0.7 MHz, the time dependence is almost linear)

Should be feasible to measure ξ as the mobility edge is approached

What happens when we vary the frequency?

Plot on log scales to show the time dependence



Near the mobility edge, we see

$$w^2(t) \propto t^{2/3} \text{ for } t < \tau_D \text{ \&}$$

$$w^2(t) \propto t^{1/2} \text{ for a limited range of } t > \tau_D$$

Agrees with estimates of $w^2(t)$ using the self-consistent theory.

Summary: Transverse confinement (3D transverse localization)

- The dynamic transverse width $w^2(t)$ has completely different properties for diffuse and localized modes

Diffuse: $w^2(t) \propto t$ and increases without bound.

Localized: $w^2(t)$ saturates at long times.

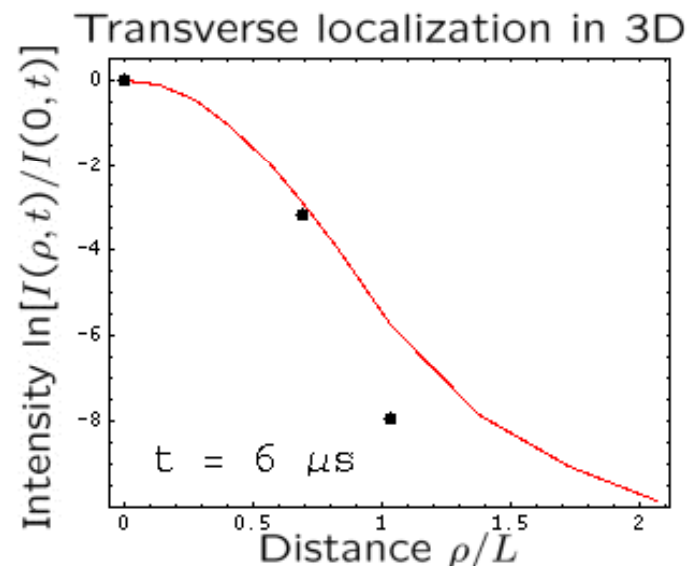
At the mobility edge: $w(t \rightarrow \infty) \approx L$

Deep in the localization regime: $w^2(t \rightarrow \infty) \approx 2L\xi(1 - \xi/L)$

- $w^2(t)$ is independent of absorption \rightarrow its measurement (*for any kind of wave*) provides a valuable method for assessing whether or not the waves are localized. (No risk of confusing absorption with localization.)

- $w^2(t)$ can be used to measure the localization length ξ .

- Measurements of transverse confinement provide the most direct evidence for localization in 3D to date.



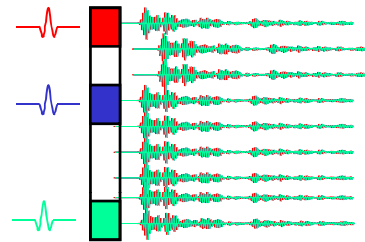
IV Backscattering experiments – initial results:

[with Laura Cobus, Alexandre Aubry and Arnaud Derode – see Laura's poster for more]

Average time-dependent backscattered intensity:

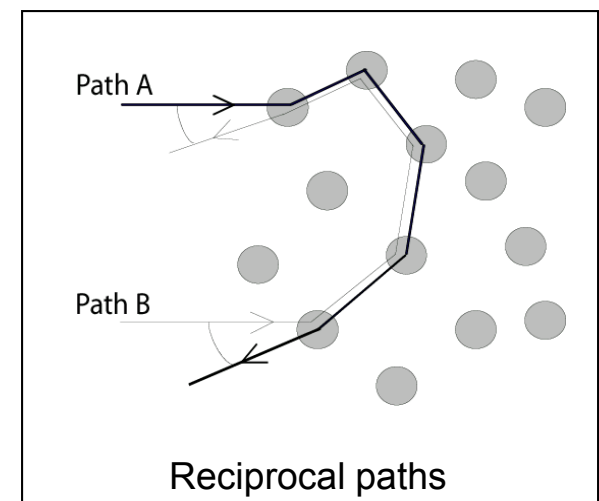
128-element
transducer array

$f = 3.2$ MHz
 $\lambda = 0.5$ mm



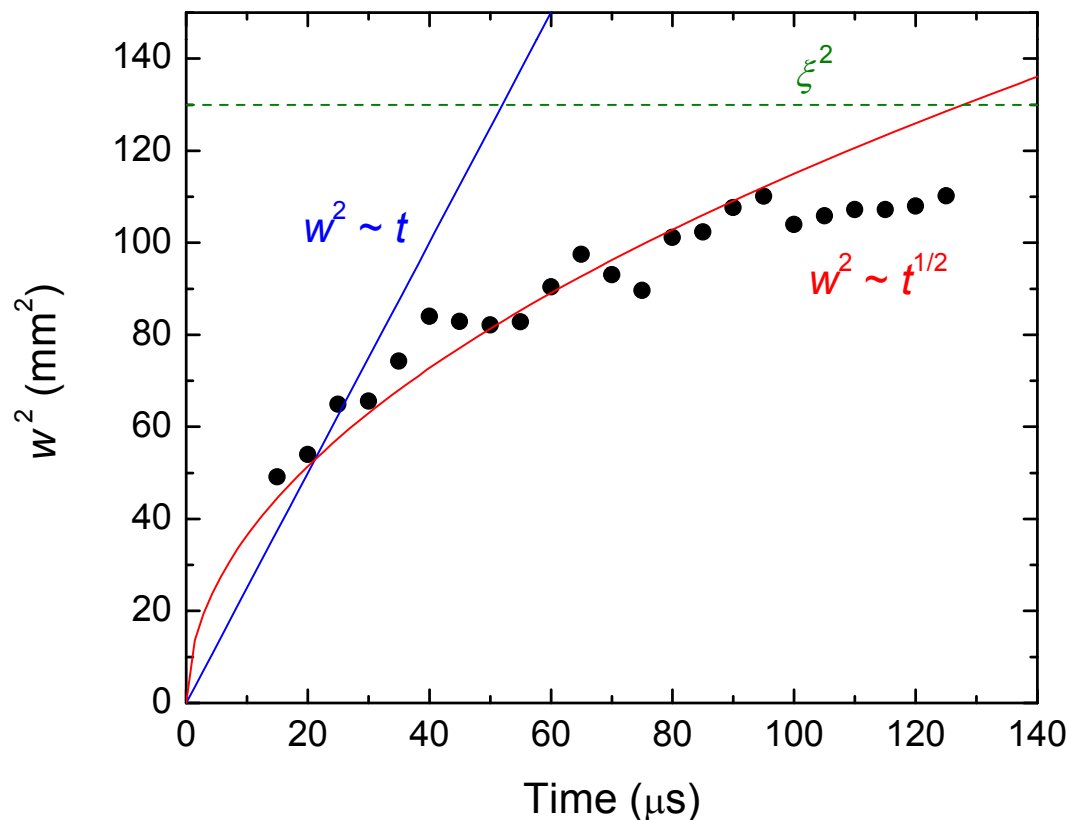
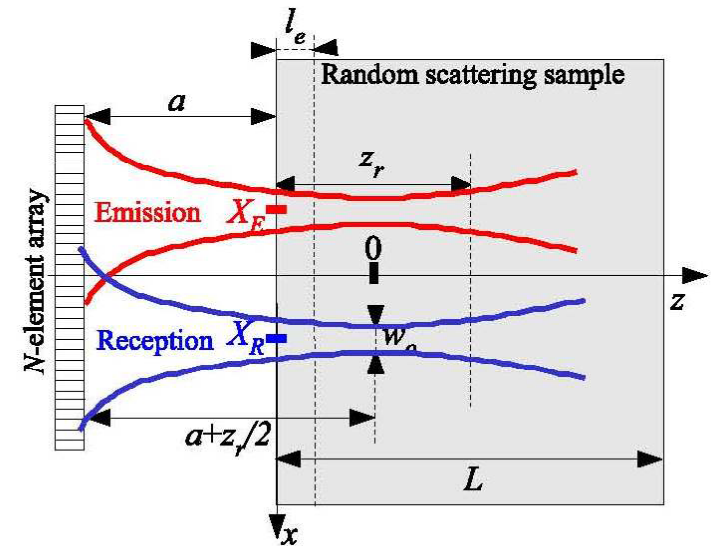
Coherent backscattering cone: - due to constructive interference in the backscattering direction of waves travelling along reciprocal paths. **Simulate far field conditions using plane wave beamforming.**

Transverse Confinement of the incoherent intensity: Gaussian beamforming permits measurements of transverse confinement in reflection.



Transverse confinement in reflection:

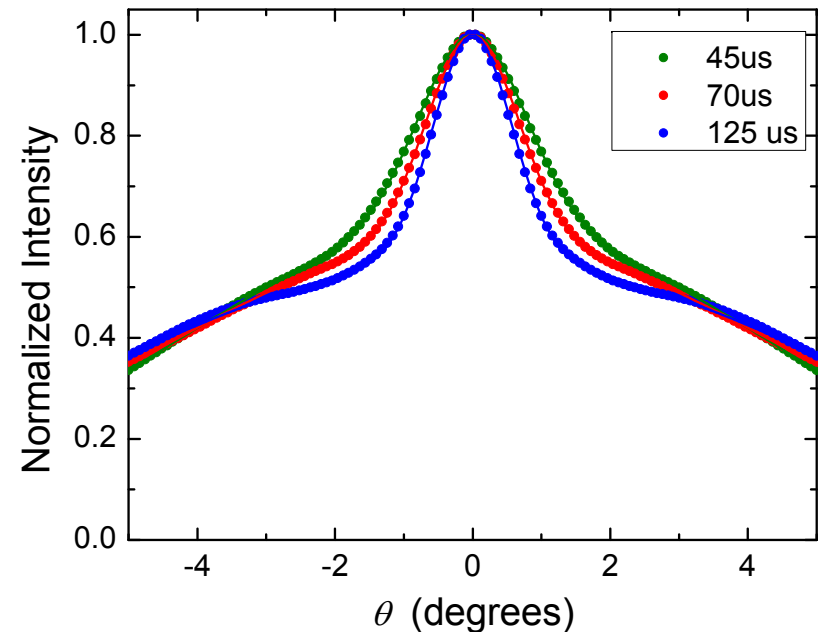
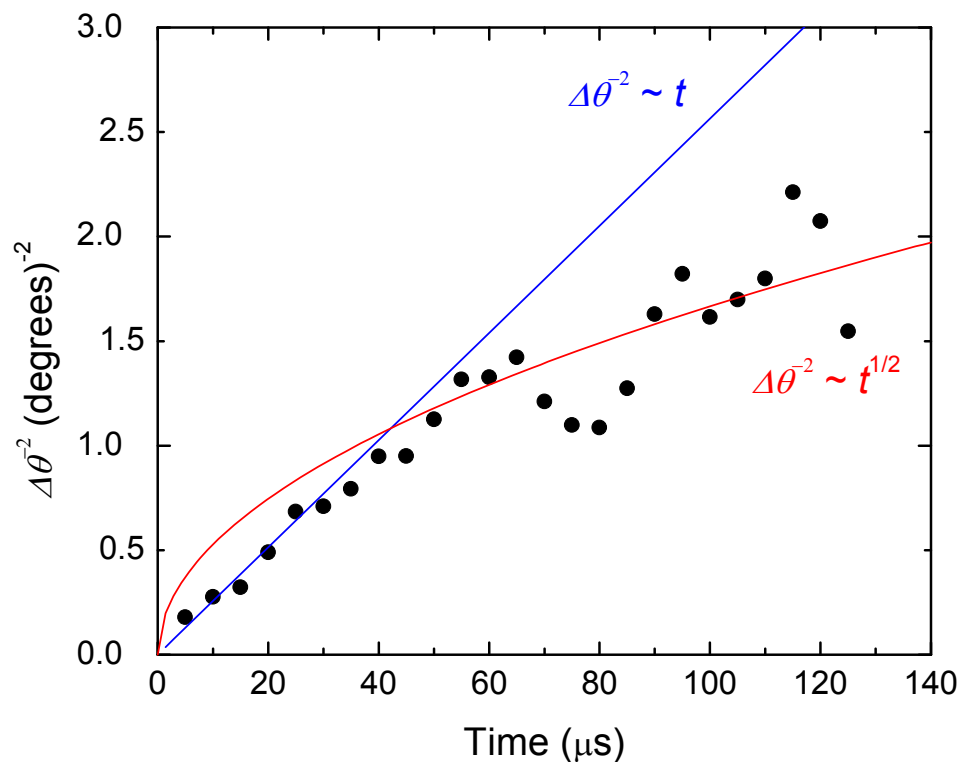
- Use Gaussian beamforming [Aubry & Derode, PRE 2007] to focus the emitted and received waves at the sample surface – measure $l(\rho, t)$ in reflection
- Incoherent background fitted by a Gaussian to measure the transverse width, w .



- Width saturates at long times → localization.
- Expect $w^2(t \rightarrow \infty) \sim \xi^2$ in reflection for thick samples (c.f., dashed green line – the measured value from transmission measurements at 2.4 MHz)

Coherent backscattering cone:

- Simulate far-field conditions using plane wave beamforming [Aubry & Derode, JASA (2007)].
- Difficult to separate cone from background at early times – preliminary analysis by fitting two Gaussians.



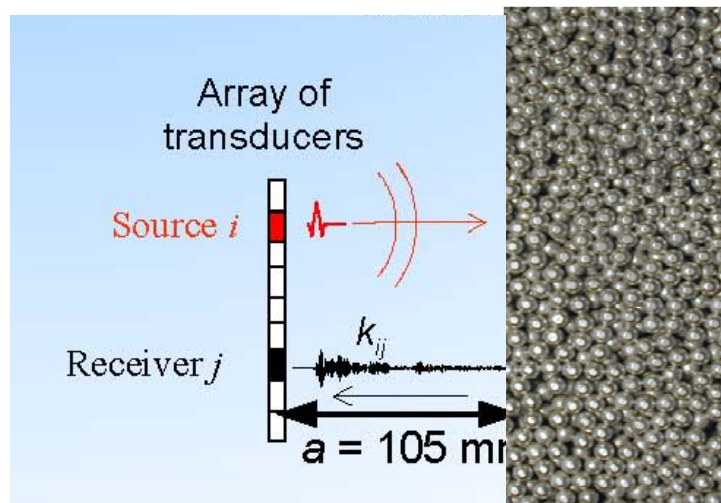
- For diffuse waves the half-width $\Delta\theta$ is:

$$\Delta\theta^{-2} = \frac{k^2 D}{\ln(2)} t$$

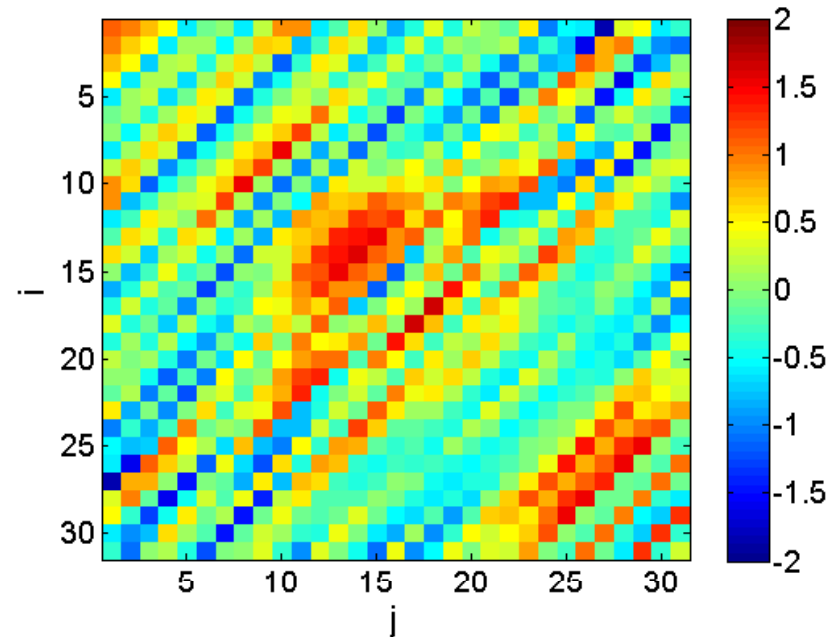
- For localized waves, expect the cone width to shrink less rapidly, and eventually saturate.

- For $t > 50 \mu\text{s}$, behaviour is consistent with the observed transverse confinement of the incoherent intensity.

The inter-element response matrix K_{ij} exhibits strong coherences along the anti-diagonals:



Matrix \mathbf{K} ($t = 35 \mu\text{s}$, $f = 2.7 \text{ MHz}$)



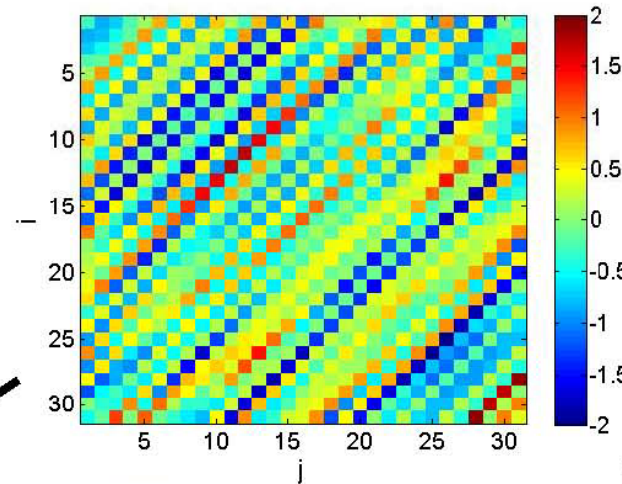
- Coherence along the antidiagonals of \mathbf{K} has been demonstrated for single scattering [Aubry and Derode, J. App. Phys. (2009), P.R.L. (2009)]
- Here, the coherence along the antidiagonals of \mathbf{K} cannot be due to single scattering, since $vt/2 > L \gg \ell_s$.
- It may be explained by the occurrence of recurrent paths (the first and last scattering events along a multiple scattering path are identical) which exhibit the same statistical properties as single scattering

Separation of recurrent paths from the total backscattered signal

Alexandre's idea:

Idea: apply the method of separation of single and multiple scattering to filter the recurrent scattering paths

$$\mathbf{K} = \mathbf{K}^R + \mathbf{K}^M$$

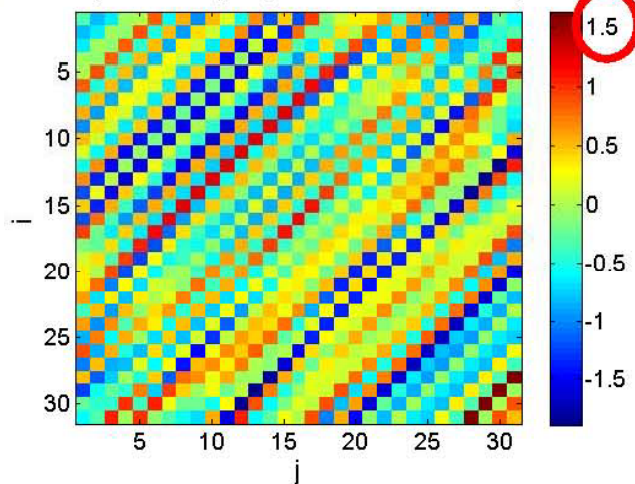


Matrix \mathbf{K}
(T=55 μs , f=3.25 MHz)

The method used is the one based on the SVD of the antidiagonals of \mathbf{K} (cf JASA 2011)

Matrix \mathbf{K}^S

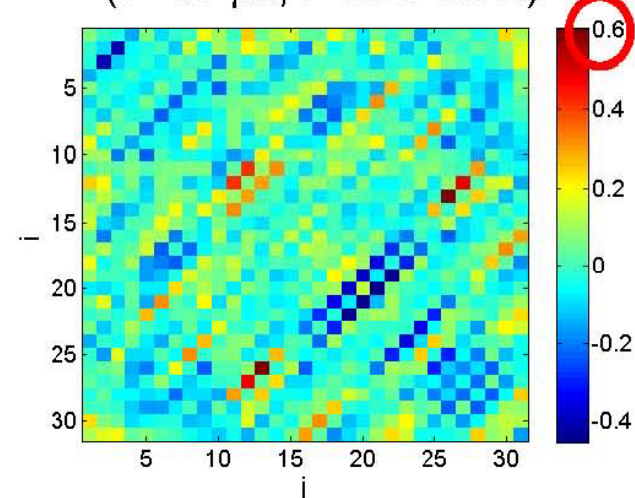
(T=55 μs , f=3.25 MHz)



Matrix characterized by a long-range coherence along the antidiagonals
→ recurrent scattering paths?

Matrix \mathbf{K}^M

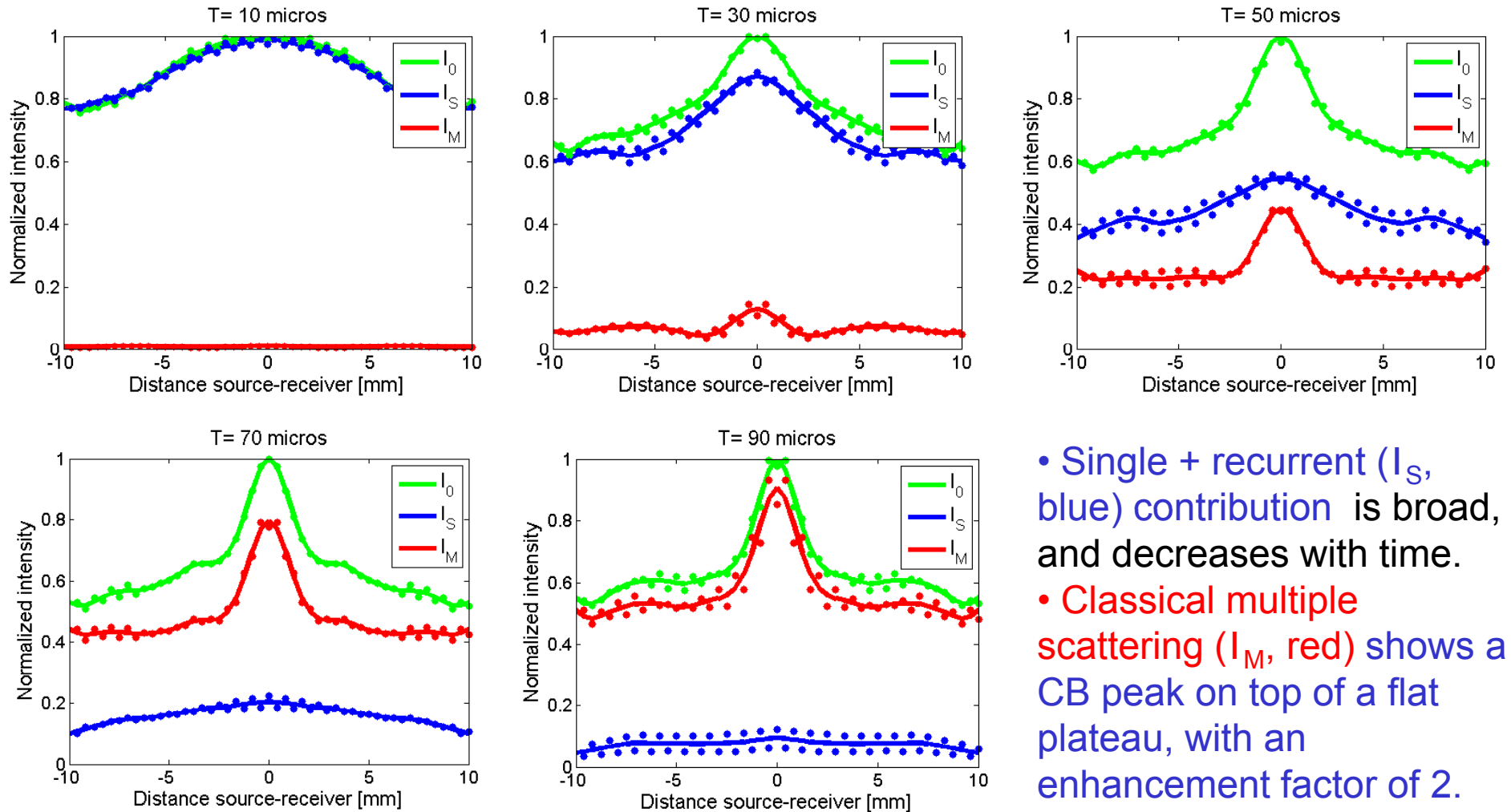
(T=55 μs , f=3.25 MHz)



Matrix typical of multiple scattering in the diffusive regime

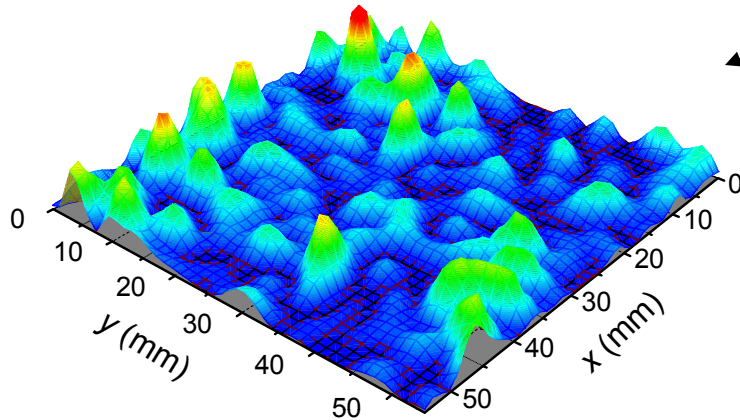
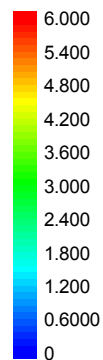
Separation of recurrent paths from the total backscattered signal

Spatial intensity profiles:



By identifying and separating the single and recurrent contributions, it should be possible to measure the time-dependent width of the backscattering cone more robustly.

V. Statistical approach to the localization of elastic waves:



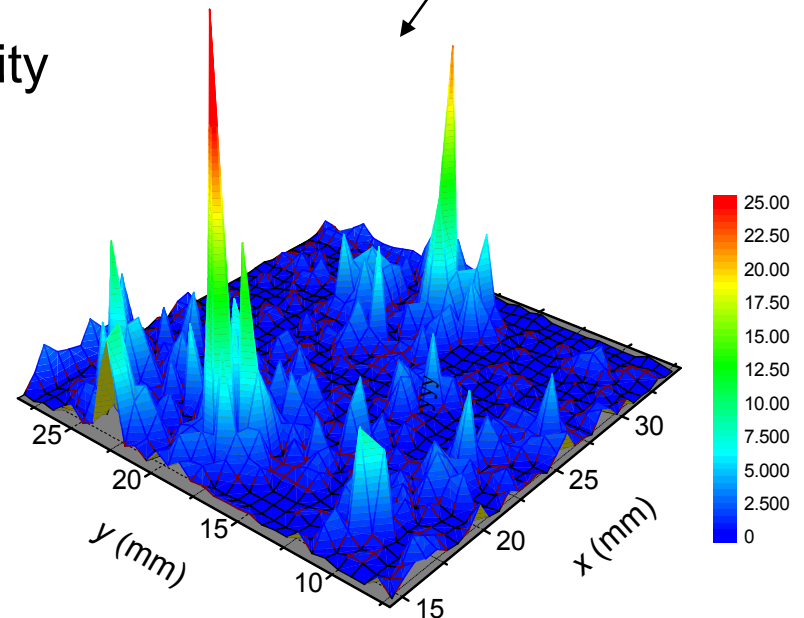
Diffuse ultrasound
(speckle pattern for our
mesoglass at 0.20 MHz)

Localized ultrasound
(speckle pattern for our
mesoglass at 2.4 MHz)

Large fluctuations in the transmitted intensity are characteristic of localized waves.

Signatures of these fluctuations are seen in:

- Near field speckle pattern
- Intensity distribution $P(I/\langle I \rangle)$
- Variance
- Multifractality



Transmitted intensity distributions for our mesoglass:

Measure the intensity I at each point in the near field speckle pattern when the sample is illuminated on the opposite side with a broad beam. When I is normalized by its average value to get $\hat{I} = I / \langle I \rangle$, its distribution is universal.

(a) Data at 0.20 MHz

Rayleigh distribution:

(random wave fields described by circular Gaussian statistics)

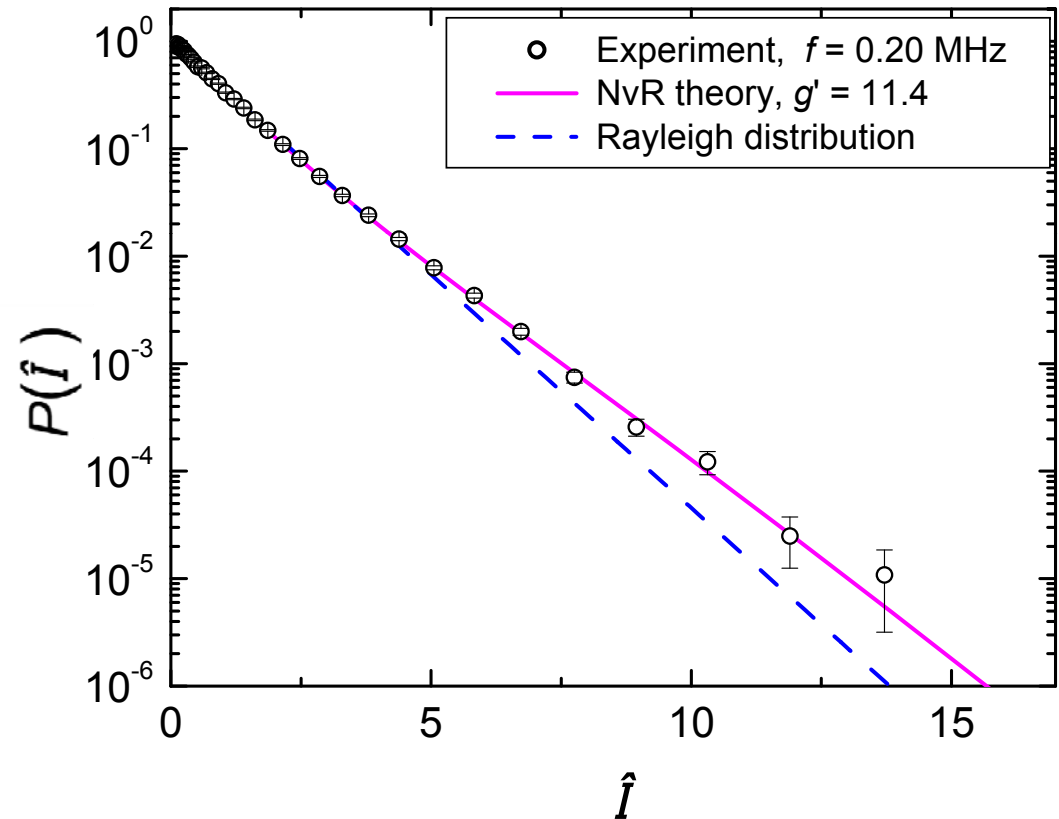
$$P(\hat{I}) = \exp(-\hat{I})$$

Leading order correction to Rayleigh statistics due to interference (no absorption)

[Nieuwenhuizen & van Rossum, PRL **74**, 2674 (1995)]

(g' = dimensionless conductance):

$$P(\hat{I}) = \exp(-\hat{I}) \left[1 + \frac{1}{3g'} (\hat{I}^2 - 4\hat{I} + 2) \right]$$



Find $g' = 11.4 \gg 1$
 \Rightarrow modes are extended

Transmitted intensity distributions for our mesoglass:

(b) Near 2.4 MHz (upper part of intermediate frequency regime), find very large departures from **Rayleigh Statistics**

Fit the entire distribution to predictions by van Rossum and Nieuwenhuizen [Rev. Mod. Phys. **71**, 313]

for a slab geometry in 3D (red curve).

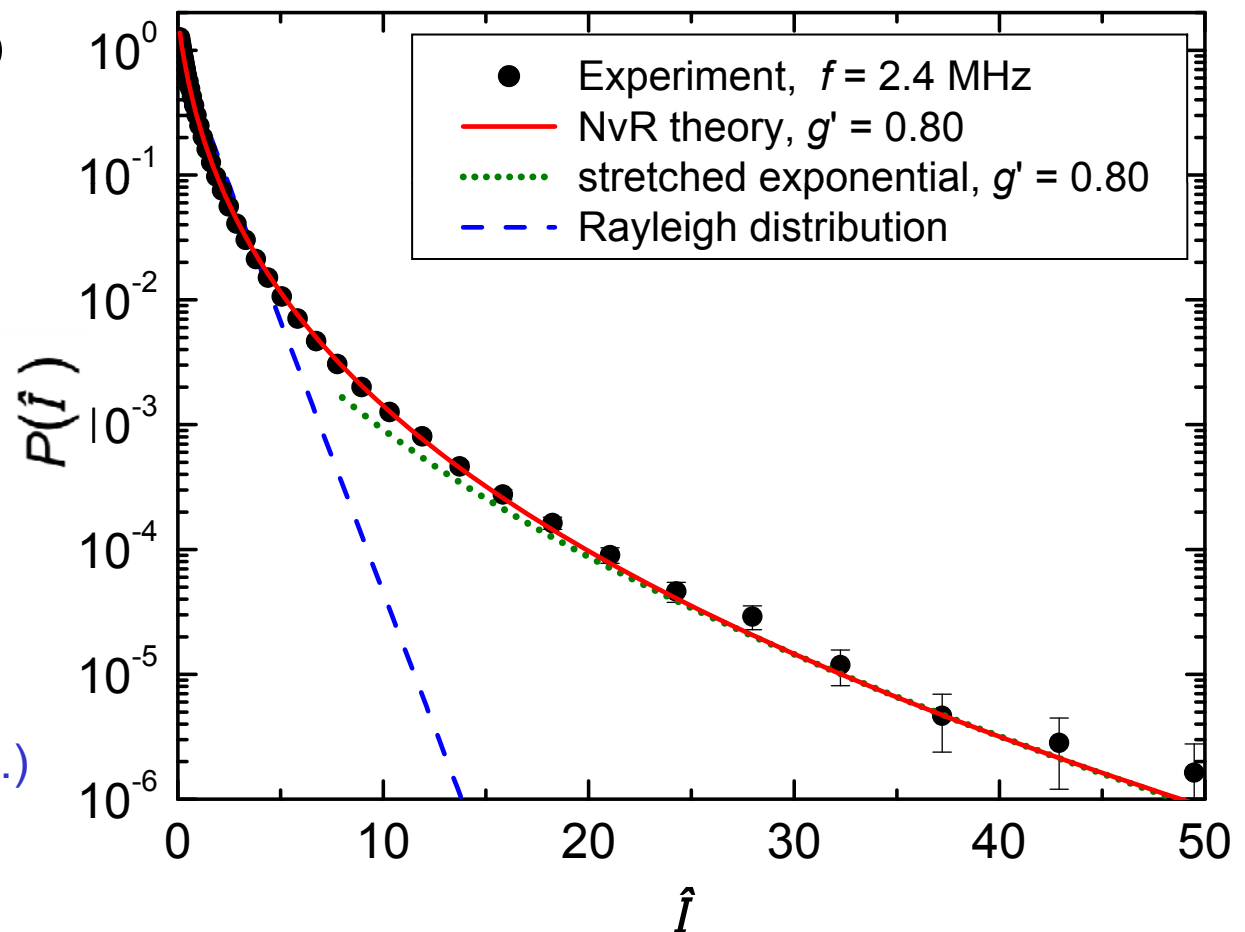
Remarkable agreement with experiment.

The tail of intensity distribution obeys a **stretched exponential distribution**

$$P(\hat{I}) \sim \exp(-2\sqrt{g'\hat{I}})$$

(g' is the effective dimensionless conductance.)

Find $g' = 0.80 < 1$, indicating localization.



Variance of the transmitted intensity – a simpler way to measure the dimensionless conductance g' :

Chabanov *et al.* [*Nature* **404**, 850 (2000)] have proposed that **localization is achieved** when the **variance of the normalized *total* transmitted intensity**,

$\hat{T} = T/\langle T \rangle$ satisfies

$$\text{var}(\hat{T}) \equiv \frac{\langle \delta T^2 \rangle}{\langle T \rangle^2} = \frac{2}{3g'} \geq \frac{2}{3}$$

whether absorption is present or not. This corresponds to the **localization condition** $g' \leq 1$.

But $\text{var}(\hat{T})$ and $\text{var}(\hat{I})$ are related: $\text{var}(\hat{I}) = 2\text{var}(\hat{T}) + 1$

Then, the Chabanov-Genack localization criterion gives $\text{var}(\hat{I}) \geq 7/3$

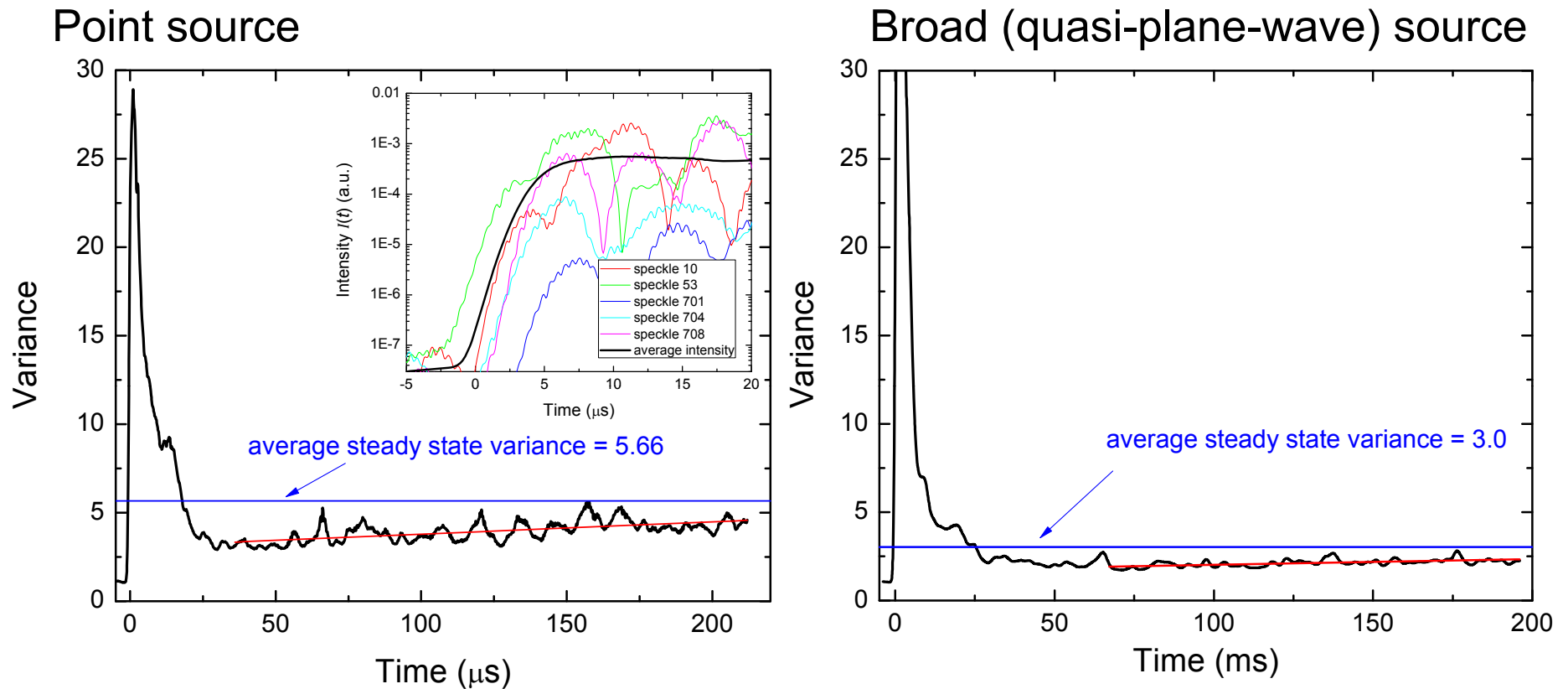
e.g., for our data at 2.4 MHz:

Measure $\text{var}(\hat{I}) = 2.74 \pm 0.09 \Rightarrow g' = \frac{4}{3[\text{var}(\hat{I}) - 1]} = 0.77 \pm 0.4$

Excellent agreement with $g' = 0.80 \pm 0.08$ measured from $P(\hat{I})$

Additional evidence that the modes are localized above ~ 2 MHz.

Time dependence of the speckle intensity variance:



- Large peak in variance at early times – due to arrival time fluctuations.
- Variance increases slowly with time at longer times (slower growth than in quasi 1D – microwave observations by Azi Genack's group).
- Both variance and its growth with time are larger for a point source.
- Time-dependent variance is less than the stationary variance for the range of times measured.

Time dependence of the speckle intensity variance:

Data are consistent with theoretical estimates by Sergey Skipetrov, based on a mode picture of wave propagation:

$$\psi(\mathbf{r}, t) = \sum A_n \psi_n(\mathbf{r}) e^{-i\omega_n t - \frac{1}{2}\Gamma_n t}$$

(quasi-mode frequencies ω_n ,
lifetimes Γ_n – for $P(\Gamma)$, see
Skipetrov & van Tiggelen, PRL (2006))

Assuming uncorrelated modes, an estimate of the variance gives

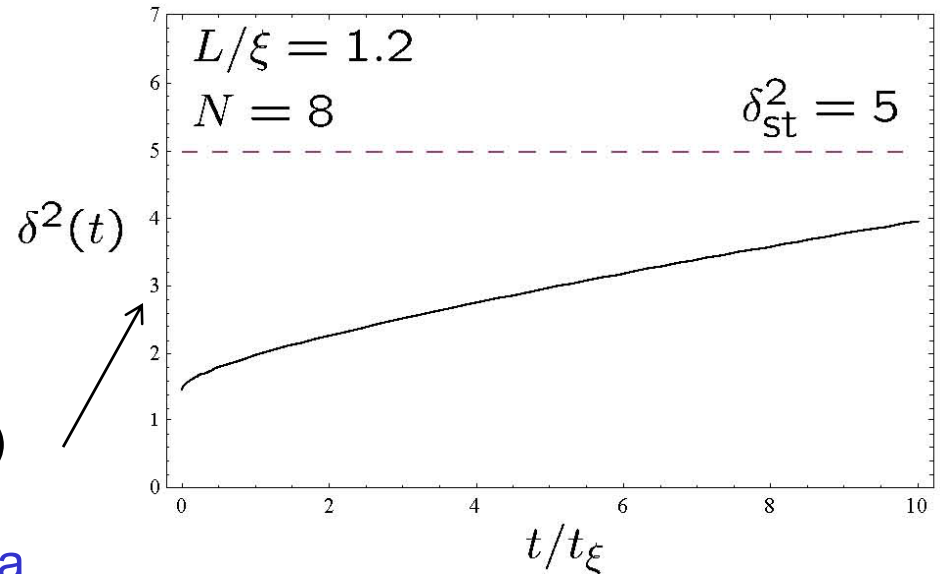
$$\delta^2(t) = \text{var}(\tilde{I}(t)) \approx 1 + \frac{1}{N} \left[\left(1 + \delta_{\text{stationary}}^2\right) f(t/t_\xi, L/\xi) - 2 \right]$$

where $t_\xi = \xi^2 / D_B$ and

$$f(t/t_\xi, L/\xi) = \frac{\langle e^{-2\Gamma t} \rangle}{\langle e^{-\Gamma t} \rangle^2}$$

$$= \begin{cases} a + b\sqrt{t/t_\xi}, & t \rightarrow 0 \\ c + d(t/t_\xi), & t \rightarrow \infty \end{cases}$$

Predictions (valid at long times, $t \gg \tau_D$)
for typical experimental parameters
reproduce the main features in the data



Multifractality (MF) of the wavefunction (with Sanli Faez, Ad Legendijk):
[Faez et al., *PRL* **103**, 155703 (2009)]

Key idea - Unusual spatial structure of the wave functions near the Anderson transition: Large fluctuations \Rightarrow the moments of the wave function intensity

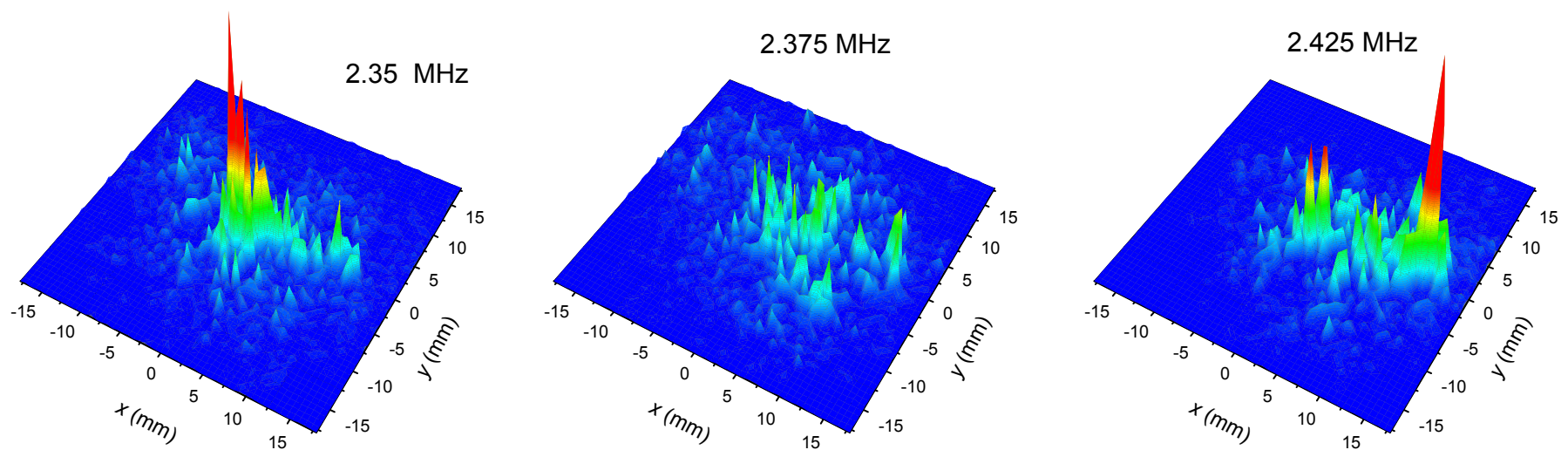
$$I(\mathbf{r}) = |\psi^2(\mathbf{r})| / \int |\psi^2(\mathbf{r})| d^d r$$

may depend anomalously on length scale , exhibiting multifractal behaviour (MF \Rightarrow each moment scales with a different power- law exponent).

- Many theoretical predictions, but almost no experimental evidence

Question: Do the ultrasonic wavefunctions exhibit MF in our samples?

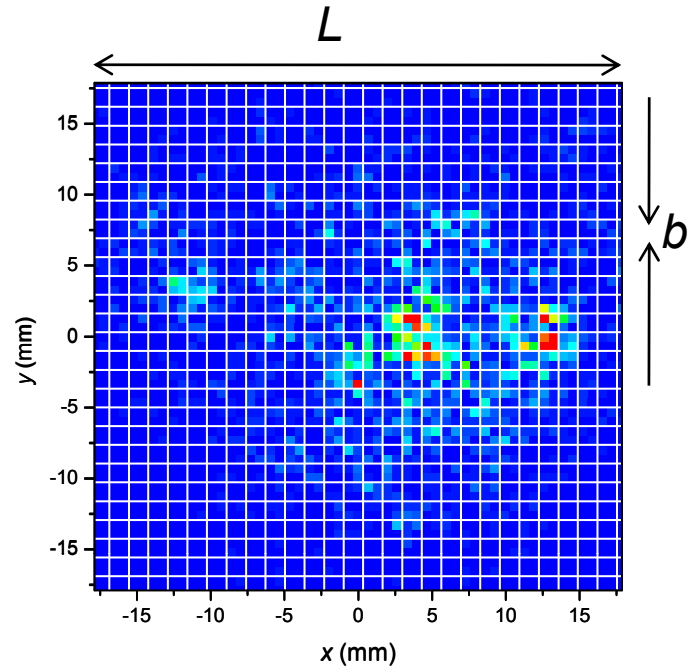
Transmitted speckle patterns $I(\mathbf{r})$ for a fixed point source (at $x = y = 0$).
Excite a single wave function at each frequency.



Multifractality (MF):

Characterizing the length scale dependence:

- Vary system size L , or
- Divide system into boxes of size b , and vary b with L fixed.
($\lambda < b < L$, L/b is the scaling length)



Generalized Inverse Participation Ratios (gIPR):

The gIPR quantify the non-trivial length scale dependence of the moments of the intensity.

$$P_q = \sum_{i=1}^n \left(I_{B_i} \right)^q = \sum_{i=1}^n \left[\int_{B_i} I(\mathbf{r}) d^d \mathbf{r} \right]^q$$

$I(\mathbf{r}) = |\psi^2(\mathbf{r})| / \int |\psi^2(\mathbf{r})| d^d r$ (normalized intensity)
 I_{B_i} is the integrated probability inside a box B_i of linear size b
 $n = (L/b)^d$ is the number of boxes.

At criticality

$$\langle P_q \rangle \sim (L/b)^{-\tau(q)} \quad \text{with}$$

$$\tau(q) = d(q-1) + \Delta_q$$

MF behaviour: τ is a continuous function of q (critical states).

normal dimension

anomalous dimension

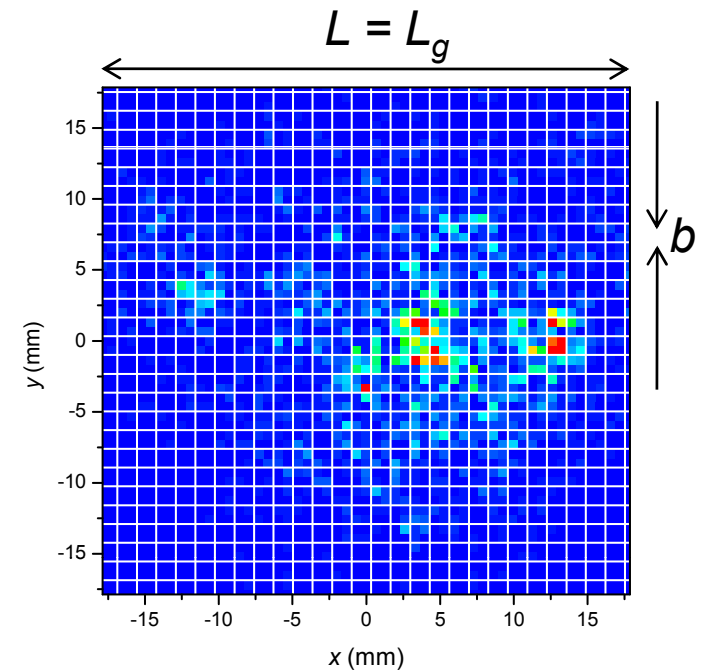
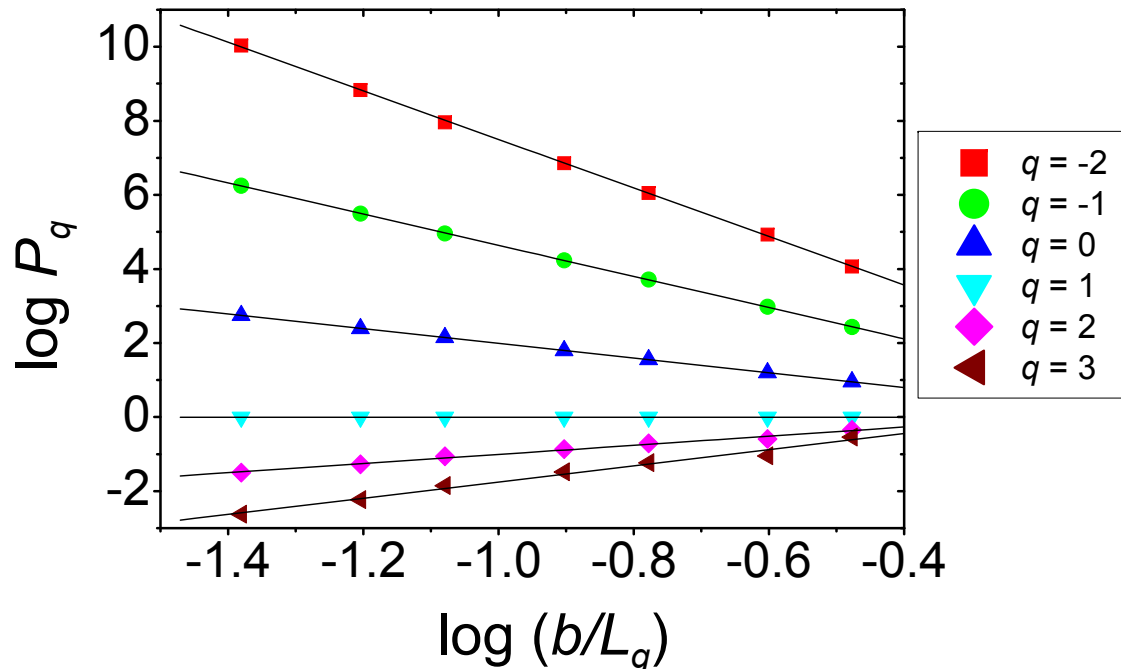
Multifractality (MF):

Generalized Inverse Participation Ratios (gIPR):

Find the “typically averaged” gIPR by box-sampling the wavefunctions (many frequencies) near the surface ($d_{\text{sampling}} = 2$, but sample is 3D) for a single realization of disorder.

$$\langle P_q \rangle_{\text{typ}} \sim (L_g/b)^{-2(q-1)-\Delta_q} \equiv (L_g/b)^{-\tau(q)}$$

Representative results at $f = 2.40$ MHz:



Extended states:

$$\tau(q) = d(q-1) \text{ [i.e., } \Delta_q = 0 \text{]}$$

Near criticality:

$\tau(q)$, Δ_q , both continuous functions of q (MF)

Deep in the localization regime: $\tau(q) = 0$

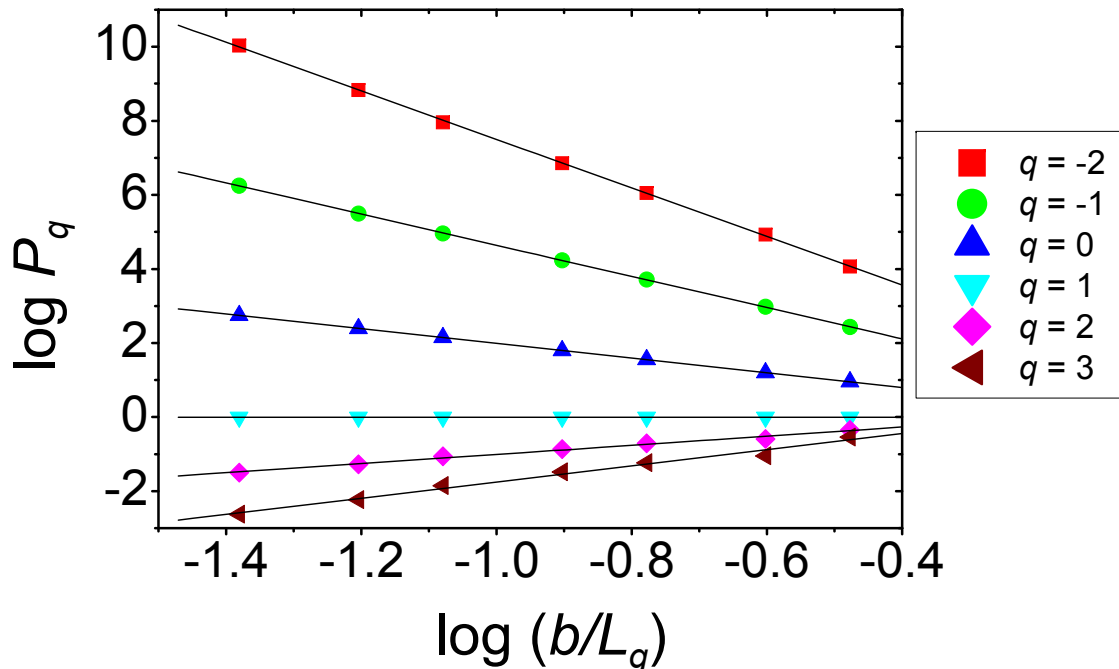
Multifractality (MF):

Generalized Inverse Participation Ratios (gIPR):

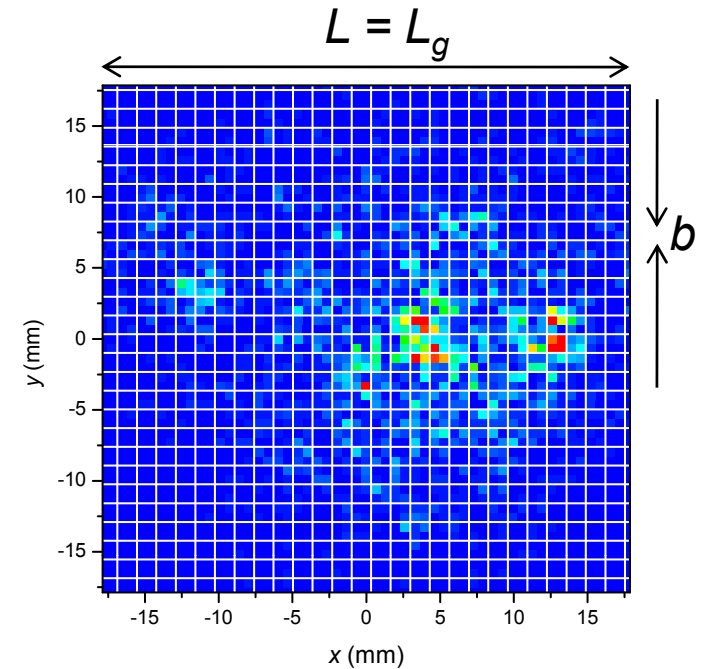
Find the “typically averaged” gIPR by box-sampling the wavefunctions (many frequencies) near the surface ($d_{\text{sampling space}} = 2$, but sample is 3D) for a single realization of disorder.

$$\langle P_q \rangle_{\text{typ}} \sim (L_g/b)^{-2(q-1)-\Delta_q} \equiv (L_g/b)^{-\tau(q)}$$

Representative results at $f = 2.40$ MHz:

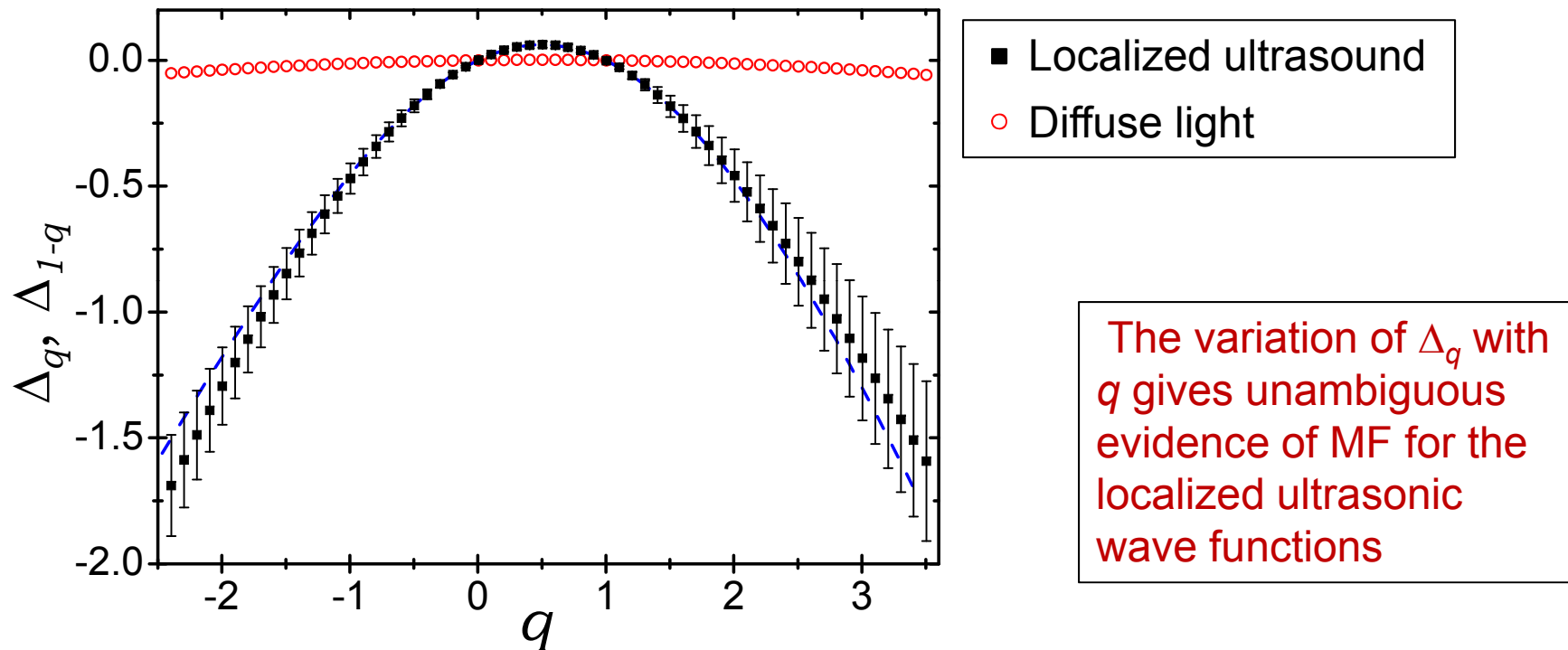


- Determine $\tau(q)$ from the slopes
- Subtract off the normal part of $\tau(q)$, $d(q-1)$, to determine Δ_q



Multifractality (MF): the anomalous exponents (from the gIPR)

Anomalous exponents Δ_q



Exact symmetry relation, predicted by Mirlin *et al.* (PRL 97, 046803, 2006)

$$\Delta_q = \Delta_{1-q}$$

Consistent with our data ✓

Multifractality (MF): PDF

Probability density function (PDF)

The gIPR are proportional to the moments of the distribution function of the intensities, $\mathcal{P}(I_B)$, implying

$$\mathcal{P}(I_B) \sim \frac{1}{I_B} \left(\frac{L}{b} \right)^{-d+f(\alpha)}, \quad \text{where } \alpha = -\frac{\ln I_B}{\ln(L/b)}$$

$f(\alpha)$ is called the singularity spectrum [the fractal dimension of the set of points \mathbf{r} where $I \sim (L/b)^{-\alpha}$]

Significance: $f(\alpha)$ is expected to be independent of (L/b) , and give a universal characterization of the MF behaviour.

Relationship with $\tau(q)$:

$$\tau(q) = q\alpha - f(\alpha) \quad q = \frac{\partial f}{\partial \alpha} \quad \alpha = \frac{\partial \tau}{\partial q}$$

i.e., $f(\alpha)$ and $\tau(q)$ are related by a Legendre transform

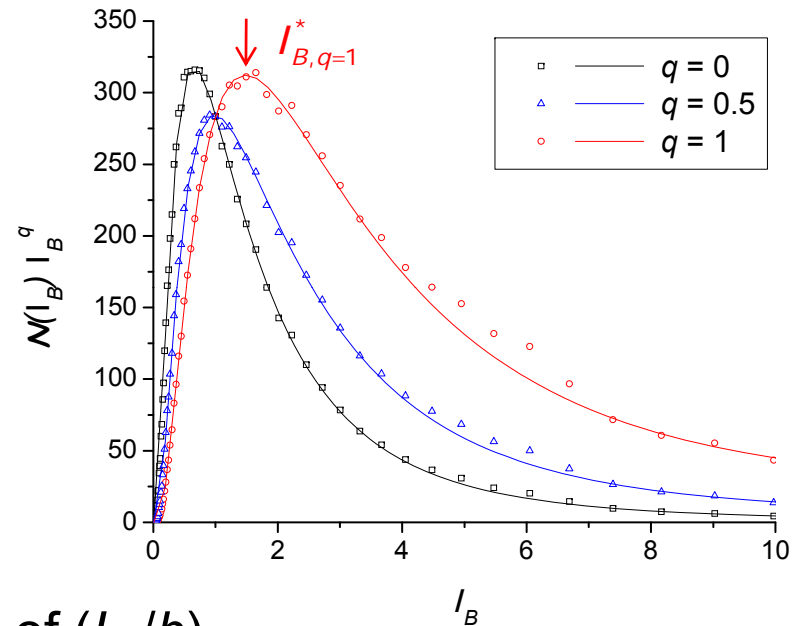
The singularity spectrum $f(\alpha)$ – relationship with $\tau(q)$

Start from: $\mathcal{P}(I_B)$ = probability that box i has I_{Bi} between I_B and $I_B + dI_B$
 $\Rightarrow \mathcal{N}(I_B) = (L_g/b)^d \mathcal{P}(I_B)$ = number of boxes with I_{Bi} between I_B and $I_B + dI_B$

Then, the gIPR can be written in terms of the PDF as

$$P_q = \int_0^1 \underbrace{\mathcal{N}(I_B) I_B^q}_{\text{sharp max at } I_{B,q}^*} dI_B$$

$$\approx \mathcal{N}(I_B^*) \left(I_B^* \right)^q$$



If both I_B^* and $\mathcal{N}(I_B^*)$ scale as powers of (L_g/b)

$$I_B^* \sim (L_g/b)^{-\alpha(q)}, \quad \mathcal{N}(I_B^*) \sim (L_g/b)^{f(q)} \quad \longrightarrow$$

$$\mathcal{P}(I_B) \sim \left(\frac{L}{b} \right)^{-d+f(\alpha)}$$

Then

$$\tau(q) = q\alpha - f(\alpha)$$

Significance of the exponents α and $f(\alpha)$:
 $f(\alpha)$ is the fractal dimension of the set of points \mathbf{r} where $I \sim (L/b)^{-\alpha}$

The singularity spectrum $f(\alpha)$ – relationship with $\tau(q)$

At the peak of $\mathcal{N}(I_B) I_B^q$

$$\left. \frac{\partial \ln [\mathcal{N}(I_B) I_B^q]}{\partial \ln I_B} \right|_{I_B^*} = 0 \quad \Rightarrow \quad \left. \frac{\partial \ln [\mathcal{N}(I_B)]}{\partial \ln I_B} \right|_{I_B^*} = -q \quad (1)$$

But from $I_B^* \sim (L_g/b)^{-\alpha(q)}$, we get $\alpha = -\frac{\ln I_B^*}{\ln(L_g/b)}$

and from $\mathcal{N}(I_B^*) \sim (L_g/b)^{f(q)}$, we get $\ln \mathcal{N}(I_B^*) \sim f(q) \ln(L_g/b)$

$$\therefore \frac{\partial \ln [\mathcal{N}(I_B)]}{\partial \ln I_B} \sim \frac{\partial f}{\partial \ln I_B} \ln(L_g/b) = \frac{\partial f}{\partial \alpha} \frac{\partial \alpha}{\partial \ln I_B} \ln(L_g/b) = -\frac{\partial f}{\partial \alpha} \quad (2)$$

$$(1) \text{ and } (2) \Rightarrow \boxed{\frac{\partial f}{\partial \alpha} = q}$$

Hence, by differentiating $\tau(q) = q\alpha - f(\alpha)$ with respect to q , we also find

$$\boxed{\frac{\partial \tau}{\partial q} = \alpha}$$

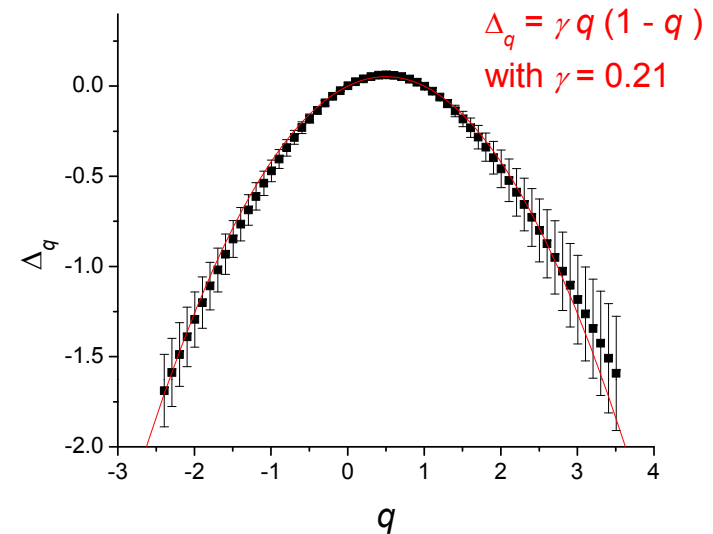
Multifractality (MF) The parabolic approx and the PDF

Parabolic approximation:

$$\Delta_q = \gamma q(1 - q) \quad (\gamma = \text{constant})$$

The Legendre transformation then yields

$$f(\alpha) = d - \frac{(\alpha - \alpha_0)^2}{4\gamma}; \quad \alpha_0 = d + \gamma$$



The PDF in the parabolic approximation:

$$\begin{aligned} \mathcal{P}(I_B) &\sim \frac{1}{I_B} \left(\frac{L}{b} \right)^{-d+f(\alpha)} \\ &\sim \frac{1}{I_B} \exp \left[-(\ln I_B - \ln I_{B,c})^2 / 2w^2 \right] \end{aligned}$$

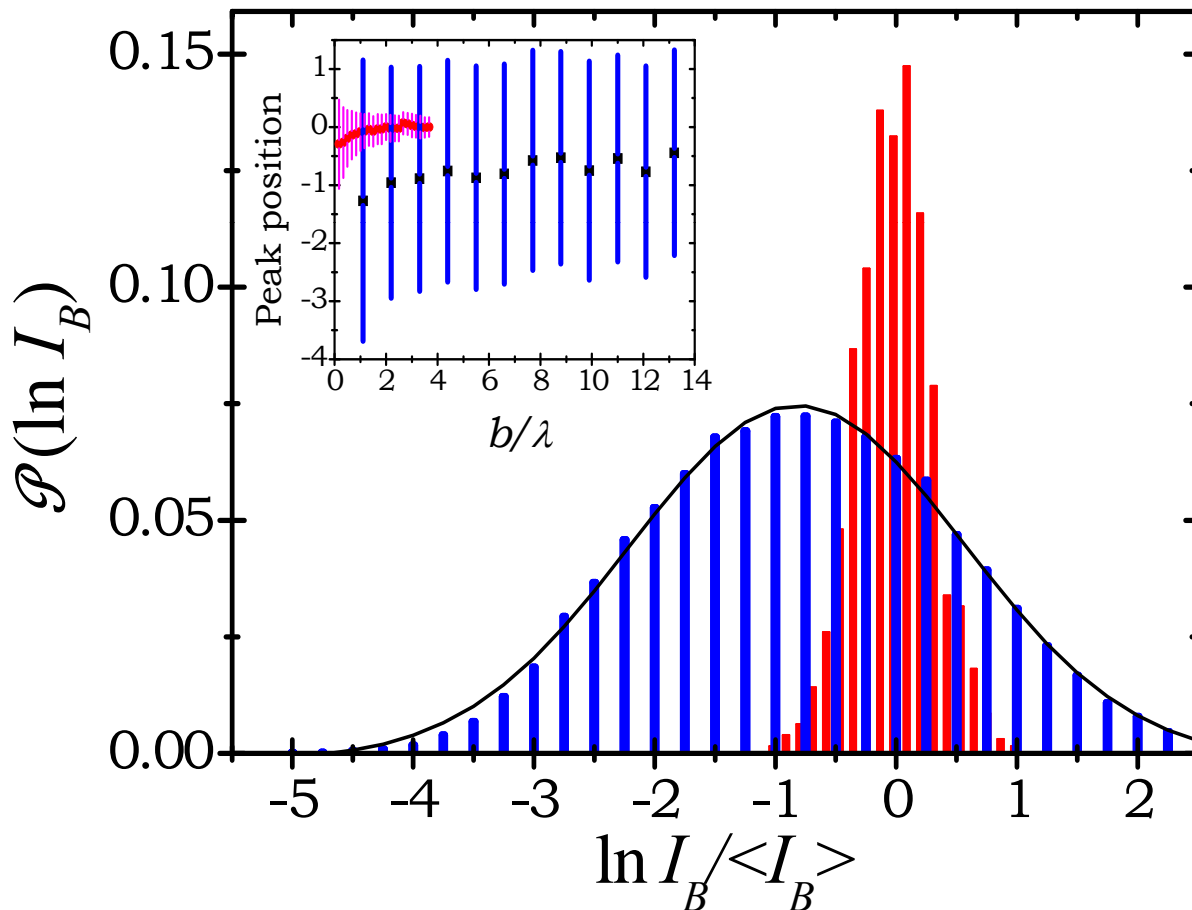
A single parameter **log-normal distribution!** (w^2 and $\ln I_{B,c}$ are related)

Multifractality (MF) PDF

$$\mathcal{P}(\ln I_B) \sim \exp\left[-(\ln I_B - \ln I_{B,c})^2 / 2w^2\right]$$

The probability density function

[Histogram of box-integrated intensities, I_B , $b \approx 2\lambda$]



Red:
diffuse ultrasound
(200-300 kHz)

Gaussian
(centred at 0)

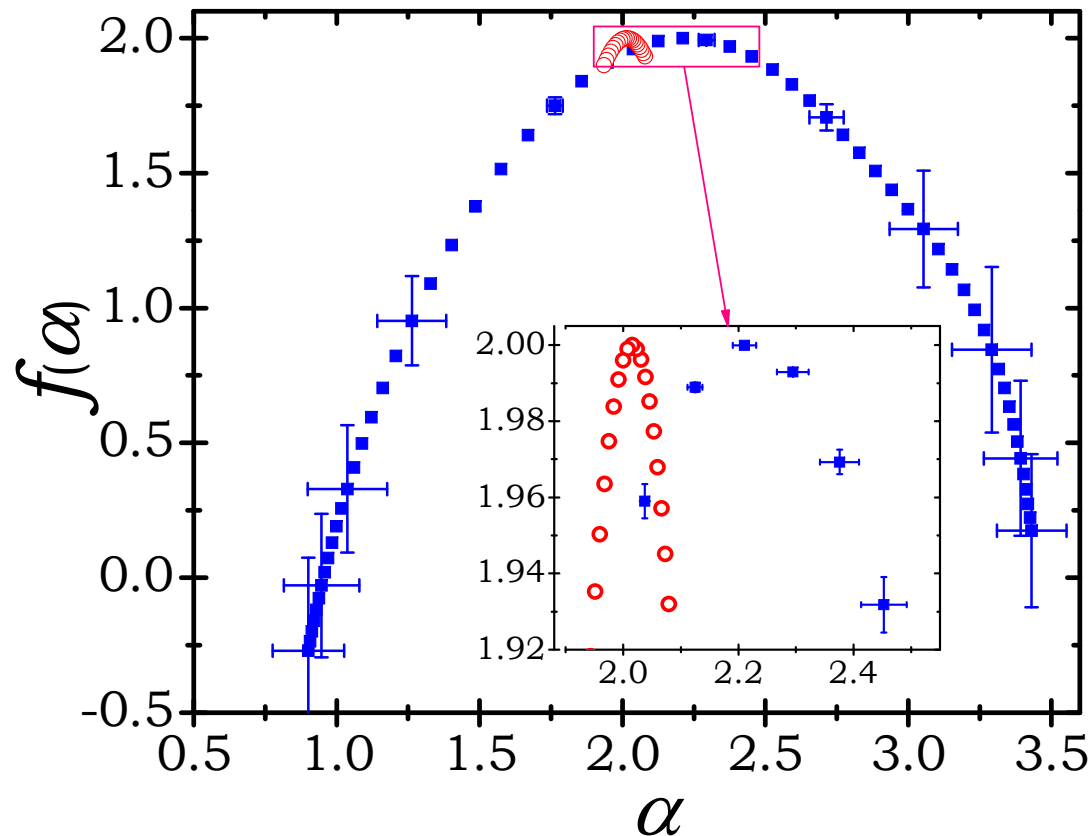
Blue:
Localized Ultrasound
(2.35-2.45 MHz)

Log normal
(peak shifted to
negative $\ln\{ I_B / \langle I_B \rangle \}$)

Multifractality (MF)

The singularity spectrum, $f(\alpha)$

Measure $f(\alpha)$ directly, using the method of Chhabra & Jensen [PRL 62, 1327 (1989)], rather than via the Legendre transform.



Question: Is $\gamma (= 0.21) \propto 1/g$?

Red: Diffuse Light

- very narrow (almost a delta function)
- no shift in the peak from $\alpha_{peak} = d_{sampling\ space} = 2$

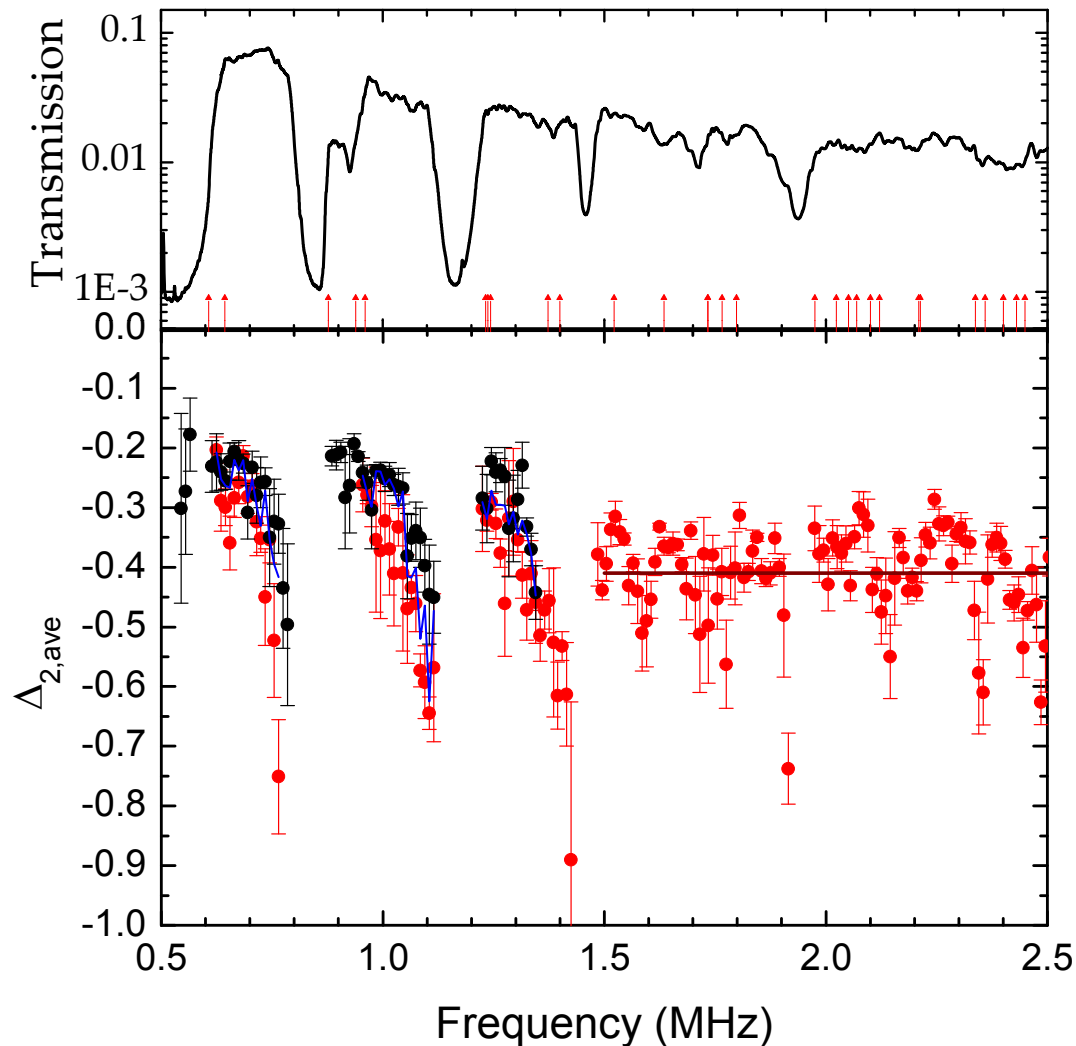
Blue: Localized Ultrasound (2.0-2.6 MHz, 700 speckles)

- Broad spectrum, indicating MF
- Max is shifted by $\alpha_{peak} - 2 = 0.21 \pm 0.02$

Multifractality (MF)

Dependence on frequency

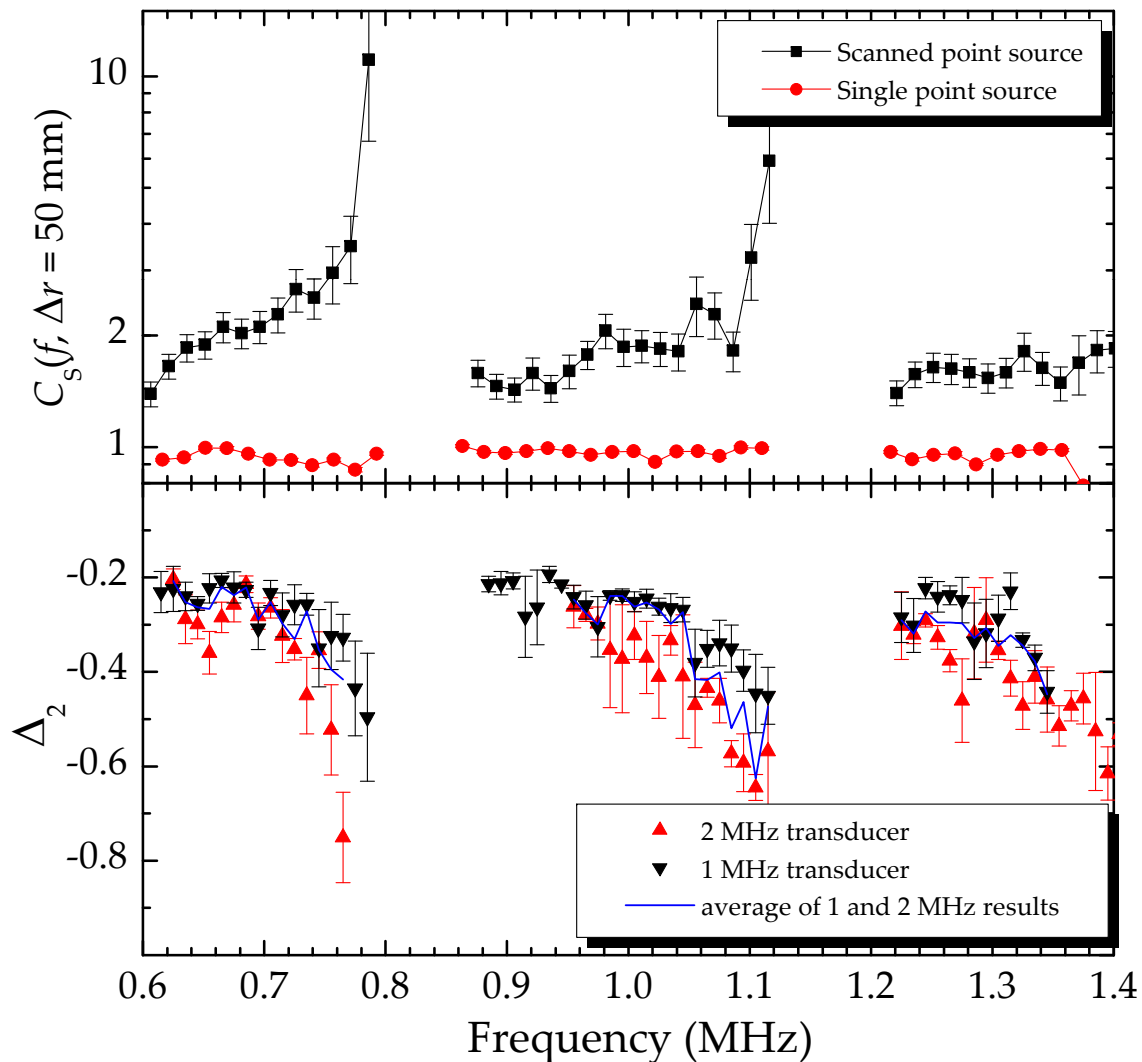
This can be illustrated by the reduced anomalous exponent for $q = 2$ (Δ_2)



- MF behaviour is seen throughout the entire frequency range (0.5 – 2.9 MHz)
- Δ_2 is nearly independent of frequency above 1.5 MHz
- Δ_2 decreases with frequency as the bandgaps are approached from below.
→ several “mobility edges!”

Long range correlations – see Kurt Hildebrand's poster for more

Spatial and frequency intensity correlations show long-range contributions. Compare near field spatial correlations using a point source and detector:

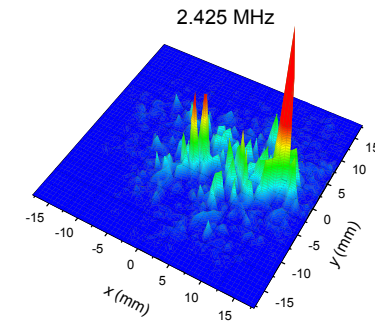
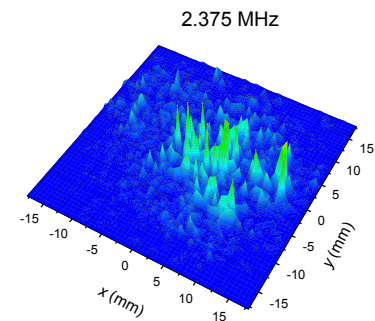
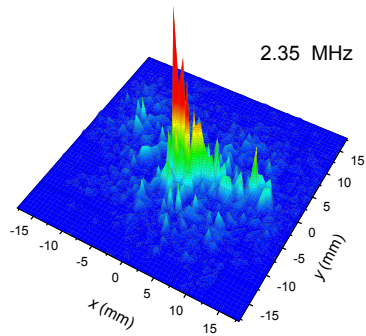


- When the source position is scanned, the transmitted intensities at *all* detector positions fluctuate together, due to LDOS fluctuations at the source positions.

Measure essentially infinite-range C_0 correlations.

- The C_0 correlations increase, while the MF exponent Δ_2 decreases, near the bandgaps
 - Consistent with recent suggestions that both LDOS and MF exponents can reveal critical behaviour.
- [Murphy et al, [arXiv:1011.0659v1](https://arxiv.org/abs/1011.0659v1)]

Statistics - Summary



- Large fluctuations in the transmitted intensity for localized modes:

non-Rayleigh statistics

large variance, $\text{var}(\hat{I})$

$$\rightarrow g < 1$$

- First experimental observations of wavefunction multifractality near the Anderson transition:

scaling of the gIPR, $\langle P_q \rangle \sim (L/b)^{-\tau(q)}$

probability density function
(PDF is log normal)

singularity spectrum, $f(\alpha)$ ($\alpha_{\text{peak}} > d$)

Some questions for future work:

- Why is the peak in the singularity spectrum is shifted above the sampling dimension by only 0.21 at 2.4 MHz?
- What are the effects on MF of open boundaries, absorption, mixed polarizations?
- Can determine critical exponents from MF behaviour?

Conclusions

We have used ultrasonic experiments and predictions of the self-consistent theory of dynamics of localization to demonstrate/explore **the localization of elastic waves in a 3D disordered mesoglass.**

➤ Time dependent transmitted intensity $I(t)$

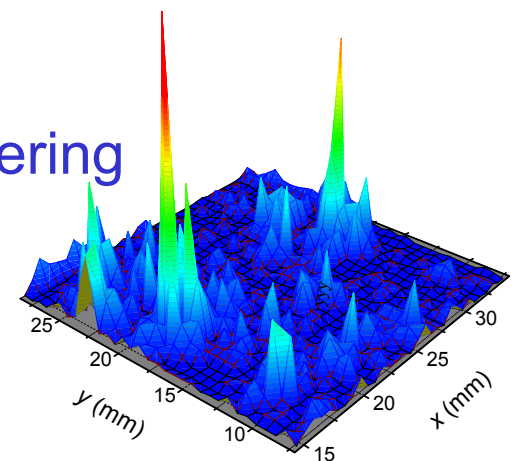
→ non-exponential decay of $I(t)$ at long times.

➤ Transverse confinement in transmission → first direct measurements and theory for $I(\rho, t)$, showing how localization cuts off the transverse spreading of the multiple scattering halo.

$w^2(t)$ is independent of absorption and depends on the localization length ξ (and L)

➤ Transverse confinement and coherent backscattering

➤ Statistics and correlations: non-Rayleigh statistics and large variance of the transmitted intensity \hat{I} ($g' = 0.8 < 1$ at 2.4 MHz); wavefunction multifractality; long range (near-field) correlations.



Transverse confinement is a **powerful new approach** for guiding investigations of **3D Anderson localization** for any type of wave.

If any of you are interested in exploring mesoscopic wave physics using ultrasound, do visit us!

Postdoctoral & graduate student opportunities are available for both fundamental and applied projects!

www.physics.umanitoba.ca/~jhpage



Mesoscopic wave physics can even be relevant to everyday life...

see *Physics Today*, May 2007

Even Anderson localization?

Anderson localization of cat...

Anderson localization of cat...

